AN ABSTRACT OF THE THESIS OF

Charles M. Wright for the degree of Master of Science in Water Resources Science presented on June 2 2023.

Title: Effects of Forest Harvest, Floods, and Wildfire on Bedload Export from Headwater Catchments in the H.J. Andrews Experimental Forest, 1957 – 2022.

Abstract approved:

_____

Julia Jones

This study examined how annual bedload export volume and bedload characteristics were related to disturbances including logging, floods, debris slides, and wildfires over 48 to 65-year periods in small, steep catchments in conifer forests of the western Cascade Range, Oregon. Bedload – the material rolling, sliding, or saltating along the stream bed – is a key indicator of landscape erosion, but few studies document multi-decade patterns of bedload export and its relationship to landscape disturbance. This study took advantage of long-term measurements of bedload export from five headwater catchments in the steep, forested H.J. Andrews Experimental Forest. Bedload was measured annually in sediment basins in five monitored catchments ranging in size from 9 to 101 ha, over the period 1957 to present, and bedload samples were collected in 2020, 2021, and 2022. In the 1950s, all five catchments were dominated by mature and old-growth forest regenerated after wildfire in the early 1500s and mid 1800s. Two catchments (WS01 and WS10) were 100% clearcut in the 1960s and 1970s, and one catchment (WS03) was 25% patch

clearcut in 1963 after roads were constructed in 1959. Major floods occurred in 1964/1965 and 1996. By 2020, clearcuts in WS01, WS03, and WS10 were 50- to 60-year-old conifer plantations. In September 2020, wildfire burned through WS01, WS02, and WS09.

Bedload export volume was related to maximum daily flow magnitude in unlogged catchments (WS02, WS09) in the period before wildfire (2020). Bedload export volume increased following clearcutting of mature and old-growth forest (WS01, WS10), patch cutting with roads (WS03) in the 1960s and 1970s, and after the 2020 wildfire (WS09). Surveys of stream channels of WS09 and WS10 in summer 2022 revealed that in-channel wood in WS09 (unlogged) stored nearly eight times more sediment than in WS10, where logging in 1975 and debris flows in 1986 and 1996 had removed large wood and depleted sediment storage in the channel. Average annual bedload export from WS09 (9 ha, burned) increased from 0.093 m^3/ha before wildfire to 0.768 m^3/ha after wildfire, while bedload export from WS10 (10 ha, unburned) was 0.031 m^3/ha during these years. Physical characterization (texture, organic matter content, and char content) of bedload samples from WS09 (burned) and WS10 (unburned) indicate that following the wildfire disturbance, a number of factors including post-fire mortality, unloading of sediment stored in channels, and hillslope ravel processes increased organic and mineral material in bedload exported from burned catchments. Bedload export from small, steep, forested catchments continued to respond for more than half a century after human and natural disturbances. These findings illustrate general principles that can be extended to

predict how catchments may respond to future forestry practices and other

disturbances including wildfire.

Effects of Forest Harvest, Floods, and Wildfire on Bedload Export from Headwater Catchments in the H.J. Andrews Experimental Forest, 1957 – 2022.

by
Charles M. Wright

A THESIS

submitted to

Oregon State University

in partial fulfillment of
the requirements for the
degree of

Master of Science

Presented June 2 2023
Commencement June 2023

<u>Master of Science</u> thesis of <u>Charles M. Wright</u> presented on <u>June 2, 2023</u>

APPROVED:

_____

Major Professor, representing Water Resources Science

_____

Director of the Water Resources Science Graduate Program

_____

Dean of the Graduate School

I understand that my thesis will become part of the permanent collection of Oregon State University libraries. My signature below authorizes release of my thesis to any reader upon request.

_____

Charles M. Wright, Author

ACKNOWLEDGEMENTS

Finally, thank you to my family and friends, old and new, for your unwavering support. I feel lucky to have a supportive, loving, group of friends and family. There is truly no chance I would be here without your support and influence.

CONTRIBUTION OF AUTHORS

Dr. Julia Jones and Dr. Frederick Swanson contributed to the development and writing of this thesis. Logan Kary assisted with the characterization of the bedload export samples. Ethan Gaddy and Michal Tutka assisted with field surveys conducted in the summer of 2022.

TABLE OF CONTENTS

LIST OF FIGURES

LIST OF FIGURES

LIST OF TABLES

LIST OF APPENDIX FIGURES

LIST OF APPENDIX TABLES

DEDICATION

This work is dedicated to Richard Talbott, I love and miss you! Until we meet again.

Effects of Forest Harvest, Floods, and Wildfire on Bedload Export from Headwater
Catchments in the H.J. Andrews Experimental Forest, 1957 – 2022.

1. INTRODUCTION

1.1. Definitions

Bedload is defined as particles that roll or saltate along a stream bed (Milhous 1973).

From a classical sediment transport perspective, the energy of the streamflow (often quantified as

shear stress) must exceed a specific magnitude force (critical shear stress) for bedload transport

to occur. The balance between the shear stress exerted by streamflow and the critical shear

stresses required for incipient motion of bedload particles depends on a variety of factors

including grain size, grain size distribution, and hydraulic slope (Parker et al., 1982; Buffington

and Montgomery 1997). The connectivity of a stream channel and the sediment being supplied to

the channel may also influence the amount of bedload transport; areas connected to an active

sediment source produced higher bedload transport rates (Harvey 2001; Heckmann and

Schwanghart, 2013). Bedload sediment makes up anywhere from 5 – 40 % of the total sediment

load carried by a stream (Czuba FS 2011; Turowski et. al., 2010).

This study examines patterns of bedload export, rather than bedload transport.

Measurement of bedload is challenging for many reasons. Many methods have been employed

to measure bedload transport, but these methods involve sampling at point locations (e.g., Pitlick

1988). In contrast, measurement of bedload export from small catchments involves

quantification of the sediment accumulated in a sediment catch basin (e.g., Grant and Wolff

1991, Safeeq et al., 2020). Bedload export to a sediment basin includes both bedload delivered

by fluvial transport and sediment contributed through mass movements, such as debris flows.

Thus, bedload export is a portion of the material transfer from a catchment (Swanson et al.,

1982). Bedload export measurements, in this study, include some suspended sediment. Early work using the H.J. Andrews bedload export dataset indicated that suspended sediment accounted for a trivial percentage of the overall bedload export volume (Swanson et al., 1987). Nevertheless, bedload export measurements may include some suspended sediment. Suspended sediment is collected separately in the H.J. Andrews using a proportional water sampler and could be combined with annual bedload export measurements to calculate annual sediment yields.

Material transported as bedload forms the bed and lower banks of the river. Bed material determines the morphology of a channel (Church 2006). When the supply of bedload sediment is less than the minimum transport capacity of a river, the channel bed may experience incision. When the sediment supply and transport capacity of a stream are equal, there are no changes in the elevation of the streambed. When bedload sediment supply exceeds transport capacity, the riverbed will aggrade (Lane 1955).

Mass-movement processes often dominate sediment delivery in forested headwater streams (Eaton et al., 2003). The influence of episodic mass wasting on channel morphology is dependent on the timing of the mass wasting events (May and Gresswell 2004). Events that occur in rapid succession will clog the channels and bury existing morphology (Benda and Dunne 1997), while occasional events may cause chronic, less extreme changes to the channel (Gomi, 2002). Sediment stored within a channel is evacuated over time through erosive debris flows, fluvial entrainment, avulsion, and bank erosion (Lancaster and Casebeer 2007). The timing of sediment evacuation through debris flows/fluvial transport, and accumulation through hillslope sediment production and deposition of massive debris flow deposits effectively shape small headwater channels through time (May and Gresswell 2004).

Bedload export influences aquatic habitat by altering channel morphology and grain size distributions (Hassan et al., 2005). Macroinvertebrate communities rely on substrate and microhabitat (Murphy et al., 1981). Fish habitat is associated with geomorphic characteristics such as elevation and channel slope (Kruse et al., 1997; Lanka et al., 1987; Shields et al., 2021). Fish assemblages respond to geomorphic variables such as valley width- to-floor ratio, gradient, and sinuosity (Shields et al., 2021), which are all in part influenced by bedload export.

1.2. Conceptual model

Many factors influence bedload export, including inherent geomorphic processes (ravel, channel erosion) and characteristics (e.g., confinement, slope, lithology), disturbances (logging, roads, fire), and ecological and human responses to disturbance (Figure 1).
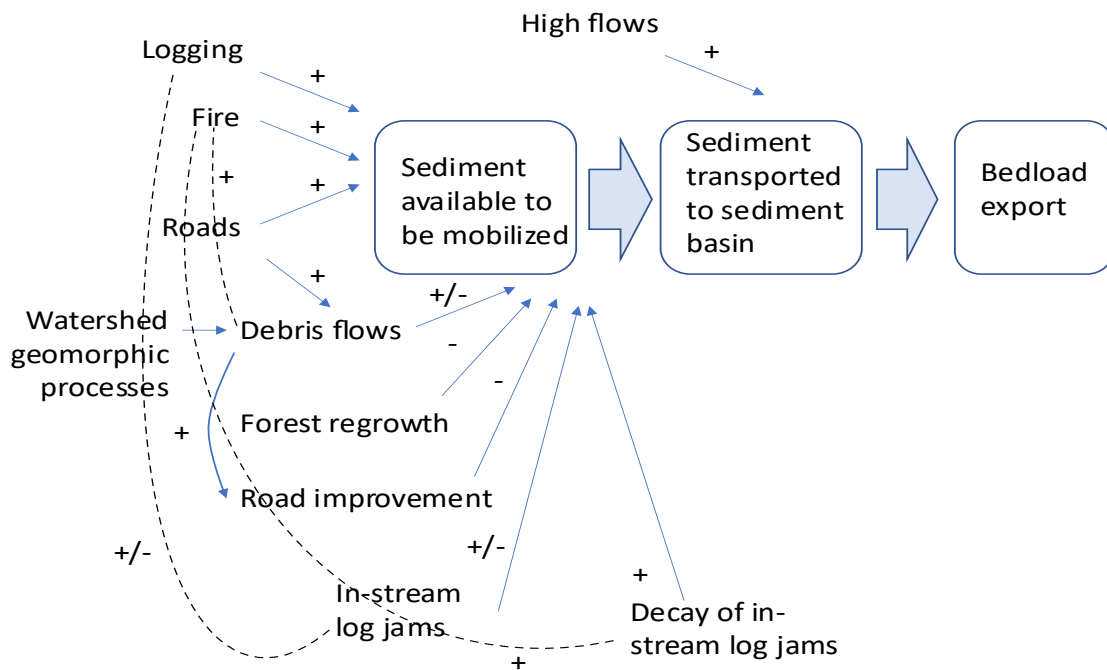
Figure 1. Conceptual diagram of processes examined in this study.

The inherent geomorphic processes and landforms of a catchment also affect bedload export based on the connectivity of hillslope and channel processes. In some cases, hillslope and channel processes are highly coupled, producing direct and sometimes immediate responses to disturbance that deliver sediment to the channel. In other cases, hillslope and channel processes response to disturbance may be lagged in time and space, producing delayed responses of bedload export to disturbance events. For example, sediment export was influenced by sediment supply, slope steepness, lithology, and streamflow metrics (Bywater-Reyers et al., 2017, Bywater-Reyes et al., 2018 and Safeeq et al., 2020). Small catchments with steep slopes and narrow valley floors would be expected to have high connectivity, whereas catchments which are larger, have wide valley floors or lower gradient channels would be expected to have lower connectivity.

High stream flows during major storm events contribute to increased bedload export by mobilizing sediment in the stream bed (Figure 1). In addition, large floods produce debris slides and debris flows (Megahan et al., 1978, Rapp et al., 1991, McClelland et al., 1997), which may move orders of magnitude more sediment than streamflow transport, solution transport, and surface erosion events (Swanson et al., 1982; Hassan et. al. 2006). Mass wasting events can influence channel morphology and sediment storage within a basin, and hence bedload export, for extended periods of time (May and Gresswell 2004, Wondzell and Swanson 1999).

Disturbances (e.g., logging, road construction, and/or fire) also contribute to increased bedload export (Figure 1), by accelerating geomorphic processes or catalyzing mass movements, such as debris slides and debris flows. Clear-cuts are associated with an increase in mass wasting events (Goodman et al., 2022, Swanson and Dyrness 1975, Brown and Krygier 1971). Roads

alter the soil stability of large sections of the hillslope, increasing mass wasting (Dyrness 1967, Swanson and Dyrness 1975, Swanson and Swanston 1977). Forest harvesting and road construction also can increase peak flows (Jones and Grant 1996, Jones 2000), which may increase fluvial transport of sediment and channel erosion, as well as mass wasting during large floods (Wemple et al., 2001).

Wildfire can influence a catchment by altering the vegetation and soil properties (Swanson 1981). Tree mortality interacts with the landscape in complex, often anti-intuitive, ways. Wildfire-related tree mortality reduces evapotranspiration and elevates soil moisture, increasing peak flows (Helvey 1973, Chen 1980, Elliot and Parker 2001), which could lead to increased sediment export through fluvial transport. Increased convective winds during a fire may increase root throw (Swanson 1981). The impact of tree toppling depends on the size of the root mass, the size of the tree bole, the position of the tree, and the mechanism of tree toppling. When a tree falls it creates a tip-up mound and mobilizes previously stable sediment; toppling of trees with larger root masses mobilize more sediment (Swanson 1981). Toppling of trees could fragment the tree into small pieces and dislodge sediment. Fragments of wood and loose soil could contribute to increased bedload export. Organic material in the form of twigs, cones, needles, and bark may fall from the recently deceased tree and contribute to the annual bedload accumulation. Additional organic material may be contributed through delayed mortality.

The removal of organic structures such as down wood and understory vegetation can increase the rate of dry ravel erosion (Dietrich et al., 1982), especially on slopes that exceed 35 degrees (Mersereau and Dyrness 1972, Bennett 1982). Ravel may increase after wildfire, even without storm events, and may remain elevated for up to ten years (Megahan et al.,1995), whereas other work showed that ravel had almost ceased by the second growing season post

wildfire (Mersereau and Dyrness 1972). Although in some settings fire may produce hydrophobic soils that can increase overland flow, infiltration excess overland flow has not been reported even after wildfire in the Pacific Northwest region, possibly due to high soil moisture and rapid rates of vegetation regrowth (Wondzell and King 2003). Fire may also increase the frequency of rapid soil movements through increased soil water (Adams et al.,1991), increased snow accumulation and melt rate (Harpold et al., 2013), and reduced root strength (Swanson 1981, Swanston 1971, McNabb and Swanson 1990). Soils with reduced root strength on a slope are more susceptible to mass wasting, especially when they are saturated. Debris flow activity is probable for five to ten years following a wildfire in the PNW (Wondzell and King 2003).

In the longer term, ecological responses to past disturbance events such as forest regrowth or wood decomposition, or human responses to disturbances such as changes in road construction, may alter geomorphic processes, and reduce sediment delivery to channels (Figure 1). A reduction over multiple decades in the volume of material delivered to channels during large floods was attributed to forest regrowth and improvements in road construction (Goodman et al., 2022). Wood decay in the channel may govern bedload export: as wood decays, sediment is liberated and can be transported as bedload (Wohl and Scott 2016).

Once sediment is in the channel, high stream flows entrain sediment and deliver it to the sediment basin (Figure 1). The capacity of a given flow to entrain sediment and deliver it to the sediment basin depends on many factors including valley width and gradient, the presence of wood in the channel, and other factors (Figure 1). Bankfull flows have been shown to be important for sediment export. Headwater streams in Idaho transport 37% of overall bedload during bankfull flows (Whiting et al., 1999). The timing of high flow events (i.e., large floods) relative to the timing of forest disturbance also affects bedload export (Grant and Wolff 1991).

Material transport on hillslopes and in channels is much higher when large floods occur soon after logging or road construction (Goodman et al., 2022).

1.3. Objectives and research questions

The objective of this study was to examine multi-decadal patterns of bedload export from small, steep forested catchments in response to various disturbances. Long-term studies of bedload export are rare. Jackson et al (2005) documented >50 years of elevated rates of bedload export attributable to sediment deposition from a century of cotton farming (1820 – 1930) in Georgia. A five-year study in an Alpine catchment revealed the role of high flows during rain-on-snow events in transporting bedload (Antoniazza et al., 2022). Multidecade rates of bedload export can be inferred from studies of reservoir sedimentation (e.g., Minear and Kondolf, 2009). At longer time scales, historical legacies of past stream disturbance, such as mill ponds in the eastern United States, can leave multi-century legacies of stored sediment (Walter and Merritts 2008).

Multi-decadal patterns of bedload export are relevant for understanding the effects of forest disturbances and climate on erosion, stream morphology, and aquatic habitat. This study evaluates 48 to 65-years of bedload export records from five small, steep, forested catchments in western Oregon affected by large floods, forestry, and wildfire. Prior studies using these data used records through 1988 (Grant and Wolff 1991) or only from one catchment (Safeeq et al., 2020). This study also evaluates the initial response of bedload export to a September 2020 wildfire, which burned portions of three of these catchments. Few studies have examined the effects of moderate to low severity fires on erosional processes in the Pacific Northwest (Wondzell and King 2003).

This study addresses three research questions:

1) What are the long-term responses of bedload export to human disturbance (e.g., roads, logging, and post-harvest burning) and natural disturbance (e.g., landslides and debris flows)?

2) What are the short-term responses of bedload export to moderate and low severity wildfire?

3) How do catchment characteristics (e.g., size, landforms, and geology) influence the bedload export response to various disturbances?

2. STUDY SITE

2.1. The H.J. Andrews Experimental Forest Physiography

The H.J. Andrews Experimental Forest (hereafter, Andrews Forest) is the 64 km^2 catchment of Lookout Creek (44.23° N, 122.17° W) in the western Cascade Range of Oregon (Figure 2). The geology is dominated by volcanic rocks; low elevations are underlain by hydrothermally altered pyroclastic flow deposits, and mid elevation areas are underlain by welded ash-flow tuff; some upper-elevation areas are composed of highly resistant basalt-andesite lava flow (Swanson and James 1975; Swanson and Jones 2002). The geomorphic landscapes expressed today are a result of the complex interactions between tectonic scale mountain building, smaller scale geomorphic processes (i.e., glacial carving, earthflows, fluvial incision, debris flows, meandering), and the varying lithology (Swanson and James 1975; Nakamura et al., 2000).
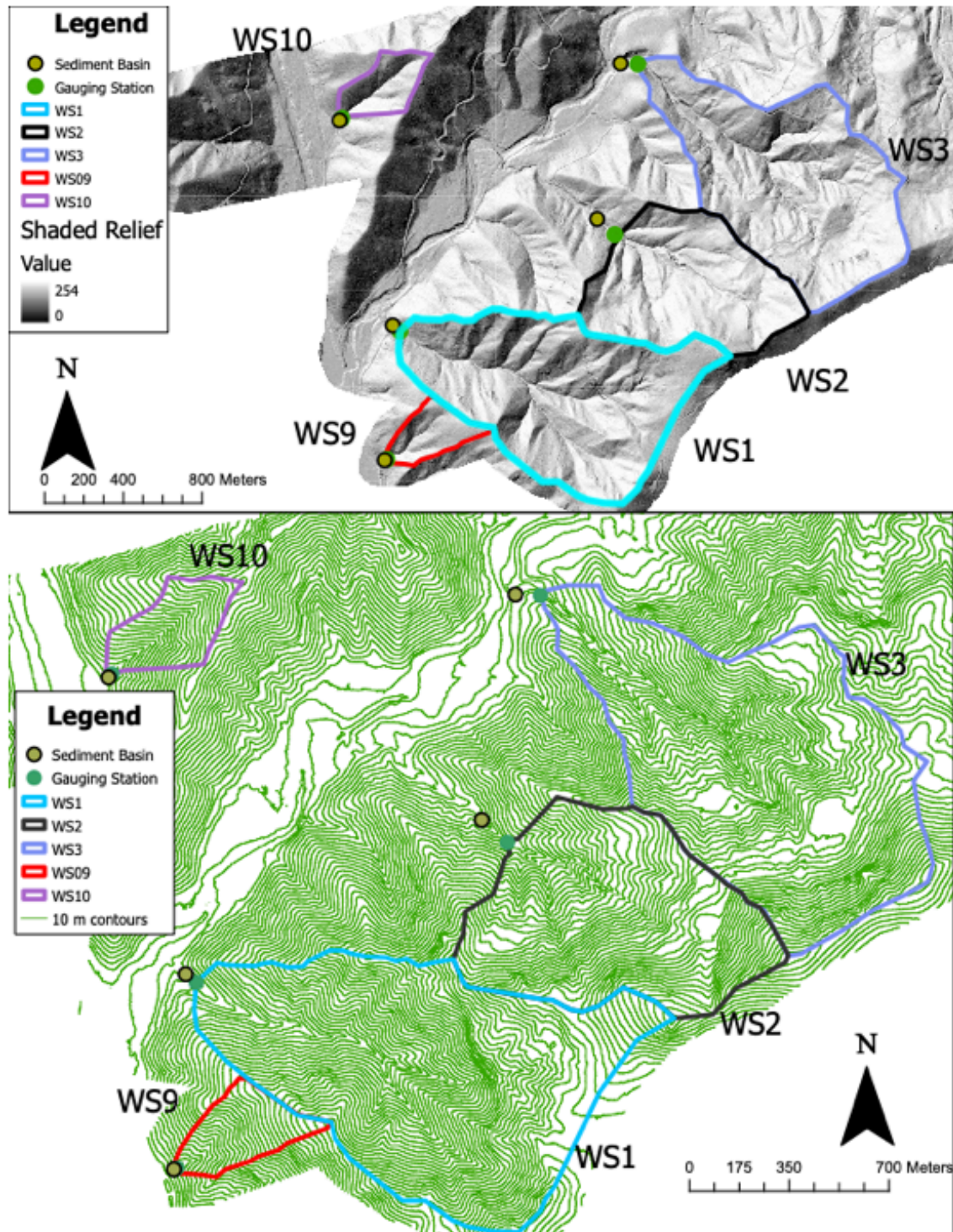
Figure 2. Site map of the small experimental catchments. Lidar flight was commissioned by Quantum spatial and occurred from July 11 - July 23 2020.

Soils in the Andrews Forest are formed from a variety of parent materials. Forty-two percent of the area consists of soil derived from glacial drift, 24 percent is from colluvial material from basalt, 11 percent is colluvial material from green breccias, and 23 percent is colluvial material from red breccias (Stephens 1964). The soils in the catchments included in this study are colluvial and alluvial; glacial processes did not affect the small catchments at lower elevation in the Andrews. Organo-mineral aggregates are present throughout the soil in the Andrews Forest (Sollins et al., 2006). Organo-mineral aggregates form when organic material binds to the outer edges of mineral material and forms layers of organic material around the mineral grain.

Climate in the Andrews Forest is characterized by mild, wet winters, and dry summers. Mean annual precipitation ranges from 2,302 to 2,785 mm, with higher values at upper elevations. More than 70% of annual precipitation falls during the fall and winter months. Mean annual temperature is 8.5 °C, ranging from 0.6 °C in December to 17.8 °C in July. Snowpack can persist into June above 1050 meters and can be up to four meters deep (Greenland 1993).

Five small (second- and third-order) catchments in the Andrews Forest have been instrumented to measure bedload export (Figure 3). These catchments range from 9 to 101 ha in size and from 438 to 1080 m in elevation. Slope gradients range from 30.7 (WS09 and WS01) to 27.7 degrees (WS03) (By-water Reyes et al., 2018). Study catchments vary in valley floor width: WS01 has the widest valley floor and WS 10 has the narrowest valley floor. Average channel gradients of tributaries in WS01, WS02, and WS03 range from 16.6 to 8.3 %, and maximum channel gradients range from 79.2 to 69.4%. Average channel gradients in WS09 and WS10 are 5.9 and 7.5%, and maximum channel gradients are 22.2 and 61.7% (Table 1).
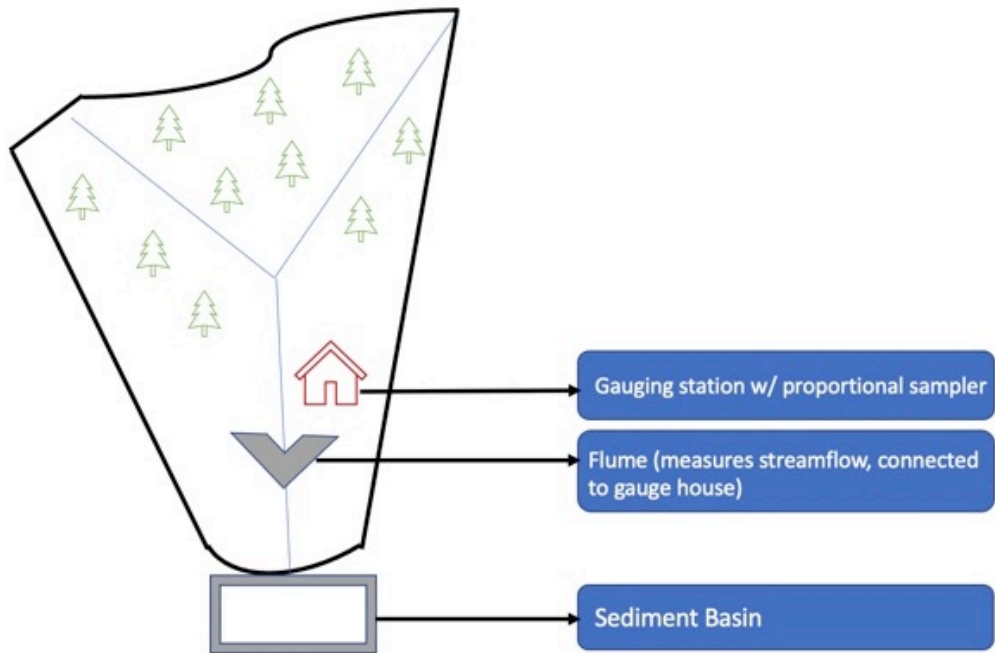
Figure 3. Schematic diagram of small catchment experimental design

Table 1. Longitudinal profiles of the tributary channels at each study site.

Watershed	Segment	average slope (Percent)	maximum slope (Percent)	maximum elevation (m)	average elevation (m)	elevation loss (m)
1	1.1	8.3	74.6	835.8	580.8	415.4
1	1.2	7.3	30.6	780.8	564.3	357.2
1	1.3	8.4	50.3	780.8	564.3	359.3
2	2.1	16.6	79.2	845	693	278.3
2	2.2	12.7	46.8	800	671	232.7
2	2.3	8.0	37.8	823.6	672.6	252.2
2	2.4	8.2	36.1	698.9	628.4	127.3
3	3.1	9.3	37.5	750	583	270
3	3.2	10.6	69.4	780	593	307
3	3.3	5.5	27.2	950	655	485
3	3.4	10.9	73.3	790	599	329
3	3.5	7.6	42.1	803	604	340
9	9.1	8.34	22.2	606.5	501	184
9	9.2	4.5	11.6	541	477	114
9	9.3	4.9	17.5	552	480	127
10	10.1	9.4	61.7	662	547	208
10	10.2	5.7	21.8	599	401	143

Massive deposits from debris flow events in 1996 remain in the WS03 channel near the mouth of the catchment, where a slump and accumulation of large wood pin this deposit in place. In WS10, the channel flows over bedrock for much of the stream length. WS09 has significant stored sediment within the channel and had a high number of log jams. The soil on the slopes is colluvial and highly unstable, especially following the wildfire (Figure 4).

Figure 4: A photograph of the hillslope in WS09, taken September 22, 2020. Photo: Mark Schulze

Hydrology of the catchments is characterized by high interception, high infiltration, and percolation. In Watershed 10, 97 % of total storm flow was subsurface storm flow, while the remaining 3% was channel interception, and overland flow did not occur (Harr 1977). Nevertheless, peak flows can occur rapidly after precipitation. The interaction between a transient shallow snowpack and rain events is important in these catchments: a large peak flow was five times more likely to occur in a rain-on-snow event than in a rain event (Harr 1981).

Vegetation of study catchments was dominated by old-growth forest in the 1950s (Table 2) dominated by native conifer species (*Tsuga heterophylla*, *Pseudotsuga menziesii, Thuja*

plicata). The amount of large wood within the channel varies between these catchments (Czarnomski et al., 2008).

WS01, WS02, and WS03 were part of the first paired- catchment study, established in 1952. WS01 was clear cut from 1962-1966 then broadcast burned at a high intensity in 1967. No forest management occurred in WS02, which has served as the reference for this experiment. Six percent of WS03 was converted to roads in 1959 in preparation for the 1963 patch cut which removed 25 % of the forest canopy (Table 2). WS09 and WS10 were part of a separate paired-catchment study, established in 1968. In 1975, WS 10 was clear-cut without the use of roads or a broadcast burn. WS09 served as a reference in this experiment (Table 2). See figures A-7 to A-11 for individual topographic maps of each catchment included in this study.

Debris flows occurred in WS03 (1964 and 1996) and WS10 (1986, and 1996), but not in WS01, WS02, or WS09 (Table 2). In WS01 and WS10, 100% of the forest was clearcut, and in WS03, 25% of the forest was clearcut in three patches (Table 2). As of 2023, vegetation in former clearcuts consists primarily of planted ~50-year-old, monoculture Douglas-fir forests.

Table 2. Characteristics of five study catchments in the Andrews Forest, Oregon.

	WS01	WS02	WS03	WS09	WS10
Area (ha)	96	60	101	9	10
Elevation (m asl)					
minimum	439	545	471	438	461
maximum	1027	1079	1080	731	679
Slope gradient (%)	59	53	53	59	58
Orientation	NNW	NNW	NNW	WSW	WSW
Original vegetation	mature and old-growth forest	mature and old-growth forest	mature and old-growth forest	mature and old-growth forest	mature and old-growth forest
Roads	none	none	2.7 km, 1959	none	None
Forest harvest	100% clear-cut, 1962-66	none	25% patch cut, 1953	none	100% clear-cut, 1975
Post-harvest burning	slash burning, 1967	none	slash burning, 1963	none	none
Debris slides, debris flows	none	none	1961, 1964, 1996	none	1986, 1996
Wildfire	moderate severity, Sept 2020	moderate severity, Sept 2020	none	moderate severity, Sept 2020	none
Bedload measurement start year	1957	1957	1957	1974	1974
Bedload measurement method	survey	survey	survey to 1996, excavation from concrete basin 1999 – present	excavation from concrete basin 1974 - present	excavation from concrete basin 1974 - present

On September 7, 2020, the Holiday Farms wildfire occurred in the Western Cascades, OR. The fire burned 173, 439 acres including the towns of Blue River, Finn Rock, Nimrod, Vida and Leaburg. The severity of the fire varied from high severity to low severity, although only low to moderate severity fire influenced the H.J. Andrews (WS01, WS02, WS09).

Using imagery from the summer of 2019 compared to the summer of 2021, the Sentinel -2 Normalized Burn Ratio was calculated to identify the overall area of each catchment impacted

by the wildfire. The total area influenced by the wildfire varied among the affected catchments. In WS09, 4.22 of 9 hectares (47% of catchment area) were impacted by the wildfire, and some sections experienced up to 50 to 75% basal mortality (Reilly et al., 2017, Bell and Powers 2023). In WS01, 20.3 of 96 ha (21% of catchment area) was influenced by the fire, while 9.6 of 60 ha (16% of catchment area) was impacted in WS02.

Repeat measurements of long-term vegetation plots in each of the catchments indicate that as of summer 2021, the wildfire killed 56% of the sampled trees (414 of 735) in WS09, 31% of the sampled trees (336 of 1087) in WS02, and 26% of the sampled trees (697 of 2756) in WS01 (Bell and Powers 2023) (Figure 5).

As mentioned above, wildfire, human disturbance, mass wasting, and large-scale geomorphic characteristics (e.g., valley width, channel gradient, arrangement of drainages, presence of coarse woody debris) differ among the five catchments. Bedload export was evaluated in the context of these differences. Much of the results and discussion of this study are organized by catchment in order to highlight the effects of catchment history and geomorphic characteristics on bedload export.
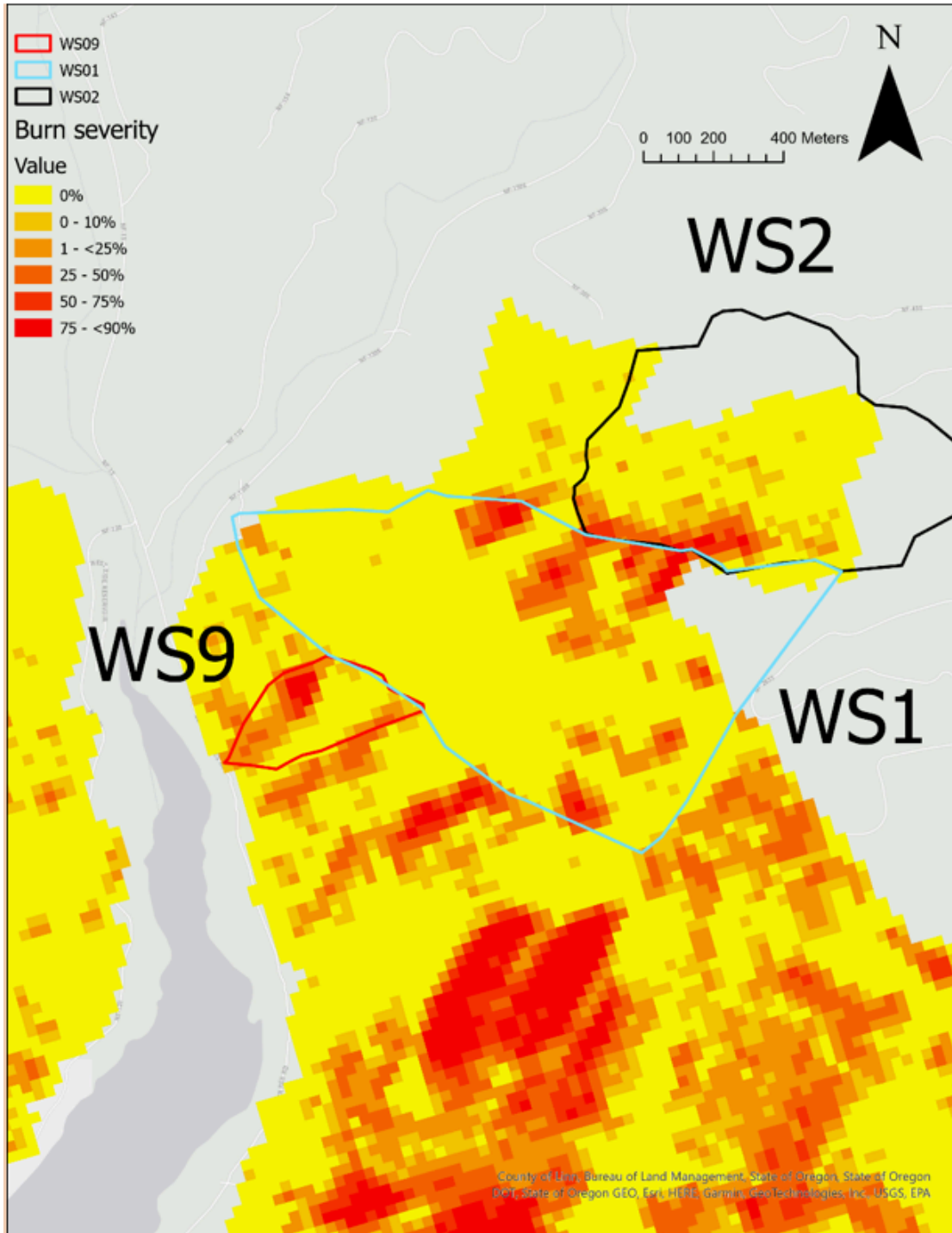
Figure 5. Burn severity map. % Indicates the percent of basal area mortality, based on Sentinel-2 Normalized Burn Ratio. (Summer 2019 vs summer 2021). Source: Bell and Powers 2023

3. METHODS

3.1. Spatial Data Analysis

Contour lines, valley floor widths, valley cross section topography, and longitudinal profiles of the tributaries were obtained using a 1-meter resolution bare earth digital elevation model and the elevation surface function in ArcGIS pro (Figure 6). Catchment boundaries were delineated using 1-m contour lines.
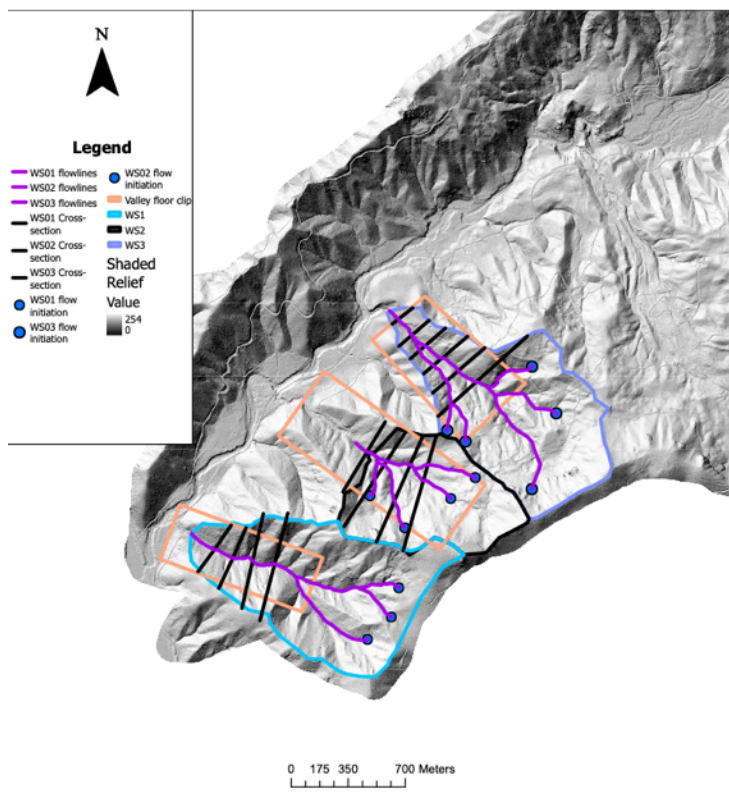
Figure 6. Site map showing locations of longitudinal profiles and cross sections

3.2 Field Methods

3.2.1 Bedload Export Sub-Sampling

A total of 22 samples of exported bedload were obtained from WS09 and nine samples were obtained from WS10 (Appendix B, Table 1). Samples of bedload export were collected from different deposits that were created during sediment basin cleaning. Each deposit represented a distinct time period of bedload accumulation in the sediment basin. The temporal range of each deposit was identified from sediment basin clean-out records from 2020 to 2022 (Greg Downing, personal communication). At WS10, we identified three distinct sediment deposits corresponding with three periods: prior to water year 2020, water year 2021, and water year 2022. At WS09, we identified three distinct sediment deposits corresponding with three periods: immediately following the 2020 Holiday Farms wildfire (accumulated from October 2020 – December 2020). The second deposit was excavated June 2021 (accumulated from December 2020 – June 2021). The last deposit was excavated in July 2022 (accumulated from June 2021 – July 2022) (Figure 7).

Figure 7. WS09 deposits, the sampling method, and samples obtained.

3.2.2. Long-term Bedload Sampling

Annual bedload accumulation has been measured since 1957 (WS01, WS02, WS03) and since 1974 (WS09, WS10) (Table 2) (Johnson and Rothacher, 2019). Sediment basins are located downstream of the flume and gauging station in each catchment (Figure 3). In the sediment catch basin, the energy from the streamflow is dissipated and the sediment carried in the flow drops out of suspension. The amount of sediment that accumulated within the sediment basin is measured annually by repeat surveys of accumulated material or by removal of the material. A portion of material that accumulates within the sediment basin can be considered suspended sediment, but Swanson et al., 1987 indicate that the amount is trivial.

Sediment basins at WS03, WS09, and WS10 are concrete-lined, but those at WS01 and WS02 are not. The concrete lined basins are excavated annually. A back-hoe and shovels are used to dig out the sediment basins. In years with low bedload production the basins can be cleared with only a shovel. When using a back-hoe and shovel to excavate, the first step is to calculate how many 5-gallon buckets of bedload sediment fits within a back-hoe bucket. Once the number of 5-gallon buckets per back-hoe bucket is calculated, the rest of the basin is dug out using mostly the back-hoe bucket. The volume of accumulated sediment is determined from the number of back-hoe buckets multiplied by the number of 5-gallon buckets per back-hoe bucket times the volume of the 5-gallon bucket.

WS01 and WS02 (and WS03 prior to 1996) do not have the concrete lined basins, so annual bedload accumulation values are calculated through repeated surveys. Approximately 15 established survey transects are located across each sediment basin at evenly spaced at 3-foot intervals (Figure 8). The elevation of the ground surface is measured every 3 feet along each transect. The survey locations are flagged as depositional or non-depositional. In all depositional zones, the elevation of the survey location is determined, and the average elevation is obtained for the area of the sediment basin. This number is compared to the average survey elevation from the previous year to determine the change in deposit depth. The volume of sediment accumulated is determined from the average change in elevation multiplied by the area of the sediment basin. In some years the sediment pile within the basin begins to breach the water surface. In those years, the basin is completely excavated, and surveys are conducted before and after the large-scale excavation to estimate the accumulation of that year.
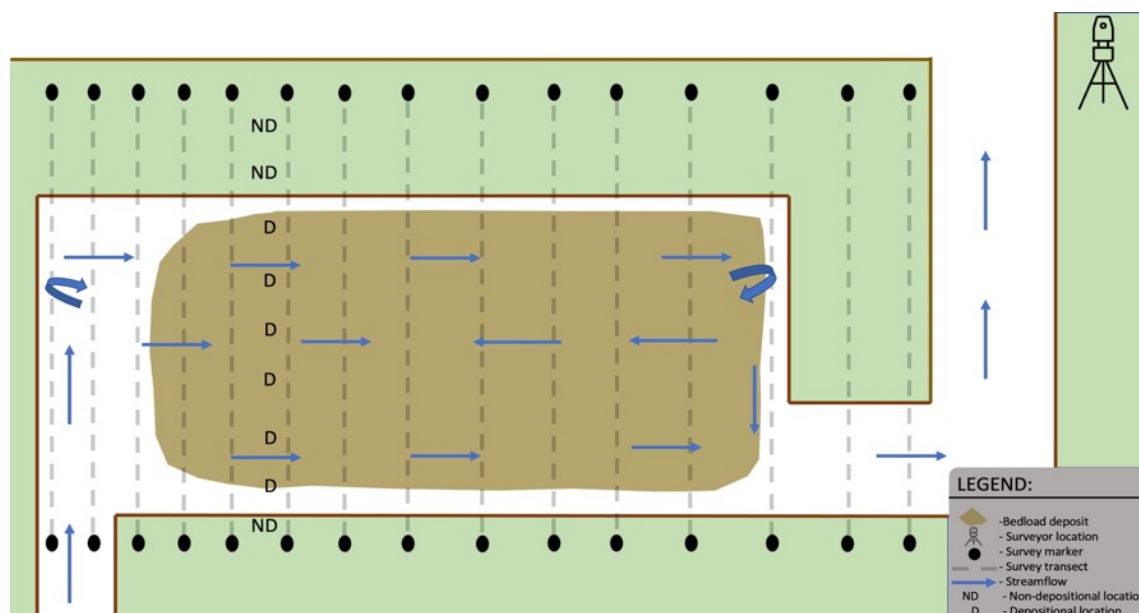
Figure 8. Schematic plan view of bedload survey method used in WS01 and WS02 (1957 to present) and WS03 (1957 to 1995).

Accumulation per catchment area is then calculated by dividing the overall volume of excavated bedload sediment accumulation by the catchment area (m³/ha). The two methods vary in their detection limits. The precision of bedload estimates was 0.02 m³ in concrete-lined basins, and 1.75 to 2 m3 in surveyed basins (Table3). The estimated annual bedload volume was less than this detection limit for two years in WS09, 5 years in WS03, seven years in WS01, and 16 years in WS02 (Table 3).

Table 3. Precision of annual bedload export in five small catchments, Andrews Forest.

	WS01	WS02	WS03	WS09	WS10
Detection limit					
(m³)	2	1.75	0.02	0.02	0.02
(m³/ha/yr)	0.02	0.03	0.0002	0.0022	0.0020
Years below					
detection limit	7	16	5	2	0
Total years	65	65	65	48	48

This study used bedload export volume rather than mass because the fraction of organic matter was important to the analysis. Organic matter content in bedload varies over time, so

given the different bulk densities of mineral and organic matter there is no simple way to convert volume to mass.

3.2.3. Field Surveys of WS09, WS10

Large wood and sediment were surveyed in a 100-meter stretch upstream of the gage in both WS09 and WS10 in the summer of 2022. During the survey, we counted pieces of large wood (> 10 cm in diameter, > 1 m in length) in the near-channel environment and estimated the amount of sediment stored by each wood piece (Figure 9). For each piece of large wood, the length, diameter, orientation, and role in storing or eroding sediment was recorded. The volume of each piece of large wood was calculated and the total wood volume was determined for the surveyed reach. The orientation of each piece of large wood was recorded in relation to stream flow (i.e., perpendicular to flow, parallel to flow) or by cardinal direction (i.e., north, west, east). Qualitative descriptions were created to assess how each piece of large wood interacted with the surrounding environment to either store or release sediment. The width, depth and length of each sediment storage zone was measured and used to estimate the volume of stored material behind each piece of large wood, assuming a wedge shape of the deposit.

Figure 9. Photographs from field surveys in WS09 and WS10. Photo: Charles Wright and Michal Tutka

3.3. Lab Methods

For each sample, we: (1) conducted a particle size analysis, (2) determined soil color for each size fraction, (3) performed loss on ignition tests for the material less than 2 millimeters, and (4) characterized the type and degree of charring in organic matter > 4 mm.

3.3.1 Particle size analysis

Immediate post fire (accumulated from October 2020 – December 2020) and the sediment excavated in June 2021 (accumulated from December 2020 – June 2021) were air-dried. The samples obtained from the deposit that accumulated from June 2021 – July 2022 were oven dried in an oven set to 105 ° C for 12 hours. After oven drying, samples were left in the oven for 48 hours to ensure that they were fully dried. A 200–400-g representative sample was obtained. This sample was separated into various size fractions using hand sieving through 4-mm

and 2-mm sieves. The >4 mm fraction was hand sorted into organic material (bark, twigs, cones, needles, etc.) and mineral material (fine gravel). The sieving procedure resulted in for distinct sedimentological classes: < 2 mm, 2 to 4 mm, > 4 mm mineral material, and > 4 mm organic material (Figure 10). Some samples lacked large pieces of organic matter. The weight of each size fraction for each sample was determined (Appendix B, Table 1). The 2-4 mm size class was of interest although it did not correspond with a distinct grain size (e.g., sand, clay, silt), because the sediment in this size class was distinctly different from the > 4 mm size class. Sediment in the 2-4 mm size class was a combination of organo-mineral aggregates. The mineral material within the 2-4mm size class was well rounded, while the greater than 4 mm size class was angular. Individual particles in the 2-4 mm size class could be broken apart by gentle pressure.

Figure 10. Particle size analysis of the bedload samples.

3.3.2. Loss on ignition

The organic fractions of the 2 to 4-mm and <2 mm fractions were determined using loss on ignition. A representative 1- to 3-g sub-sample was obtained using the following procedure.

A 20-g sample was poured out on a flat surface. Using a straight edge, the 20-gram pile was split into four separate sections. Two of the four sections were removed and replaced with the overall sample. The remaining two sections were mixed and then split again into four sections. This process was repeated until a 1- to 3-g subsample was obtained (Figure 11).

Figure 11. Splitting process used to obtain a 1-3 gram representative subsample for loss on ignition tests

Loss on ignition was determined using a procedure from Nelson et al., (1996). Each 1- to 3-g sample was poured into a pre-weighed crucible. The crucibles were placed into a muffle furnace, preheated at 450 ° C, heated for two hours, and cooled for approximately eight hours. Cooled samples and crucibles were reweighed. The percent organic content was calculated as:

OM% = (SC1 - SC2) / (SC1 - C)

where OM % = organic matter percent, SC1 and SC2 = Sample + Crucible Weight before and after ignition, respectively, C = crucible weight.

For each sample (n = 22 from WS09, n = 9 from WS10), the total weight of sampled sediment was calculated. The weights and percent of each size fraction were calculated, and these were subdivided by organic and mineral fractions (Appendix B, Table 1).

3.3.3. Char Assessment

Using a Munsell color book (edition 1949), charred particles (defined as Munsell colors 5y 2/1 and 5Y 2/2) were separated from the >4 mm organic fraction. The weight and percentage of charred organic material in the 4mm size class was calculated (Figure 12)

Figure 12. Photo of char separated from larger sample.

3.4. Data Analysis

3.4.1 Data used in regression techniques

Instantaneous records of streamflow have been collected since 1952 (at WS01, WS02, and WS03) and since 1968 (at WS09, WS10) (Johnson and Rothacher, 2020). The annual unit-

area maximum daily flow (cubic feet per second per square mile, cfsm) in each water year in each catchment was determined from the daily mean streamflow data series. A Log-Pearson III flood frequency analysis was conducted for the annual daily mean streamflow data series for each catchment using data for the full available record (1953 – 2018 for WS01, WS02, and WS03, 1968 – 2018 for WS09 and WS10).

The 1.25-year recurrence interval flood was identified and used to represent bank full conditions (Castro and Jackson 2007) for each catchment (Figure 13). The number of days that exceeded the 1.25-year return period flow were counted and the total volume of flow that exceeded the bank full discharge was calculated for each water year for each catchment (Appendix Table A-1). Annual bedload accumulation values (m^3/ha) and maximum daily flow (cubic feet per second per square mile, cfssm) were plotted over time for each catchment. Disturbance events (forest management activities such as clear-cuts, burns, road building, etc.) and debris flow events were noted on the plots.
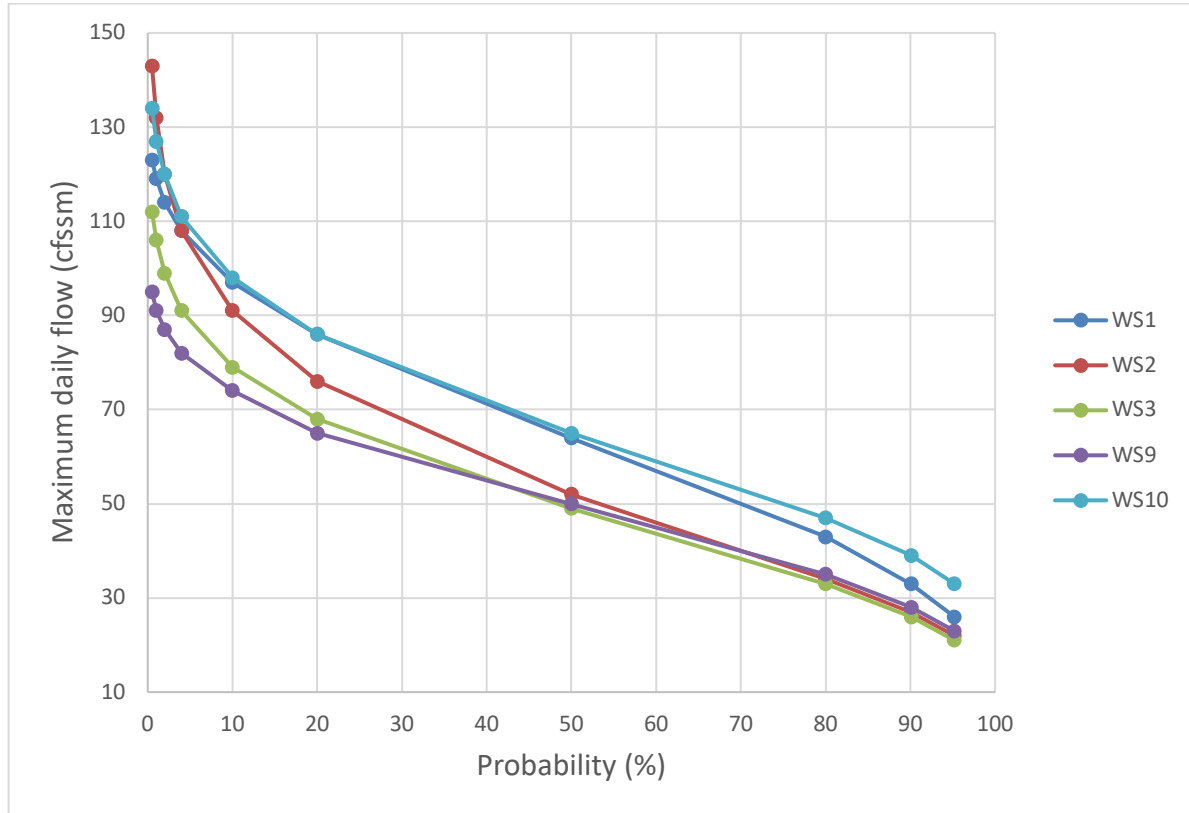
Figure 13. Log-Pearson III flood-frequency analysis using the mean daily flows from each water year in each study catchment, used in multiple regression analyses. Cfssm = cubic feet per second per square mile.

3.4.2 Statistical methods

Ordinary least squares regression models were fitted to relate natural-log- transformed annual bedload accumulation (dependent variable) to natural-log-transformed maximum daily streamflow for the corresponding year (independent variable). Models were fitted for various time periods for each catchment, including the pre-harvest period and various post-harvest periods. Multiple linear regression models were fitted to relate natural-log- transformed annual bedload accumulation (dependent variable) to natural-log-transformed maximum daily streamflow, the annual volume that exceeded bank full discharge, and the number of days in which a bank full flow occurred (independent variables). Debris flow events (in WS03 and

WS10) were excluded from the analysis (Appendix Table A-1). Maximum daily flow and bedload data were not normally distributed. A natural log transformation was applied to maximum daily flow and annual bedload accumulation to normalize the data prior to statistical analysis.

3.4.3 Calculating percent change

To calculate percent change through time, a bedload export ratio (treated export / reference export) was calculated for pre-harvest and compared to the bedload export ratio calculated for each 5-year period after treatment.

4. RESULTS

4.1 Long-term Patterns of Bedload Export

4.1.1 Bedload Export and Maximum Daily Flow by Year

WS01. Average bedload export from WS01 was higher than reference catchments (WS02, WS09) but considerably lower than the two catchments that experienced debris flows (WS03, WS10). Bedload export remained relatively low during the logging period but increased after the broadcast burn and remained relatively high for about 10 years. From 1967 to 1972, bedload export was higher than we would expect based on the maximum daily flow. The highest flow in the decade after logging (1972) produced the second highest export on record. From 1972 to 1977, bedload export seemed elevated relative to the maximum daily flow in those years. High streamflow events in the third to fifth decade after logging (1986, 1996, 1999, 2006) also produced high annual bedload accumulations. By the mid-1980s, bedload accumulation in years without high maximum daily flows was lower than in the early post-logging decade. Following

1995, the annual bedload export was approximately proportional to the magnitude of the maximum daily flow. Since 2020, there has been little indication that the wildfire caused an increase in bedload export. There was a moderate increase in 2021, but in 2022 bedload export returned to pre 1967 values (Figure 14a, Figure 15, Table 4).

WS02. Average bedload export from WS02 was lower than from all logged catchments (Figure 15). Years with the highest annual bedload accumulation coincide with the highest maximum daily flows (1965, 1976, 1986, 1996, and 2006). Bedload export appears to be closely related to the magnitude of maximum daily streamflow. However, in 1973 there was considerably more bedload export than in 1972, even though the maximum daily streamflow of 1973 was 55 cfssm lower than 1972 maximum daily streamflow. In WY 2021 (a year after the 2020 wildfire), a small debris torrent of approximately 5 to 10 m^3 occurred just upstream of the gage. Because streamflow data are lacking for these years (data were collected, but not yet processed), the role of streamflow for this event cannot be determined (Figure 14b, Table 4).

WS03. The average bedload export from WS03 was an order of magnitude higher than in catchments that did not experience debris flows (WS01, WS02, WS09) (Figure 15). There was little change in annual bedload accumulation from WS03 immediately following road construction (1959) and patch clearcutting (1963). In 1965 and 1996, the two largest floods on record produced multiple debris flows in WS03. Debris flow activity dominates the bedload export in this catchment. Bedload export has been quite low despite high maximum daily streamflow in1999 and 2006. For example, in 2006 the maximum daily flow was just 20 cfssm lower than in 1996, but bedload export was 1000 times less than in 1996. Very high bedload export from debris flows occurred in years with maximum daily streamflow >60 cfssm (Figure 14c, Table 4).

WS09. Average annual bedload export from WS09 was relatively low compared to the other catchments in this study, especially those that experienced debris flows (WS10 and WS03) (Figure 15). Annual bedload accumulation appears to be related to maximum daily flow in most years. The largest flood on record (1996) produced the highest bedload export ($1.02m^3$/ha) (Figure 14d). However, bedload export did not increase in other years with high maximum daily streamflow (1984, 1986, 2004, 2006, 2011, and 2012). Following the wildfire in 2020 there was a noticeable increase in unit-area sediment export (Figure 14d, Table 4).

WS10. Average annual bedload export from WS10 was the second highest of all five catchments in this study and an order of magnitude higher than catchments that did not experience mass wasting (Figure 15). From 1974 to 1975, export was less than 1 m^3/ha. Following the clear-cut, bedload export increased to more than 1 m^3/ha (an increase of 6 times compared to pretreatment average) in 1976 (3.0 m^3/ha) and 1978 (2.0 m^3/ha), but remained relatively low until the debris flow during the flood of 1986, which produced the highest export for this catchment at 65 m^3/ha (increased by 141 times compared to pretreatment average). Although the maximum mean daily flow of 1996 was higher than the maximum daily flow of 1986, the estimated export was only 8.5 m^3/ha (increased by 18 times compared to pretreatment average) (Figure 14e, Table 4).

Although WS03 and WS10 both experienced debris flows, bedload export differed between these two catchments. The debris flow events in WS03 were larger than those from WS10. When debris flows are excluded, bedload export from WS03 is almost the same as from the reference catchment WS02. However, when debris flows are excluded, bedload export from WS10 exceeds that from the reference catchment WS09 (Figure 15). Prior to 2020, reference catchments WS02 and WS09 consistently produced less unit-area bedload export.

Table 4. Annual bedload export from five small catchments in the Andrews Forest, 1957-2022, by water year (e.g., 1957 is bedload accumulated from October 1956 to summer 1957). Large values in 1965, 1986, and 1996 are debris flows associated with major floods of December 1964 and January 1965, February 1986, and February 1996; these values were estimated in the field based on the deposit, which extended beyond the sediment basin. Values for WS10 have high confidence because the source and deposit were contained, but values for WS03 are underestimated because there were multiple sources, multiple sites, and material was delivered into Lookout Creek and removed by the high flows (F.J. Swanson, personal communication). -- indicates data not collected. SE = standard error.

	Annual export (m^3)					Annual unit-area export (m^3/ha/yr)				
Year	WS01	WS02	WS03	WS09	WS10	WS01	WS02	WS03	WS09	WS10
1957	18.4	11.5	10.9	--	--	0.19	0.19	0.11	--	--
1958	6.3	15.5	27.3	--	--	0.07	0.26	0.27	--	--
1959	0.0	2.6	1.9	--	--	0.00	0.04	0.02	--	--
1960	0.6	1.0	2.9	--	--	0.01	0.02	0.03	--	--
1961	1.4	7.7	11.5	--	--	0.01	0.13	0.11	--	--
1962	8.2	2.6	0.5	--	--	0.09	0.04	0.00	--	--
1963	0.9	2.9	9.1	--	--	0.01	0.05	0.09	--	--
1964	0.7	0.5	3.9	--	--	0.01	0.01	0.04	--	--
1965	18.9	46.9	20745.7	--	--	0.20	0.78	205.40	--	--
1966	5.1	8.7	23.3	--	--	0.05	0.15	0.23	--	--
1967	89.3	0.0	25.5	--	--	0.93	0.00	0.25	--	--
1968	109.5	0.4	19.6	--	--	1.14	0.01	0.19	--	--
1969	126.9	4.5	63.1	--	--	1.32	0.08	0.62	--	--
1970	37.9	4.5	35.5	--	--	0.39	0.08	0.35	--	--
1971	107.6	8.1	51.3	--	--	1.12	0.14	0.51	--	--
1972	198.6	1.7	58.4	--	--	2.07	0.03	0.58	--	--
1973	123.5	22.7	8.5	--	--	1.29	0.38	0.08	--	--
1974	131.0	1.3	14.5	0.5	3.2	1.36	0.02	0.14	0.06	0.32
1975	129.3	3.0	7.9	0.8	6.2	1.35	0.05	0.08	0.09	0.62
1976	130.8	22.7	19.1	2.6	30.2	1.36	0.38	0.19	0.29	3.02
1977	3.1	0.0	0.0	0.2	3.1	0.03	0.00	0.00	0.02	0.31
1978	106.0	9.7	22.8	0.6	20.3	1.10	0.16	0.23	0.07	2.03
1979	60.1	0.7	4.4	0.8	3.9	0.63	0.01	0.04	0.09	0.39
1980	78.9	9.1	2.1	0.4	1.4	0.82	0.15	0.02	0.04	0.14
1981	74.8	5.4	9.1	0.6	8.5	0.78	0.09	0.09	0.07	0.85

1982	94.9	11.5	14.2	1.0	0.9	0.99	0.19	0.14	0.11	0.09
1983	34.5	6.0	8.1	1.9	0.1	0.36	0.10	0.08	0.21	0.01
1984	45.1	1.8	9.1	0.6	1.1	0.47	0.03	0.09	0.07	0.11
1985	1.9	0.0	1.0	0.0	0.1	0.02	0.00	0.01	0.00	0.01
1986	137.1	33.8	29.3	0.0	659.1	1.43	0.56	0.29	0.00	65.91
1987	53.7	9.6	5.1	0.3	0.3	0.56	0.16	0.05	0.03	0.03
1988	28.8	0.0	0.0	0.3	3.2	0.30	0.00	0.00	0.03	0.32
1989	80.6	20.5	24.3	3.2	10.4	0.84	0.34	0.24	0.36	1.04
1990	34.5	0.0	8.1	0.9	3.2	0.36	0.00	0.08	0.10	0.32
1991	3.7	1.3	5.4	0.2	0.7	0.04	0.02	0.05	0.02	0.07
1992	15.3	3.0	4.0	0.2	0.5	0.16	0.05	0.04	0.02	0.05
1993	16.9	4.6	3.2	0.2	0.4	0.18	0.08	0.03	0.02	0.04
1994	12.9	0.0	0.0	0.2	0.4	0.13	0.00	0.00	0.02	0.04
1995	98.8	17.5	14.2	0.6	0.8	1.03	0.29	0.14	0.07	0.08
1996	252.2	77.8	7736.2	8.7	85.0	2.63	1.30	76.60	0.97	8.50
1997	56.6	13.3	0.0	1.2	3.6	0.59	0.22	0.00	0.13	0.36
1998	14.8	2.4	0.0	0.3	0.7	0.15	0.04	0.00	0.03	0.07
1999	99.7	28.9	114.1	1.9	9.9	1.04	0.48	1.13	0.21	0.99
2000	38.4	16.3	25.2	1.0	1.0	0.40	0.27	0.25	0.11	0.10
2001	2.9	0.6	0.7	0.2	0.5	0.03	0.01	0.01	0.02	0.05
2002	30.7	9.0	3.4	0.3	1.6	0.32	0.15	0.03	0.03	0.16
2003	23.0	1.2	1.1	0.2	0.8	0.24	0.02	0.01	0.02	0.08
2004	29.7	7.2	2.0	0.2	0.8	0.31	0.12	0.02	0.02	0.08
2005	10.5	4.8	0.7	0.3	0.9	0.11	0.08	0.01	0.03	0.09
2006	93.0	52.5	12.3	0.5	3.2	0.97	0.88	0.12	0.06	0.32
2007	17.3	5.4	6.5	0.2	1.5	0.18	0.09	0.06	0.02	0.15
2008	19.6	3.0	1.9	0.3	0.9	0.20	0.05	0.02	0.03	0.09
2009	38.1	20.8	12.1	1.4	2.7	0.40	0.35	0.12	0.16	0.27
2010	--	--	--	--	--	--	--	--	--	--
2011	68.8	20.1	7.2	0.8	2.9	0.72	0.34	0.07	0.09	0.29
2012	65.6	13.6	3.8	0.4	2.1	0.68	0.23	0.04	0.04	0.21
2013	22.1	5.6	1.3	0.2	0.9	0.23	0.09	0.01	0.02	0.09
2014	50.8	6.3	2.6	0.3	2.0	0.53	0.11	0.03	0.03	0.20
2015	61.4	9.6	2.6	0.6	2.7	0.64	0.16	0.03	0.07	0.27
2016	30.9	4.9	3.1	0.4	1.6	0.32	0.08	0.03	0.04	0.16
2017	32.6	8.4	4.0	0.5	0.8	0.34	0.14	0.04	0.06	0.08

2018	5.8	6.6	0.2	0.2	0.4	0.06	0.11	0.00	0.02	0.04
2019	14.0	4.2	3.6	0.4	0.6	0.15	0.07	0.04	0.04	0.06
2020	0.1	7.2	1.3	0.2	0.4	0.00	0.12	0.01	0.02	0.04
2021	24.6	0.2	1.5	5.8	0.5	0.26	0.00	0.01	0.64	0.05
2022	18.5	7.9	1.4	7.3	0.1	0.19	0.13	0.01	0.81	0.01
ave	51.5	9.9	450.1	1.0	18.5	0.54	0.16	4.46	0.12	1.85
SE	6.5	1.7	341.3	0.3	13.8	0.1	0.0	3.4	0.0	1.4

(a)WS01
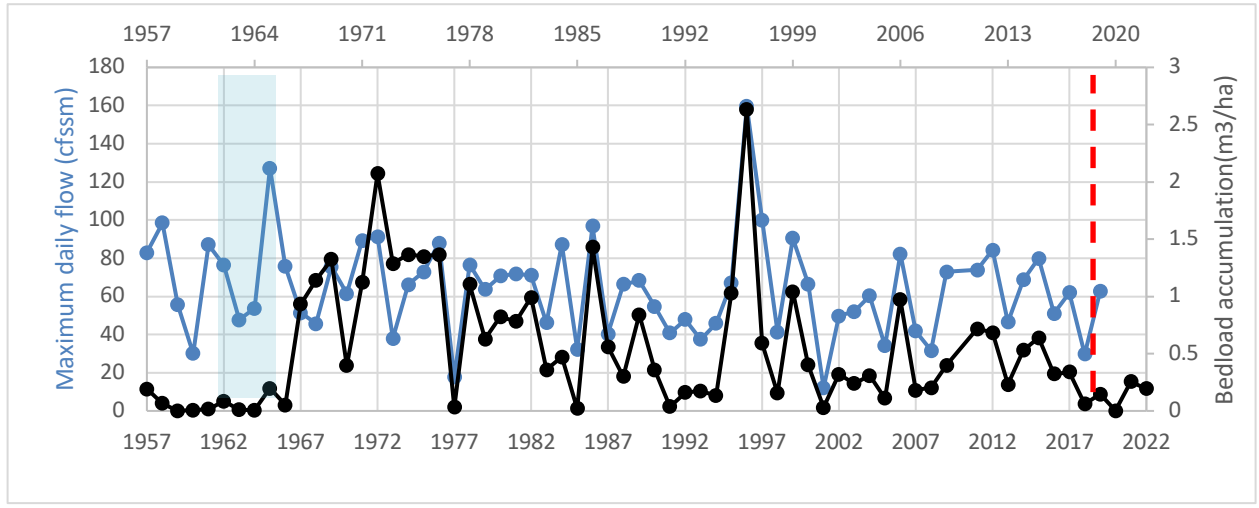
(b)WS02
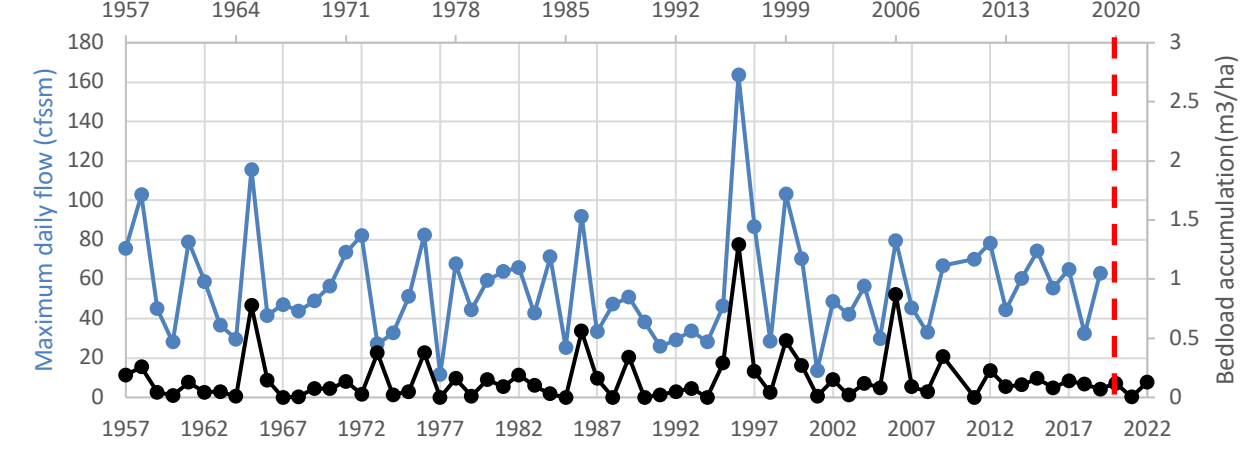
(c)WS03
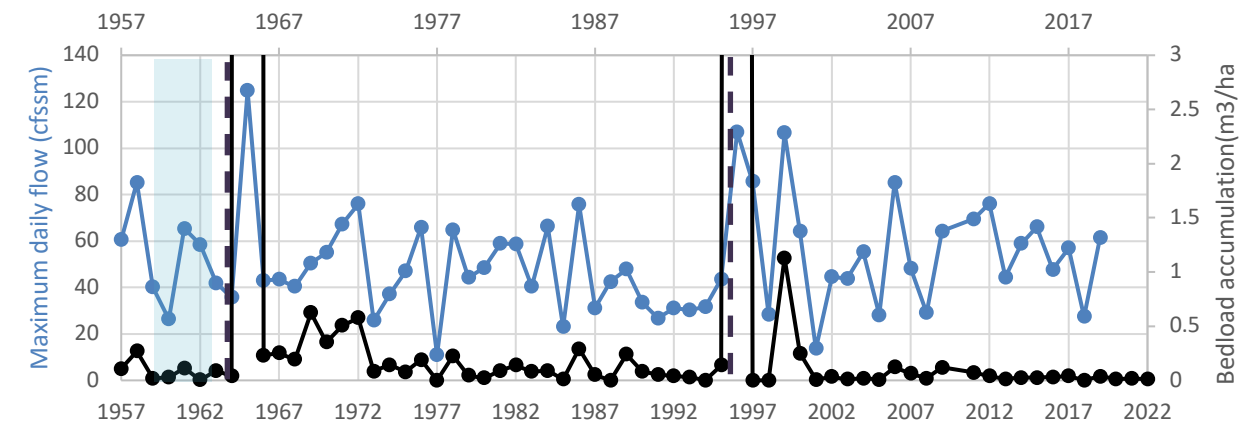
(d)WS09
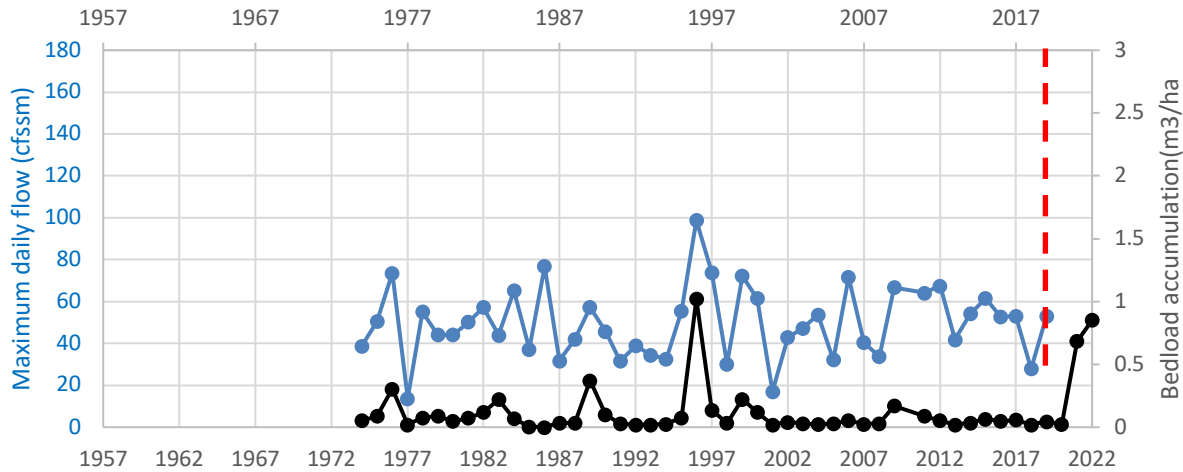
(e)WS10
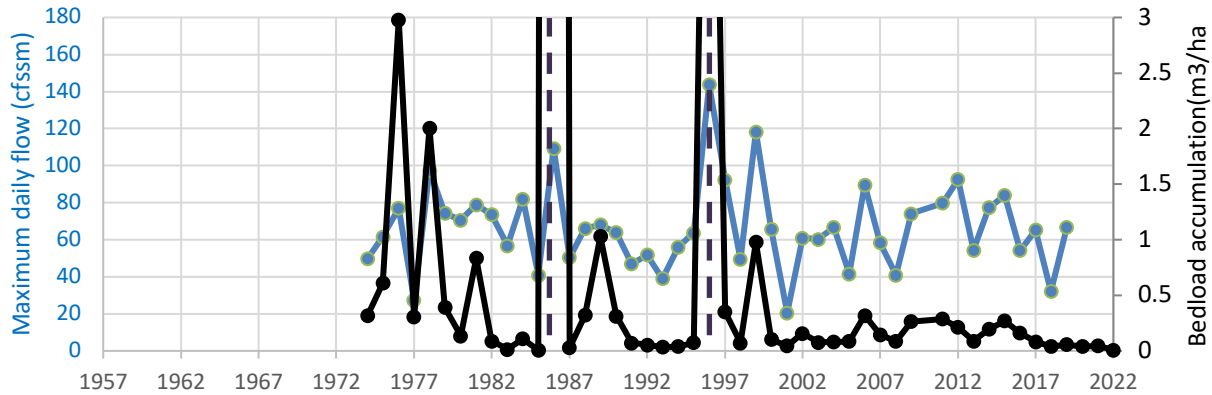
Figure 14 (a). Long-term trends in annual bedload export (m³/ha/yr) (black) and maximum daily flow (cfssm) (blue) by water year (October of prior year to September of current year) from small catchments in the Andrews Forest. (a) WS01, 1957 – 2022, (b) WS02, 1957 – 2022, (c) WS03, 1957- 2022, (d) WS09, 1974-2022, (e) WS10, 1974-2022. Study catchment characteristics are in Table 2. Blue boxes and vertical dashed blue lines indicate logging and roads, vertical brown dashed lines indicate debris flows, and vertical red dashed lines indicate fire.
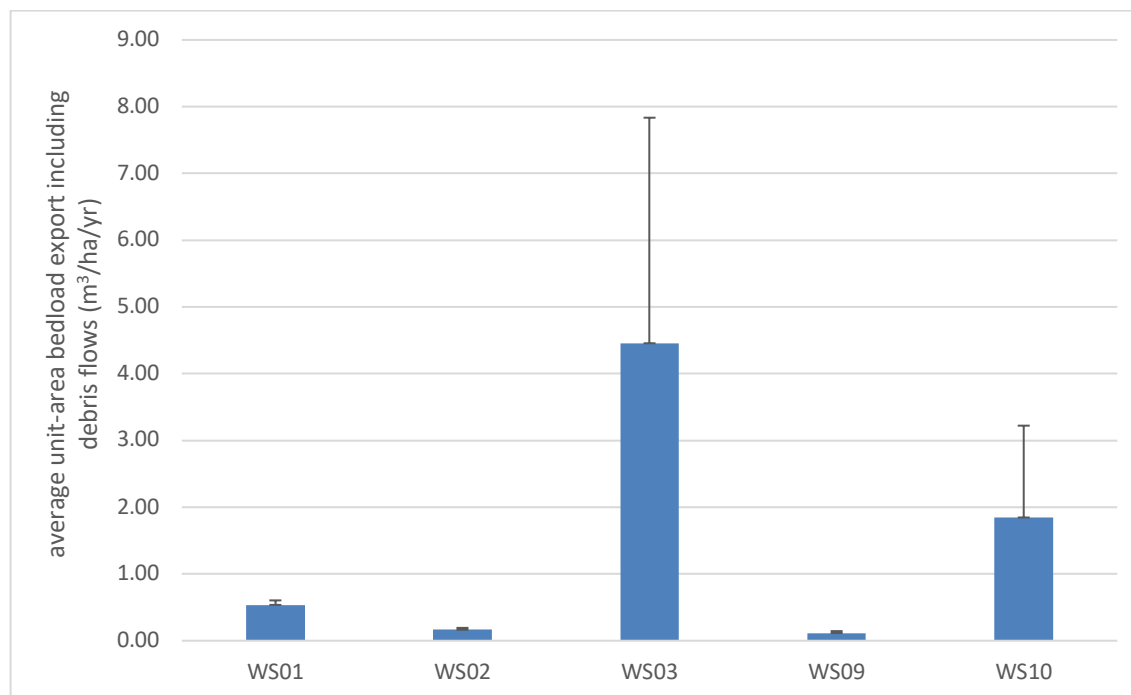
Figure 15. Mean and standard errors of the annual unit-area bedload export, including debris flows, for the full period of record, for study catchments. Error bars show the standard error associated with the mean unit-area bedload export for each catchment.

4.1.2 Bedload export response to logging and roads by 5-yr periods

Unit-area bedload export (excluding debris flows) increased after logging in two 100% clearcut catchments (WS01, WS10) and one patch-cut catchment with roads (WS03) relative to their reference catchments (WS02, WS09) (Figure 16). Initial post-logging bedload export values (logged minus unlogged) were least in the driest year on record (1977). Differences in post-logging bedload export values (logged mine unlogged, excluding debris flows) were greatest in wet years or years with high magnitude maximum daily flows (e.g., 1972, 1986, 1996, and 1999) (Figure 16).

Differences in post-logging bedload export values (logged minus unlogged) remained relatively high from the patch-cut catchments with roads (WS03) after debris flows in 1996. However, bedload export (excluding debris flows) were less at the patch-cut catchment with

roads (WS03) than from the reference catchment (WS02) after debris flows in WS03 in 1996. Also, export values (excluding debris flows) were less at the clearcut catchment (WS10) after debris flows in 1986 and 1996 (Figure 16).

Starting in 2021, unit-area bedload export was higher at WS09 (burned) than WS10 (unburned). There was little change in bedload export after the wildfire in WS01 or WS02, based on the relationship of WS01 (burned) or WS02 (burned) to WS03 (burned). Over the full period of record prior to the September 2020 wildfire, bedload export remained higher at the 100% clearcut catchments (WS01, WS10) than their reference catchments (WS02, WS09), based on the 7-year running mean of differences in bedload export, logged minus unlogged (Figure 16).

Over the full period of record, the average bedload export became lower at the patch-cut catchment with roads (WS02) relative to its reference catchment (WS02) starting in 1976, based on the 7-year running mean of differences in bedload export, logged minus unlogged. The only exception to this long-term reduction in bedload export from WS03 was high bedload export from WS03 relative to WS02 during the flood event of 1999. Over the full period of record, the 100% clearcut catchments (WS01, WS10) delivered more sediment as bedload export than their reference catchments (WS02, WS09), based on the difference in unit-area bedload export excluding debris flows, logged minus unlogged catchments. Bedload export excluding debris flows was higher from the 100% clearcut catchment without debris flows (WS01) than the 100% clear-cut catchment with debris flows (WS10), based on the long-term difference in unit-area bedload export excluding debris flows, logged minus unlogged catchments (Figure 16).

WS01.Bedload export increased in WS01 during 11 and decreased in 1 of the 12 five-year post-logging periods. Percent increases ranged from 3762 to 259 %, while the percent decrease was -21%. Bedload export decreased by 21% during harvest in WS01 and increased by

3762 % 1 to 5 years after logging and broadcast burn. Bedload export was lower than during pre-treatment in only one year. Following treatment there was at least a 259% increase in bedload export. Fifty-one to 55 years following the broadcast burn in 1967 there was still an observed 298% increase in bedload export (Table 5).

WS03. Bedload export increased in WS03 during 7 and decreased in 6 of the 13 five-year post-logging periods. Percent increases ranged from 27,300 to 14%, while percent decreases ranged from -76 to -14%. Time periods in which debris flows occurred had the largest percent increases (1964 to 1968 and 1994 to 1998). Percent decreases were observed 5-10 years after the first round of debris flows, then 10 – 25 years after the second round of debris flows (Table 5).

WS09. Unit-area sediment export from WS09 increased by 7 to 9 times (0.684 m^3/ha in 2021 and 0.852 m^3/ha in 2022) compared to pre-wildfire averages (1974 – 2019) (Table 4).

WS10. Bedload export from WS10 increased in four of eleven 5-year time periods after logging, relative to the reference catchment (WS09). Percent increases coincided with periods that experienced debris flows and ranged from 2148 to 21%. Percent decreases relative to WS09 ranged from -99 to -28%, and were greatest in 2021-2022 after wildfire increased bedload export from WS09 (Table 5).

Table 5. Percent change in bedload export from logged catchment vs. reference catchment for five-year periods after logging in three pairs of small catchments, Andrews Forest, 1957-2022. % change is the change relative to the pre-treatment ratio (i.e., WS01/WS02, WS03/WS02, WS10/WS09).

	Years	WS01	WS02	WS01/WS02	% change
Pre-harvest	1957-1961	5.3	7.7	0.7	0
Harvest	1962-66	6.8	12.3	0.5	-21
1-5 yrs after	1967-71	94.2	3.5	26.9	3762
6-10 yrs after	1972-76	142.6	10.3	13.9	1890
11-15 yrs after	1977-81	64.6	5.0	13.0	1760
16-20 yrs after	1982-86	62.7	10.6	5.9	747
21-25 yrs after	1987-91	36.9	5.5	6.8	871
26-30 yrs after	1992-96	79.2	20.6	3.8	452
31-35 yrs after	1997-01	42.5	12.3	3.5	395
36-40 yrs after	2002-06	37.4	14.9	2.5	259
41-45 yrs after	2007-11	36.0	12.3	2.9	318
46-50 yrs after	2012-16	46.2	8.0	5.8	728
51-55 yrs after	2017-22	15.9	5.7	2.8	298
	Years	WS02	WS03	WS03/WS02	% change
Pre-harvest	1957-1962	6.8	9.2	1.3	0
Harvest	1963	2.9	9.1	3.1	133
1-5 yrs after	1964-68	11.3	4163.6	368.5	27300
6-10 yrs after	1969-73	8.3	43.4	5.2	288
11-15 yrs after	1974-78	7.3	12.9	1.8	30
16-20 yrs after	1979-83	6.5	7.6	1.2	-14
21-25 yrs after	1984-88	9.0	8.9	1.0	-27
26-30 yrs after	1989-93	5.9	9.0	1.5	14
31-35 yrs after	1994-98	22.2	1550.1	69.8	5092
36-40 yrs after	1999-03	11.2	28.9	2.6	92
41-45 yrs after	2004-08	14.6	4.7	0.3	-76
46-50 yrs after	2009-13	15.0	6.1	0.4	-70
51-55 yrs after	2014-18	7.2	2.5	0.3	-74
56-60 yrs after	2019-22	4.9	2.0	0.4	-70
	Years	WS09	WS10	WS10/WS09	% change
Pre-harvest	1974	0.5	3.2	6.4	0
Harvest	1975	0.8	6.2	7.8	21

1-5 yrs after	1976-80	0.9	11.8	12.8	100
6-10 yrs after	1981-85	0.8	2.1	2.6	-59
11-15 yrs after	1986-90	0.9	135.2	143.9	2148
16-20 yrs after	1991-95	0.3	0.6	2.0	-69
21-25 yrs after	1996-00	2.6	20.0	7.6	20
26-30 yrs after	2001-05	0.2	0.9	3.8	-40
31-35 yrs after	2006-10	0.6	2.1	3.5	-46
36-40 yrs after	2011-15	0.5	2.1	4.6	-28
41-45 yrs after	2015-20	0.4	1.1	2.8	-56
46-50 yrs after	2021-22	6.6	0.3	0.0	-99

(a)
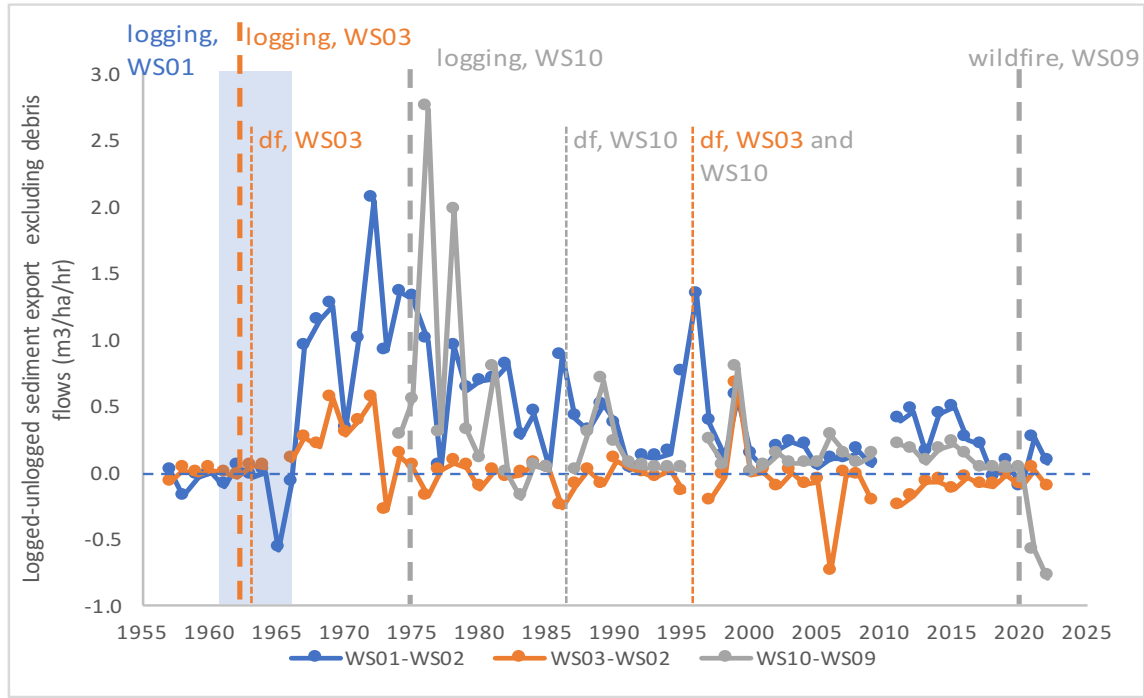
(b)
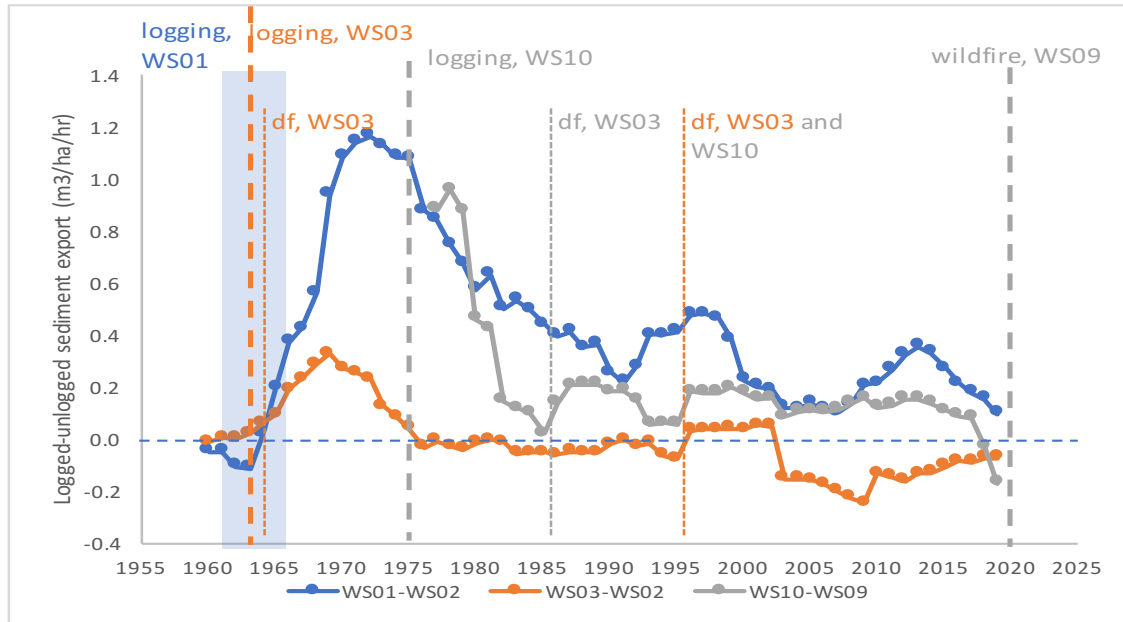
(c)
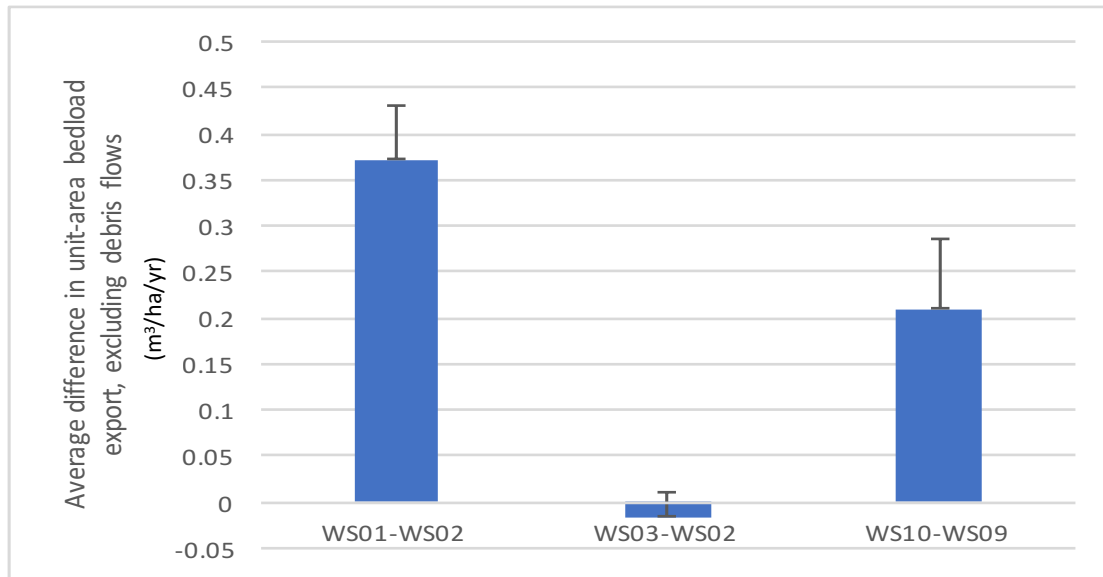
Figure 16. Differences in unit-area bedload export excluding debris flows, logged minus unlogged catchments (a) by water year, (b) 7-year running mean of differences, and (c) mean and standard errors of the differences over the full period of record. See Table 6.

Table 6. Differences in annual unit-area bedload export (m³/ha/yr), excluding debris flows, logged catchment minus reference catchment, for three pairs of small catchments in the Andrews Forest, 1957-2022. -- indicates data not collected; df = debris flow amount omitted.

Year	WS01-WS02	WS03-WS02	WS10-WS09	WS01-WS02	WS03-WS02	WS10-WS09
1957	0.00	-0.08	--			
1958	-0.19	0.01	--			
1959	-0.04	-0.02	--			
1960	-0.01	0.01	--	-0.05	-0.01	
1961	-0.11	-0.01	--	-0.05	0.00	
1962	0.04	-0.04	--	-0.11	0.00	
1963	-0.04	0.04	--	-0.11	0.02	
1964	0.00	0.03	--	0.02	0.06	
1965	-0.58	df	df	0.20	0.09	
1966	-0.09	0.09	--	0.37	0.19	
1967	0.93	0.25	--	0.42	0.23	
1968	1.13	0.19	--	0.56	0.29	
1969	1.25	0.55	--	0.94	0.32	
1970	0.32	0.28	--	1.08	0.27	
1971	0.99	0.37	--	1.14	0.25	
1972	2.04	0.55	--	1.16	0.23	
1973	0.91	-0.29	--	1.13	0.12	
1974	1.34	0.12	0.26	1.08	0.08	
1975	1.30	0.03	0.53	1.08	0.04	
1976	0.98	-0.19	2.73	0.87	-0.03	
1977	0.03	0.00	0.29	0.84	-0.01	0.88
1978	0.94	0.06	1.96	0.75	-0.03	0.96
1979	0.61	0.03	0.30	0.68	-0.04	0.88
1980	0.67	-0.13	0.10	0.57	-0.02	0.46
1981	0.69	0.00	0.78	0.63	-0.01	0.42
1982	0.80	-0.05	-0.02	0.50	-0.01	0.14
1983	0.26	-0.02	-0.20	0.53	-0.06	0.12
1984	0.44	0.06	0.04	0.50	-0.05	0.10
1985	0.02	0.01	0.01	0.44	-0.05	0.02
1986	0.86	-0.27	df	0.40	-0.06	0.14
1987	0.40	-0.11	0.00	0.41	-0.05	0.21
1988	0.30	0.00	0.29	0.35	-0.05	0.21
1989	0.50	-0.10	0.68	0.36	-0.05	0.21
1990	0.36	0.08	0.22	0.25	-0.02	0.18
1991	0.02	0.03	0.05	0.22	-0.01	0.19
1992	0.11	-0.01	0.03	0.28	-0.03	0.15
1993	0.10	-0.04	0.02	0.40	-0.02	0.06

Year						
1994	0.13	0.00	0.02	0.40	-0.07	0.06
1995	0.74	-0.15	0.01	0.41	-0.08	0.06
1996	1.33	df	df	0.48	0.03	0.18
1997	0.37	-0.22	0.23	0.48	0.04	0.18
1998	0.11	-0.04	0.04	0.47	0.04	0.18
1999	0.56	0.65	0.78	0.38	0.04	0.20
2000	0.13	-0.02	-0.01	0.23	0.03	0.18
2001	0.02	0.00	0.03	0.20	0.05	0.15
2002	0.17	-0.12	0.13	0.19	0.05	0.16
2003	0.22	-0.01	0.06	0.12	-0.15	0.08
2004	0.19	-0.10	0.06	0.12	-0.15	0.10
2005	0.03	-0.07	0.06	0.14	-0.16	0.11
2006	0.09	-0.75	0.26	0.12	-0.17	0.11
2007	0.09	-0.03	0.13	0.10	-0.20	0.11
2008	0.15	-0.03	0.06	0.13	-0.23	0.14
2009	0.05	-0.23	0.11	0.20	-0.25	0.16
2010	--	--	--	0.21	-0.14	0.12
2011	0.38	-0.26	0.20	0.27	-0.15	0.13
2012	0.46	-0.19	0.17	0.32	-0.16	0.15
2013	0.14	-0.08	0.07	0.35	-0.13	0.15
2014	0.42	-0.08	0.17	0.33	-0.13	0.13
2015	0.48	-0.13	0.20	0.27	-0.11	0.11
2016	0.24	-0.05	0.12	0.22	-0.08	0.09
2017	0.20	-0.10	0.02	0.18	-0.09	0.08
2018	-0.05	-0.11	0.02	0.15	-0.07	-0.03
2019	0.08	-0.03	0.02	0.09	-0.07	-0.17
2020	-0.12	-0.11	0.02			
2021	0.25	0.01	-0.59			
2022	0.06	-0.12	-0.80			
ave	0.37	-0.02	0.21			
SE	0.06	0.03	0.08			
min	-0.58	-0.75	-0.80			
max	2.04	0.65	2.73			

4.1.3. Flow frequency analysis results and relation of bedload export to high flows (max daily flows and bankfull flows)

Log-Pearson III flood-frequency analysis indicated that WS01 and WS10 had the highest discharge for all flow probabilities. WS03 and WS09 had relatively lower flows. WS02 discharge was intermediate, except for the lowest probability flow levels, where it has the highest discharge (Figure 13).

The strongest relationship of bedload export to maximum daily flow occurs in WS02 ($R^2 = 0.58$) while the weakest relationship occurs in WS03 ($R^2 = .016$) (Table A-1 appendix). Annual bedload export over the period of record was weakly related to maximum daily streamflow in WS01 ($R^2 = 0.32$), WS09 ($R^2 = 0.35$) and WS10 ($R^2 = 0.13$).

The strongest predictors for bedload export based on multiple regression varied among the catchments. Maximum mean daily flow was a significant independent variable in WS01, WS02, WS03, and WS09 (p-value < 0.05). In WS02, WS09, and WS10 days above bankfull was a significant variable. The volume of flow that exceeded bankfull annually was a significant variable in WS02 and WS10 (p-value < 0.05), and close to significant in WS09 (p-value = 0.06) (Table 7). See Appendix Table A-1 for a summary of the independent parameters used for the multiple linear regressions (the annual maximum daily flow, 1.25 RI bank full flow, the volume of flow over bank full, and the number of days that bank full flow was exceeded).

Table 7. Relationship of annual bedload export to maximum daily flow, days of flow above bankfull (1.25-year return interval) flow, and volume above bankfull flow, based on multiple linear regression. $* = p < 0.05$, $** = p < 0.01$, $*** = p < 0.001$.

	WS01	WS02	WS03	WS09	WS10
Multiple R	0.57	0.83	0.54	0.69	0.77
R^2	0.33	0.69	0.29	0.48	0.59
Max daily flow	0.01**	0.003*	0.004*	0.004*	0.02
Days > bank full	0.04	-0.05***	0.006	0.004*	-0.44**
Volume > bank full	-0.0004	0.003***	0.00002	-0.03	0.03***

4.1.4. Change in relationship of bedload to max daily flows for selected post-logging decades, by catchment

Forest harvest in WS01 increased the annual bedload export controlling for maximum daily flow. For an equal magnitude max daily flow, bedload export was highest in the first ten years after logging, followed by 30 to 50 and 10 to 20 years post treatment. During the clear cut and burn treatment period bedload export was higher than the pre-treatment period, but less than the 10-, 20-, and 30-50-years post treatment periods. Although the slope for all these lines is similar, the main difference between the treatment groups can be seen in the intercept value (Figure 17a). In WS02 (reference) the relationship of bedload accumulation to maximum daily flow did not change for different time periods (Figure 17b). Based on the natural log of the detection limit, the pretreatment relationship is significantly different than all post-treatment periods other than the logging period (1962 to 1967).

In WS03, when debris flows are excluded, there was little change in bedload export after logging and roads, controlling for maximum daily flow. However, the slopes of the regression relationships changed over time. The 1957 – 1963 period had the shallowest slope. From 1964 – 1968 the slope increased. Thirty years after

treatment, the slope of the relationship was steeper than before logging (1957 – 1963) but shallower than just after logging (1964 –1968) and the intercept was higher than during treatment and 50 years post treatment. Fifty years after logging, the slope and intercept of the relationship was very similar to the pre-logging (1957 – 1963) period. With increasing years post-management, a given magnitude maximum daily flow produced less bedload export, compared to immediately after logging (Figure 17c).

In WS09 the relationship of bedload accumulation to maximum daily flow did not change for different time periods (Figure 17d).

In WS10, there are clear differences in the relationship between maximum daily flow and annual bedload accumulation through time. Ten to 20 years and 30 to 50 years after the clear cut, a given maximum daily flow produced less bedload export, compared to the first five years after the clear cut (Figure 17e).

(a) WS01
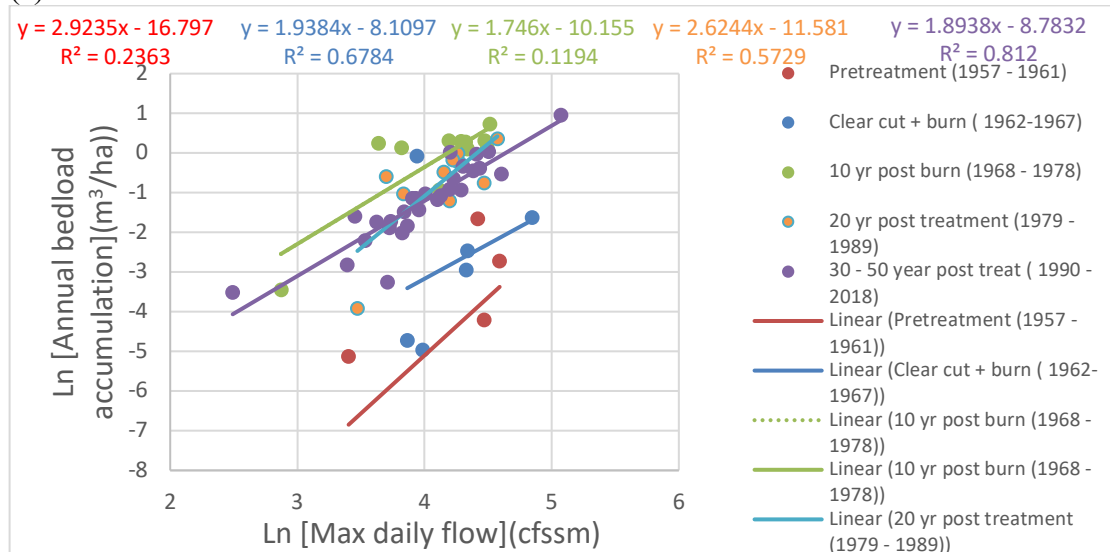
(b) WS02
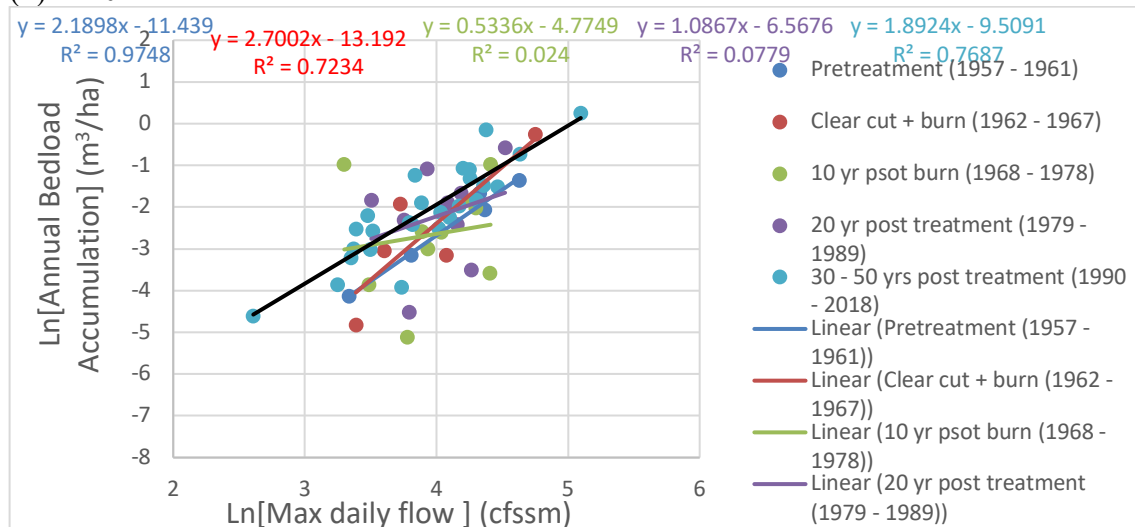
(c) WS03
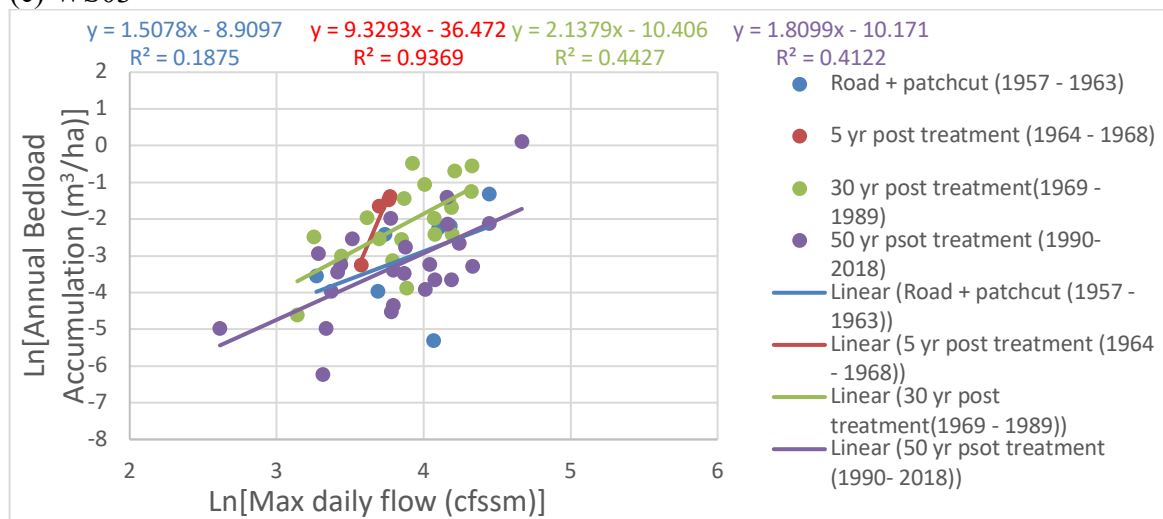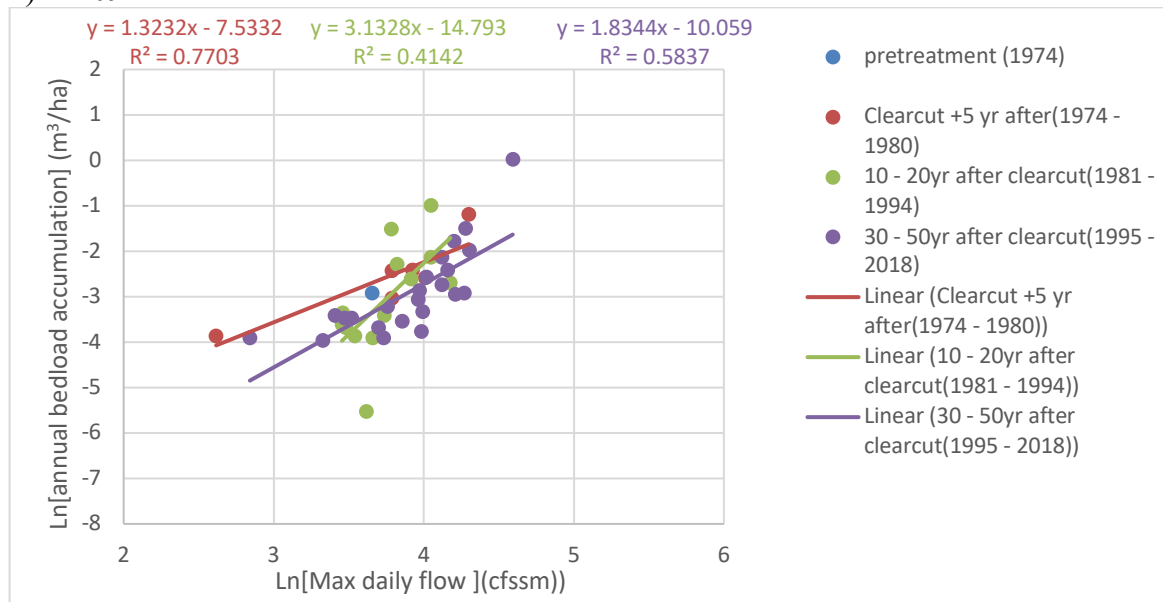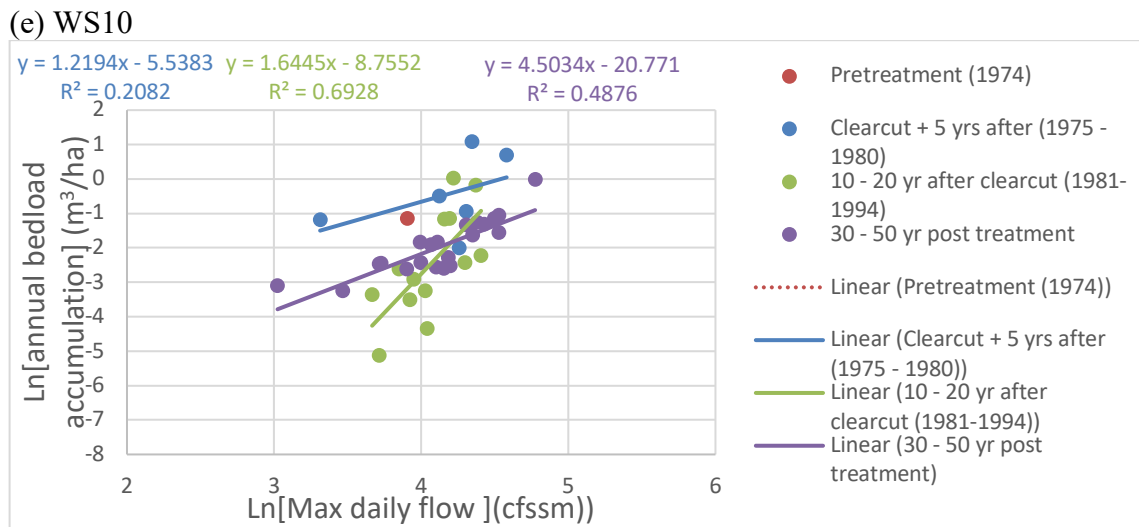
d) WS09

(e) WS10

Figure 17. Relationship of annual bedload, excluding debris flows, to maximum daily flows in selected post-logging periods for (a) WS01, (b) WS02, (c) WS03, (d) WS09, and (e) WS10.

4.1.5. Change in relationship of bedload to max daily flows for WS01, WS02, and WS03.

Logging altered the relationship of annual bedload export to maximum daily flow in WS01 throughout the post-logging period, but the relationships did not change in WS02 (reference old-growth forest) or WS03 when debris flow events were excluded (25% patch cut with roads). Before logging, WS01 (yellow) had lower bedload export than WS02 (green) and WS03 (blue) controlling for maximum daily flow, but bedload export increased for 50 years after logging for all sizes of flows in WS01 (red) (Figure 18). In contrast, bedload export excluding debris flows did not increase after logging and roads in WS03 (blue) (Figure 18).
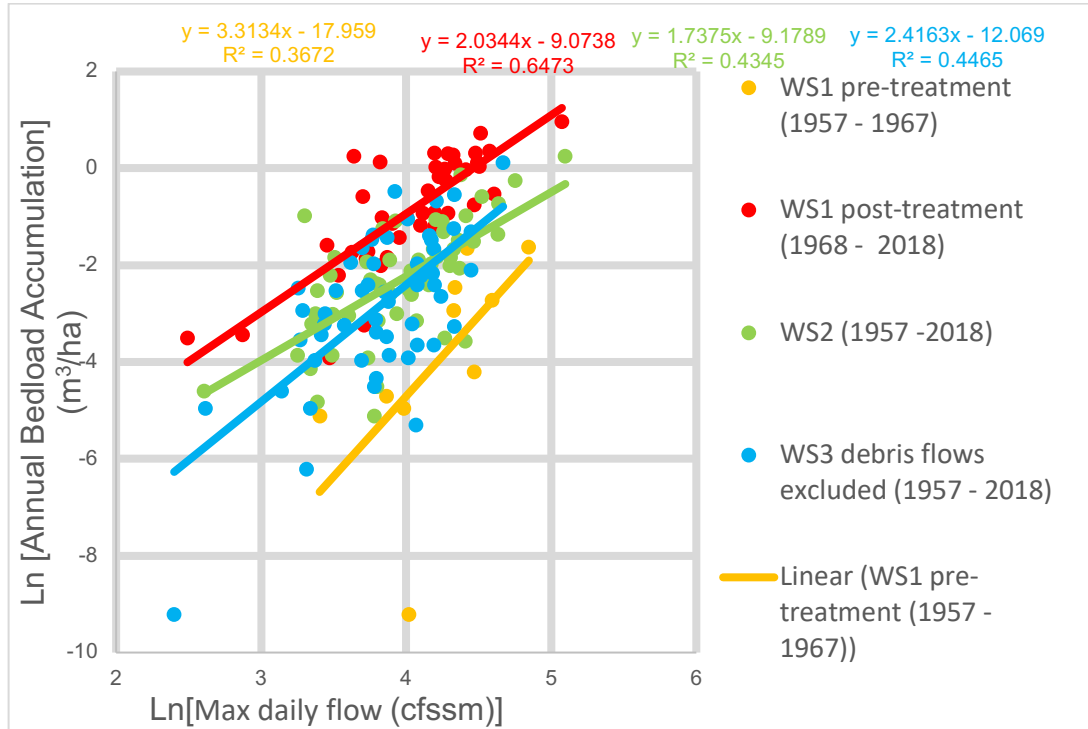
Figure 18. Changing relationship of bedload to max daily flow before and after logging at WS01, compared with WS02 and WS03.

4.2 Post-fire Bedload Characteristics, WS09 and WS10

4.2.1 Grain size distributions WS09 and WS10 bedload export

Grain size distributions of bedload export subsamples changed over the first two years after wildfire in WS09, but there were no changes in bedload export grain sizes from WS10. The bedload export sample from WS09 in the first fall after wildfire (October –December 2020) was composed of mostly fine-grained sediment (68%) and large organic matter (20%). In the first winter and spring after wildfire (February - May 2021), the sample was predominantly coarse grained mineral material (57%) and material within the 2-4mm size class (25%), with few large organics (<5%) and little fine-grained sediment (12%). The proportions of grain sizes were consistent for WS10 through time, although there was a small increase in fine-grained sediment in the May 2021 – June 2022 deposit (35% vs 31%) and a small increase in large mineral material in the deposit from October – December 2020 (32% vs 21%). By May 2021 – June 2022, the grain size distribution of the bedload export from WS09 was comparable to WS10 although there was more >4 mm and less 2-4 mm mineral material (Table 8).

Table 8. Particle size distribution of samples from WS09 and WS10 over the period October 2020 to August 2022.

		WS09				WS10
		Oct-Dec 2020	Jan-May 2021	Jun-Aug 2022	Oct 2020- Aug 2022	Oct 2020- Aug 2022
	n	6	10	6	22	9
weight (g)	ave	274	332	327	315	271
	stdev	113	88	50	87	124
<2 mm (g)	ave	174	52	176	99	121
	stdev	99	19	50	76	37
2-4 mm (g)	ave	11	79	24	46	52
	stdev	19	91	16	69	28
>4 mm (g)	ave	89	201	200	170	98
	stdev	34	117	74	100	89
ave as %	<2 mm	64	16	31	37	45
	2-4 mm	4	24	7	12	19
	>4 mm	33	61	61	52	36
stdev as %	<2 mm	36	6	15	24	14
	2-4 mm	7	27	5	22	10
	>4 mm	13	35	23	32	33
SE as %	<2 mm	15	2	6	5	5
	2-4 mm	3	9	2	5	3
	>4 mm	5	11	9	7	11

Grain size distributions averaged over the full period (October 2020 to June 2022) did not differ between WS09 and WS10. Fine- and coarse- grained sediment dominated the export at both sites (more than 80% of export). The 2-4 mm size fraction was no more than 20% of the total bedload in either catchment (Figure 19).
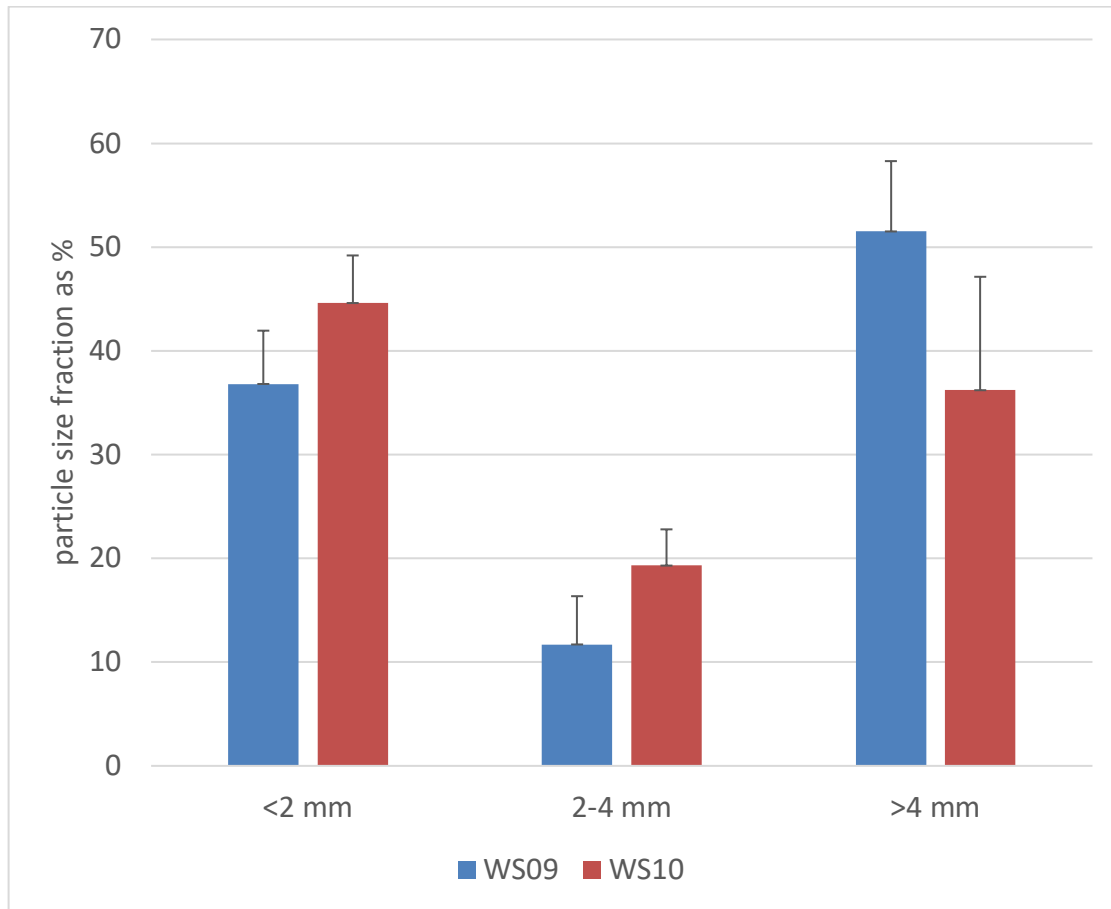
Figure 19. Mean and standard errors of the grain size distributions of bedload export, October 2020 to August 2022, WS09 and WS10.

There are clear variations in the particle size distribution of the bedload export from WS09 through time. The fine-grained sediment was greatest in early fall (>60%), decreased in the winter of 2020 (<20%) then increased again in the second year after wildfire (31%). The coarse-grained fraction was lowest in the early fall of the first-year post fire (33%) but increased significantly in the first year and second year after wildfire (61%). Coarse-grained sediment made up the largest percentage of bedload export in the winter of the first-year post-wildfire. The 2-4mm fraction was 4% of the bedload export in early fall of the first-year post-fire, 24% in the winter of the first year, and 7% in the second water year post wildfire (Figure 20, Table 8).
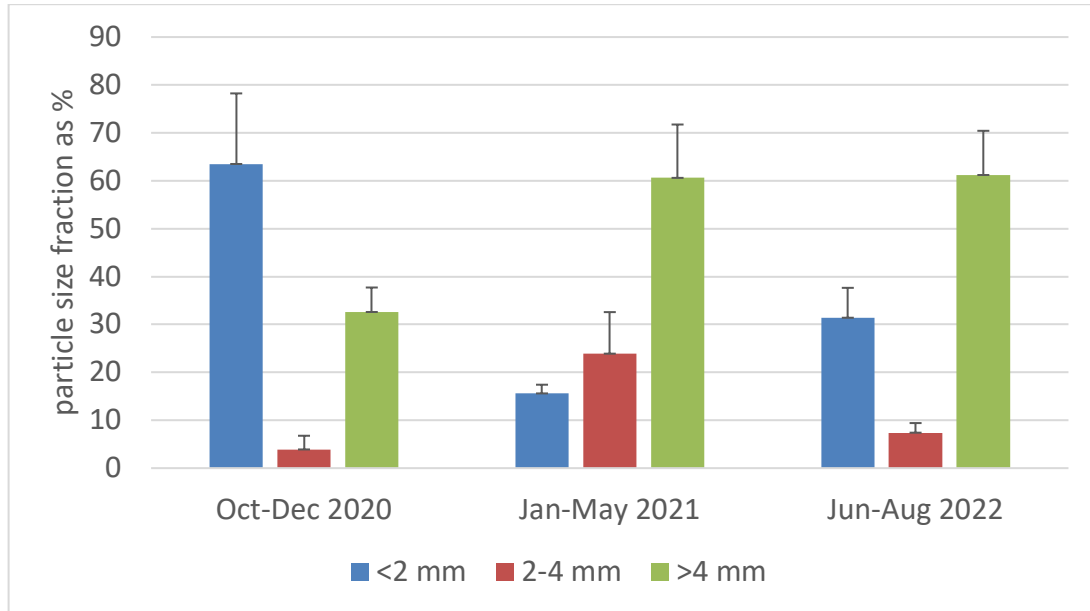
Figure 20. Mean and standard errors of the grain size distributions of bedload export for three time periods after the September 2020 wildfire in WS09.

4.2.2 Organic percent of WS09 and WS10 of bedload export

Organic material was a similar fraction of the total in WS09 and WS10 for the <2 and >4 mm fractions, but WS09 had significantly lower organics present in the 2-4 mm size fraction (Figure 21, Table 9).
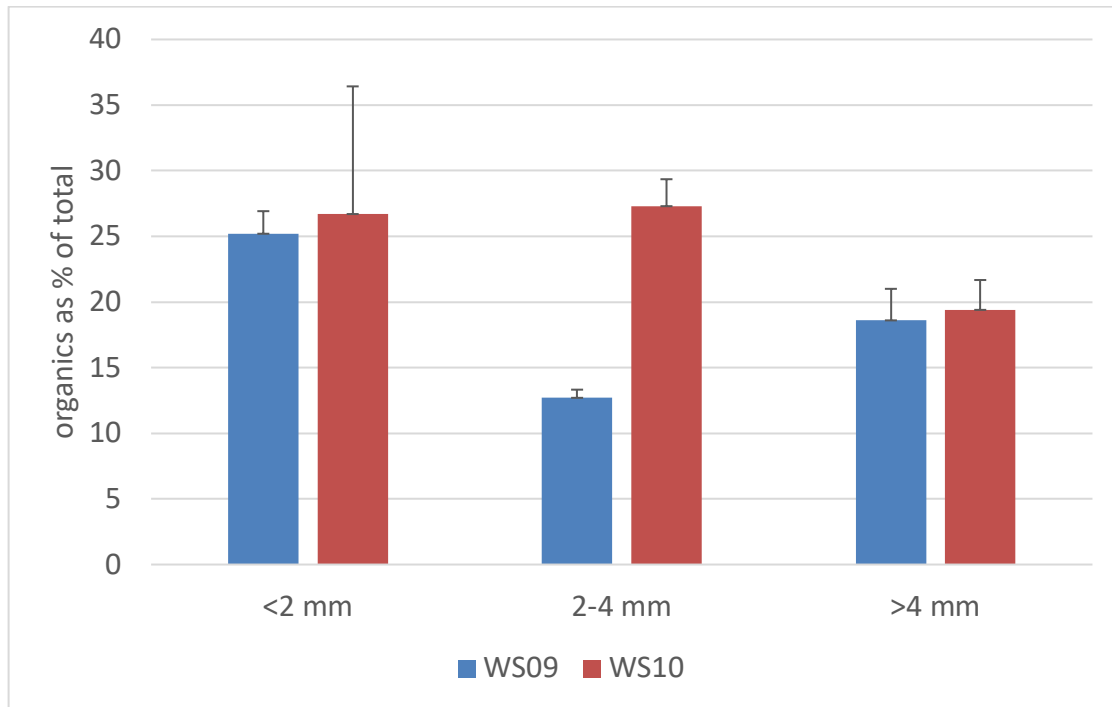
Figure 21. Mean and standard errors of the organic material as percent of total sample, WS09 and WS10, October 2020 to August 2022.

Table 9. Organic and mineral proportions of particle size fractions from WS09 and WS10, October 2020 to August 2022. Values are from dried samples.

| | | WS09 | | | | WS10 |
		Oct-Dec 2020	Jan-May 2021	Jun-Aug 2022	Oct 2020-Aug 2022	Oct 2020-Aug 2022
n of samples		6	10	6	22	9
All fractions (g)	ave	274	332	327	315	271
	stdev	113	88	50	87	124
<2 mm (g)						
Organic	ave	53	6	28	25	97
	stdev	29	3	12	25	79
Mineral	ave	9	66	16	40	266
	stdev	16	78	10	61	205
2 - 4mm (g)						
Organic	ave	2	6	8	6	43
	stdev	4	12	6	9	17
Mineral	ave	9	66	16	40	114
	stdev	16	78	10	61	41
>4 mm						
Organic	ave	73	3	39	6	57
	stdev	32	4	21	36	19
Mineral	ave	16	180	39	139	237
	stdev	3	128	65	115	36
Organics (%)	<2 mm	31	12	27	25	27
	2-4 mm	18	9	32	13	27
	>4 mm	82	1	19	19	19
stdev	<2 mm	11	1	4	8	29
	2-4 mm	1	4	2	3	6
	>4 mm	12	1	6	11	7
SE	<2 mm	4	0	2	2	10
	2-4 mm	1	1	1	1	2
	>4 mm	5	0	3	2	2

Organic as % of total was highest in the >4mm fraction, but only in the first period after the wildfire (Figure 22, Table 9). Organics as a percent of total in the <4mm fractions were highest in the first fall after fire, declined in the first winter after fire, then increased again in the second year after fire (Figure 22). Organics as a percent of total in the 2-4 mm fraction were highest in the second year (Figure 22, Table 9). The character of the bedload export in WS09 had considerable variation through time. Just a few months after the wildfire, the material was split relatively evenly between organic and mineral material (47% organic, 53% mineral). Up to a year after the wildfire the export shifted to predominately mineral material (95%), with a very small percentage being organic (5%). In the second year after the wildfire the bedload was about 23% organic and 77% mineral, which is similar to the organic vs mineral percentages of the bedload export sampled in WS10 (Figure 22, Table 9)
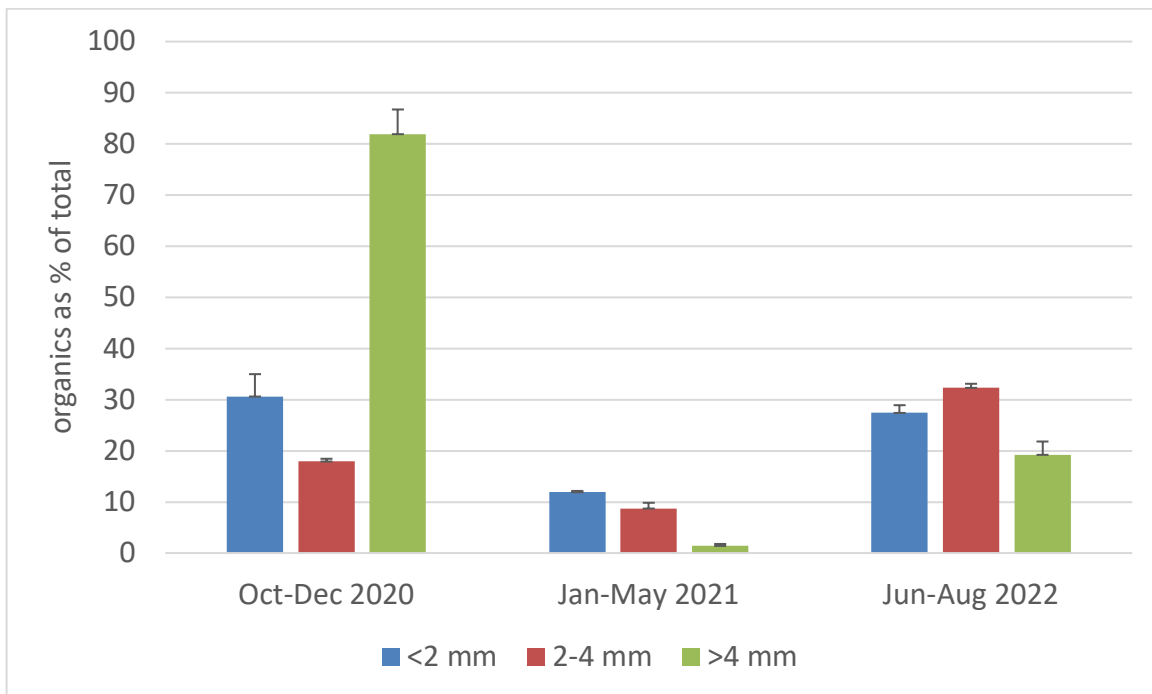
Figure 22. Mean and standard errors of the organic material as percent of sample in bedload export for three time periods after the September 2020 wildfire in WS09.

Charred organic material represented 22% of the >4mm organic material in bedload export from WS09 after wildfire in October- December 2020, 48% in January – May 2021, and 19% in May 2021 – June 2022. However, charred organic material represented 25 % of >4mm mineral and organic bedload export from WS09 after wildfire in October – December 2020, 24% in January – May 2021, and 9% in May 2021 – June 2022 (Figure 23, Table 10).

Char was a larger fraction of organic material in the coarse (> 4mm) fraction exported in the first winter after wildfire, compared to the first fall or the second year after wildfire in WS09. Overall, char decreased as a proportion of the >4mm fraction in the second year compared to the first year after the wildfire (Figure 23, Table 10).
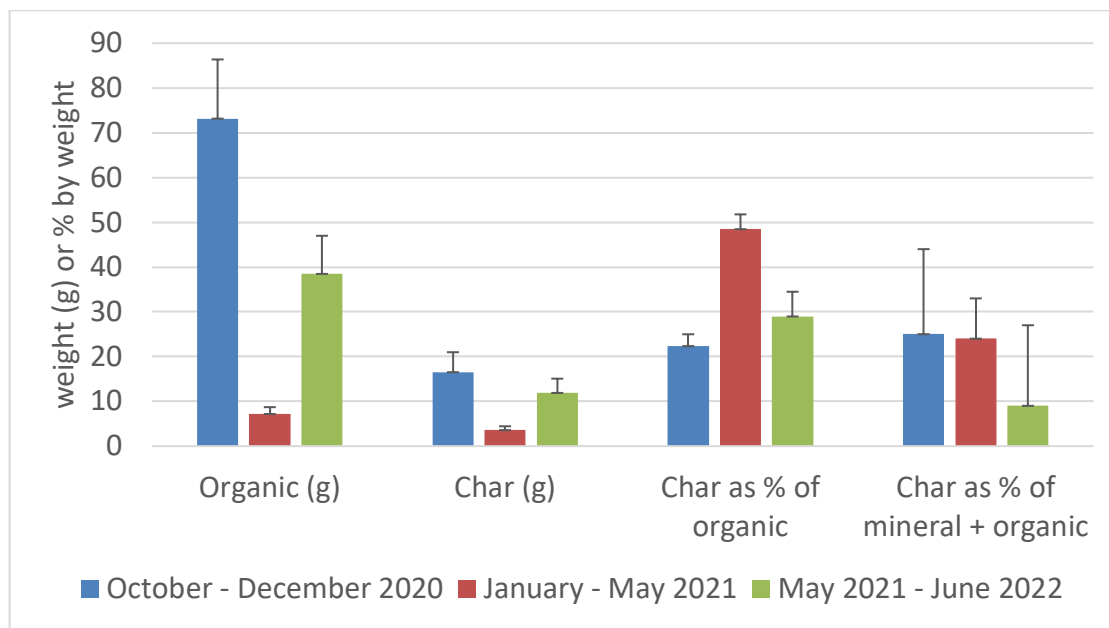
Figure 23. Mean and standard errors of the weight of organic material and char in >4 mm fraction of bedload export from WS09, and char as percent of >4 mm organic fraction and >4 mm mineral plus organic fraction, for three time periods after wildfire. See Table 10.

Table 10. Charred organic matter as percent of total organic matter in the >4 mm fraction, WS09, three time periods: October-December 2020, January-May 2021, and May 2021-June 2022.

Sample no.	Organic weight (g)	Charred organic weight (g)	Percent charred
October - December 2020			
1	128	38	30
2	73	15	20
3	43	10	23
4	93	11	12
5	53	15	28
6	49	10	21
January - May 2021			
1	4	1	39
2	10	5	48
3	6	3	52
4	9	5	53
May 2021 - June 2022			
1	53	13	24
2	16	5	29
3	51	22	43
4	39	18	46
5	62	13	22
6	10	1	11
October - December 2020			
ave	73	17	22
SE	13	4	3
January - May 2021			
ave	7	4	48
SE	2	1	3
May 2021 - June 2022			
ave	38	12	29
SE	9	3	5

4.2.3 Field surveys of channel and hillslope landforms (WS09 and WS10)

In summer 2022, WS09 (mature and old growth forest, burned in 2020) had more pieces of wood, larger wood pieces, and greater total wood volume, as well as more sediment wedges accumulated upstream of large wood, larger volumes of sediment wedges, and greater total sediment storage by wood, compared to WS10 (clearcut in 1975, debris flows in 1986 and 1996, not burned in 2020) (Table 11).

Table 11. Large wood and sediment in the first 100 m of channel upstream of the gages in WS09 and WS10, based on a field survey of conducted in summer 2022.

	WS09	WS10
Number of near of instream large wood pieces	44	36
Average volume per wood piece (m³)	181.4	28.3
Total measured wood volume (m³)	7802	1019
Number of sediment wedges identified	29	6
Average volume of sediment wedge (m³)	1.3	0.7
Total volume of stored sediment wedges (m³)	36.6	4.4

5. Discussion

5.1 Sediment budget in undisturbed forest

In undisturbed steep, forested catchments, bedload export depends on geomorphic processes and landforms. Sediment is contributed from hillslopes to channels through slow moving soil creep, biological activity (bioturbation), root-throw from individual treefall, and organic litterfall. Sediment also is contributed to channels from episodic mass movements events, such as debris slides, or chronic mass movements, such as slumps or deep-seated earthflows. Sediment moving along the hillslope can be trapped within depressions of pit-mound topography, downed wood, or understory vegetation. Sediment that reaches the channel may be stored for

long periods of time, transported by streamflow as bedload export, or exported by

mass movement processes (debris flows). Episodic mass wasting events such as

debris slides and debris flows can occur in undisturbed forests, but the frequency is

not as high as disturbed forests (Snyder 2000) (Figure 24).
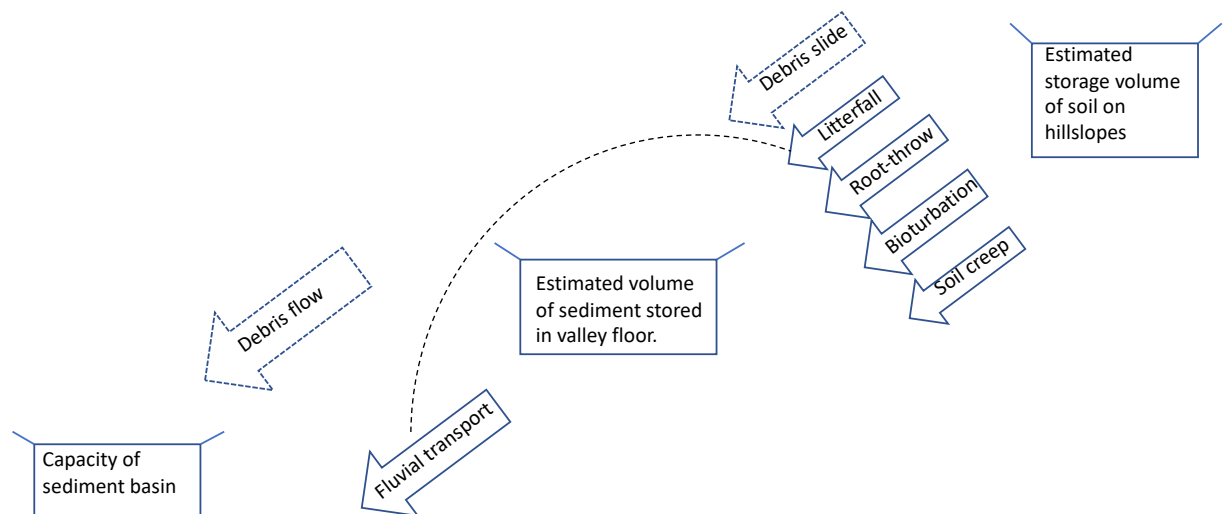
Figure 24. Schematic diagram of storages and flows of sediment in the reference
catchments (WS02 and WS09) before the wildfire (2020).

5.2 Complex interactions and their impact on sediment budget

This study demonstrates that bedload export varies over multiple decades

based on multiple factors, including inherent geomorphic processes (e.g., slumps, soil

creep, ravel, fluvial transport etc.), landforms (e.g., valley width, slope, tributary

slope gradient), disturbances (logging, wildfire, roads), and ecological and human

responses to disturbance (Figure 1). In time periods following forest disturbance

(logging, roads, wildfire) bedload export generally increased, although the magnitude of that increase was variable, and varied among catchments based on their geomorphic processes and landforms (Figures 24 to 27). Various examples of how these factors varied between sites, and how the factors interacted to produce different bedload export are discussed below.

WS01. Disturbance events, such as clearcuts and slash burning can increase sediment production on hillslopes (Brown and Krygeier 1971) especially through increases in dry ravel (Bennet 1982). Sediment produced from the slash burning event can deposit in different zones (e.g. hillslope, channel), depending on the size and shape of the sediment, sediment connectivity (Brunsden and Thornes, 1979; Harvey, 2001; Heckmann and Schwanghart, 2013), and the amount of roughness elements on the slope that retard the transit of sediment (DiBiasee et al., 2017). Sediment can have relatively short transit times from the hillslope to a catchment outlet, or it can remain stored for many years. Roughness elements within a channel also influence the transit time of sediment from the hillslope to basin outlet (Rice and Church, 1996; Hogan et al., 1998). After the 100% clear-cut and broadcast burn, in-stream wood was manually cleaned (Figure A-12). A path was cleared in the middle of the valley to enable the passage of streamflow and sediment following the disturbance. The large export values immediately after the broadcast burn could be due to the stream cleaning. Over time as the coarse wood fragments were re-organized, the transit time of the sediment from hillslope to outlet likely increased, reducing bedload export.

WS01 has the widest valley floor of all the study sites, a shallow stream gradient, and has high amounts of coarse woody debris and vegetation within the

channel. As of 1982, Swanson and Fredriksen (1982) estimated that 4300 t of material had entered temporary storage within the channel, and they predicted that this stored sediment would prolong the post-logging and slash burning increase in bedload export for another decade. In fact, annual bedload export from WS01 has remained elevated compared to WS02 through 2022, 55 years after logging and slash burning were completed.

Annual bedload export is closely related to maximum daily flow for the period of available streamflow record, 1957 to 2018 ($R^2 = 0.57$ to 0.81), indicating that streamflow plays a large role in bedload export in this catchment (Figure 15). A strong relationship exists between bedload export and maximum daily flow. No debris flows have occurred since the 1950s, so it appears that fluvial transport is the dominant export mechanism in this catchment.

The combined effect of elevated and more frequent high flows (Jones and Grant 1996), increased sediment production from the hillslope, channel storage promoted by large wood in the wide valley floor, and the gradual decay and reorganization of wood contribute to the half-century of elevated bedload export from WS01 compared to WS02 (Figure 25).

A combination of the treatment's influence on the hillslope, vegetation, near-channel environment, the overarching geomorphic setting, the spatial arrangement of the drainages, the long-term ecological response of the treatment, and the timing of the treatment in relation to a large flood event (Swanson and Fredriksen 1982) could help explain the lack of debris flow activity within this catchment.
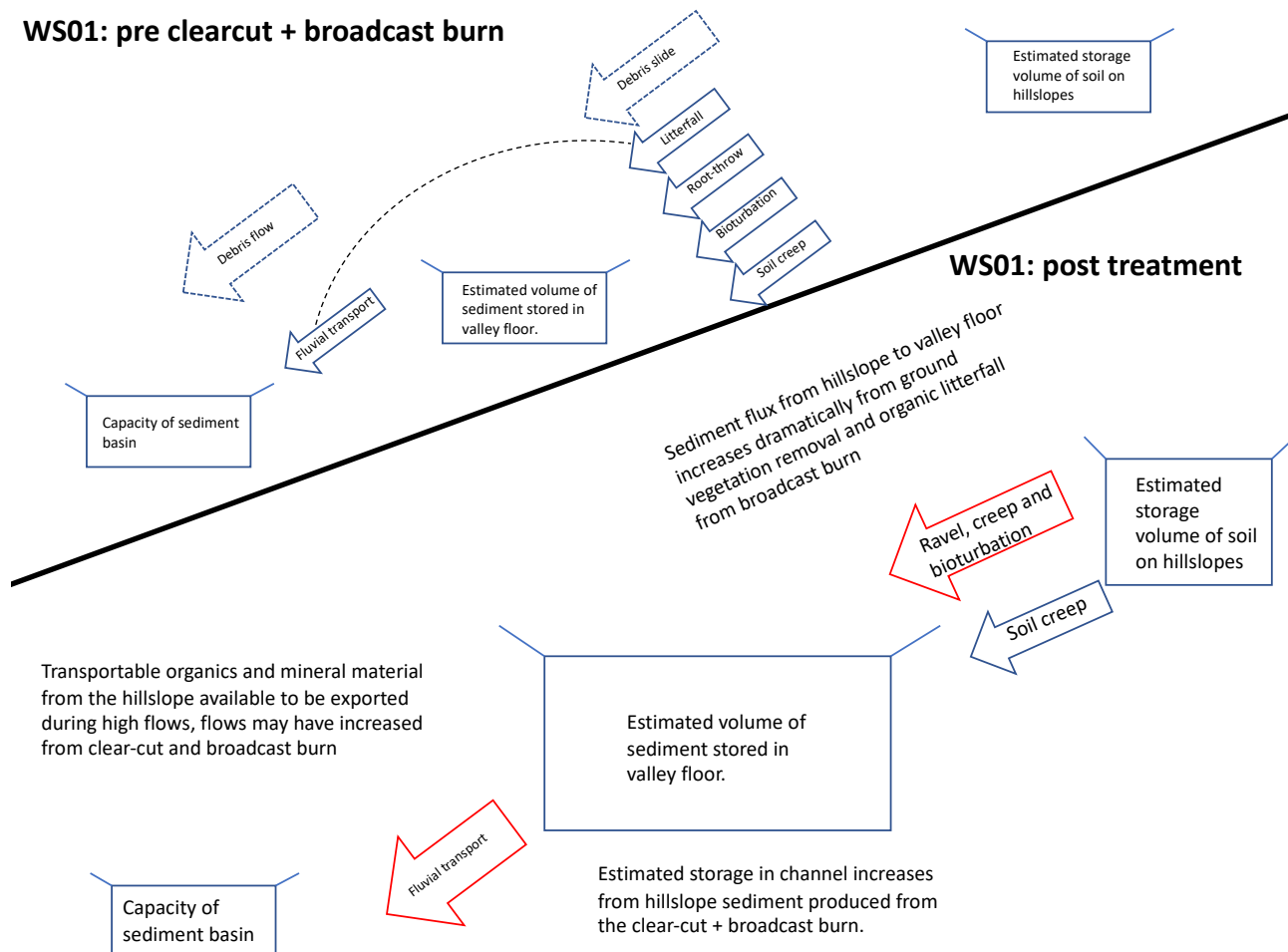
Figure 25. Schematic diagram of storages and flows of sediment in WS01, before and after logging (1962-66) and slash burning (1967).

WS03. Disturbance events such as clear cuts and road building on the

hillslope can increase the likelihood of mass wasting events (Swanson and Dyrness

1975, Wemple et al., 2001; Fredriksen 1965; Dyrness 1967; Fredriksen 1970). Roads

had been recently constructed (in 1959), and patch clearcutting and slash burning had

occurred (in 1963), just prior to water year 1965. In December 1964 and January

1965, two storm events triggered multiple debris slides and debris flows in WS03,

and an estimated 20,000 t of material was exported from the catchment. Swanson and Fredricksen (1982) estimated that 90 percent of the exported material was sourced from road fills, while the rest was sediment that was stored in the channel prior to road construction and logging or contributed during debris flows of 1961 (Fredriksen 1965). Debris flows in 1964 and 1965 scoured much of the channel length and exported much of the sediment stored in the channels (Fredriksen 1970, Goodman et al., 2022). Additional debris flows occurred in WS03 during the major flood of February 1996, but these events exported less material than previous debris flow events, possibly due to reduced sediment available from roads because of prior road-related debris slides, reduced storage within the channel from scour by previous debris flows, and lack of time for sediment to accumulate over the 30 years between the 1964/1965 and 1996 floods (Goodman et al., 2022) (Figure 26).

When the volume of material exported by debris flows is excluded, average annual bedload export from WS03 is similar to the reference catchment (WS02). Bedload export from WS03 may be limited by the narrow valley floor in the lower reaches of WS03, which is pinched by a slump just upstream of the WS03 outlet, the lack of sediment stored in the channel, or the large grain sizes of instream sediment delivered by mass movements to WS03 channels (F. Swanson, personal communication) (Figure 26). Streamflow metrics and bedload export have a weak relationship in this catchment, indicating that fluvial transport may influence export to a lesser degree. A change in the streamflow-export relationship following debris flow events may indicate that debris flow events influenced fluvial transport of bedload in this catchment. The material delivered to the channel from mass movements may be

too coarse to be transported through fluvial transport. Additionally, debris flow events

scoured stored sediment within the channel (in some cases to bedrock) (see Figure A-

13) leaving less material available for fluvial transport in the following years.

WS03: pre roads + 25% patch-cut
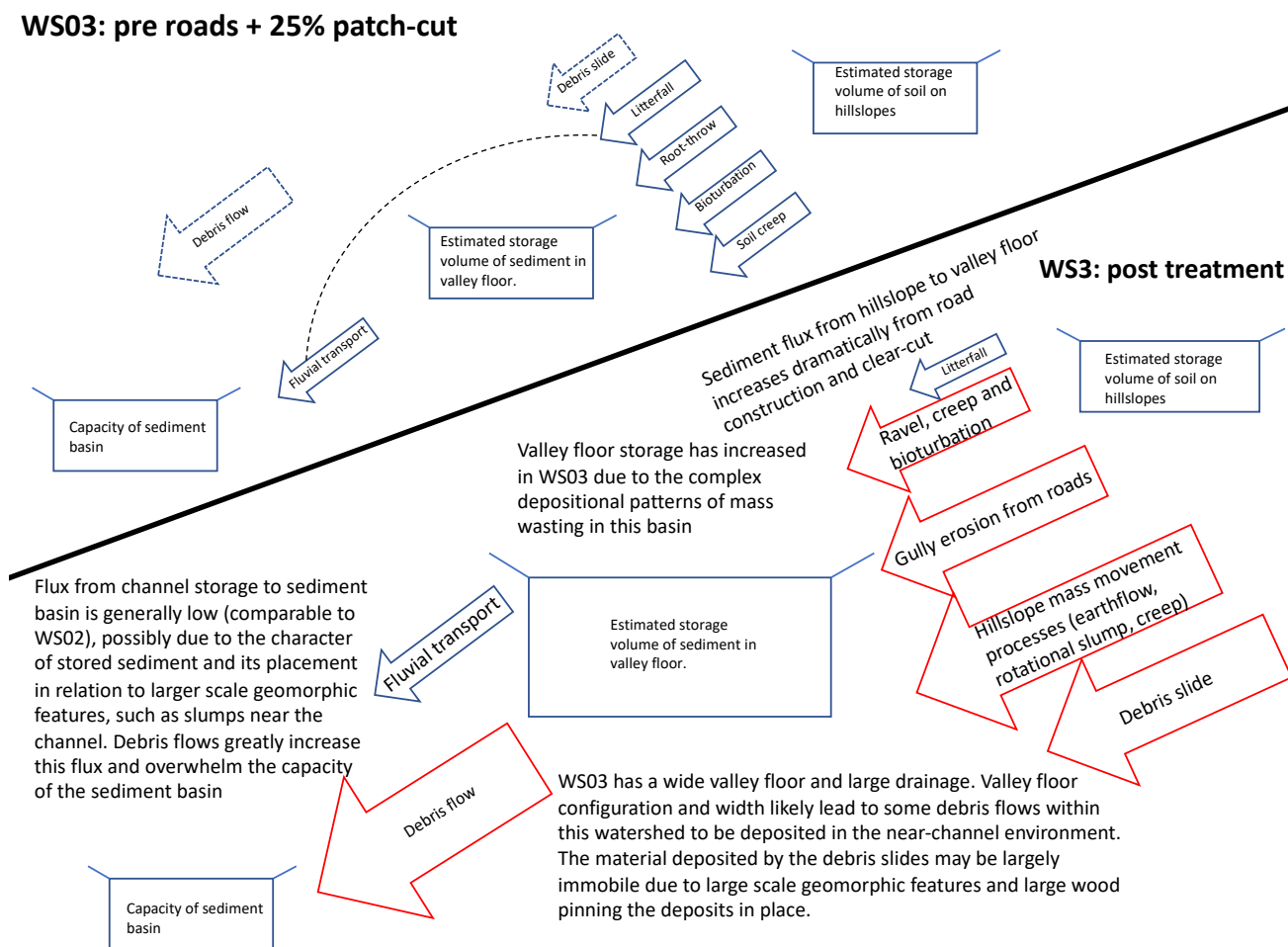
Figure 26. Schematic diagram of storages and flows of sediment in WS03, before and after roads (1959) and patch-cuts (1963).

WS10. In this catchment, 100% clearcutting occurred in 1975 using skyline

yarding, with no roads, and no burning of logging slash. Bedload export increased

after the clear-cut, and much of this export occurred during moderate flood events.

Harr and McCorison (1979) reported a decrease in the size of peak flows following

rain events in WS10 compared to WS09 in the first few years after logging, but replacement of the flumes in WS10 and WS09 in the year prior to the logging treatment may have confounded these results. Jones (2000) reported a 25% increase in peak flows in WS10, similar to the increase in flows in WS01, in the first ten years after logging. Higher peak flows, the removal of logs within the channel, which effectively decreased storage capacity, and increased sediment production on the hillslope (Swanson et al., 1982), may all have contributed to the increase in bedload export after logging in WS10 (Figure 27).
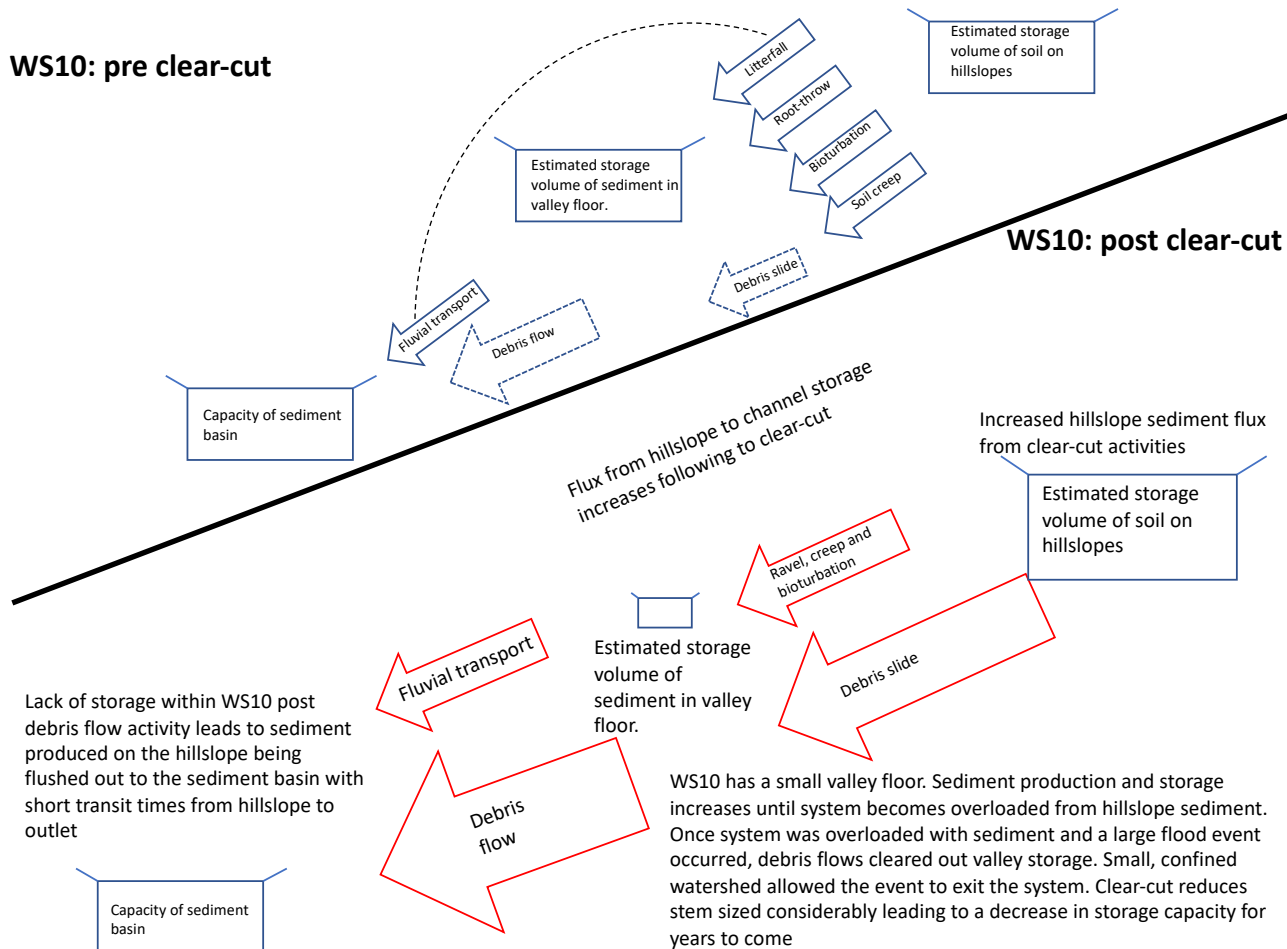
Figure 27. Schematic diagram of storages and flows of sediment in WS10, before and after logging in 1975.

Debris flows occurred in WS10 during the large floods of February 1986 and February 1996. Clear-cuts increase the probability of mass wasting by decreasing root strength (Swanston 1970), decreasing transpiration (Bethlahmy 1962), and increasing snowmelt runoff (Anderson 1959). The 1986 debris flow initiated from a debris slide in a bedrock hollow in WS10 (Swanson et al., 1987). Loss of root strengths, unstable, shallow soils, little vegetation, and a lack of large wood on hillslopes may have also contributed to the 1986 debris flow from WS10 (Swanson et al., 1987). The 1996 debris flow initiated from a streamside slide, and it exported much less material than the debris flow of 1986. Swanson and Jones (2002) speculated that the smaller size of the 1996 debris flow could be attributed to a majority of unstable sites already being activated in previous storms, and a lack of time to reload sediment into the channel.

When debris flows are excluded, bedload export from WS10 (100% clearcut) was 0.2 m^3/ha/yr greater than from WS09 (reference) over the full period of record. This high level of bedload export from WS10 compared to WS09 may be the result of the initial increases in bedload export from 1976 to 1978, immediately after the clear-cut, when annual bedload export increased by 34 times in WS10 compared to WS09 during that same time period. The lack of sediment storage capacity in the channel of WS10 may also have contributed to consistently higher annual bedload export from WS10 compared to WS09. Field surveys indicate that the channel of WS10 has less coarse woody debris within the channel, leading to WS10 having less capacity to trap and store sediment. This lack of storage may lead to rapid movement of sediment contributed from hillslopes to bedload export, whereas in WS09, sediment

contributed from hillslopes may be stored in the channel for a long time (Figure 27). See Figure A-14 for historical photographs of some of the events labeled above.

5.3 High flows and bedload export, in the context of forestry

Results from this study indicate that, as expected, high flows play a role in bedload export. The combination of maximum daily flow, volume above bankfull flow, and number of days above bankfull flow provided variable predictions of annual bedload export over the full period of record (R^2= 0.33 for WS01, 0.69 for WS01, 0.29 for WS03, 0.48 for WS09, and 0.59 for WS10). The relationship of annual bedload export to maximum daily flow varied depending on time since treatment. Inclusion of bankfull flows as independent variables improved model fits over models using only maximum daily flow. These findings are consistent with mechanisms controlling fluvial entrainment and transport of bedload. Flows above bankfull stage may access sediment stored in locations inaccessible to lower flows. High flows also may have the capacity to liberate sediment by mobilizing wood jams (Figure 28), and they exert shear stress that may exceed the critical shear stress for particle motion (Figure 29). However, the relationship of annual bedload export to high flows (maximum daily flow and bankfull flows) varied among the catchments, as discussed below.

Although a 1.25 year return-period flood was used to define bankfull flow in this study, results would be similar if a different recurrence interval, such as a two or five year return-period flood had been used. A 1.25 year return-period flood captures more flow events than a higher return-period flood, and the flow events exceeding a

higher return-period flood are a subset of flow events exceeding the 1.25 year return-period flood.

*** Size of arrow indicates relative energy carried within the stream
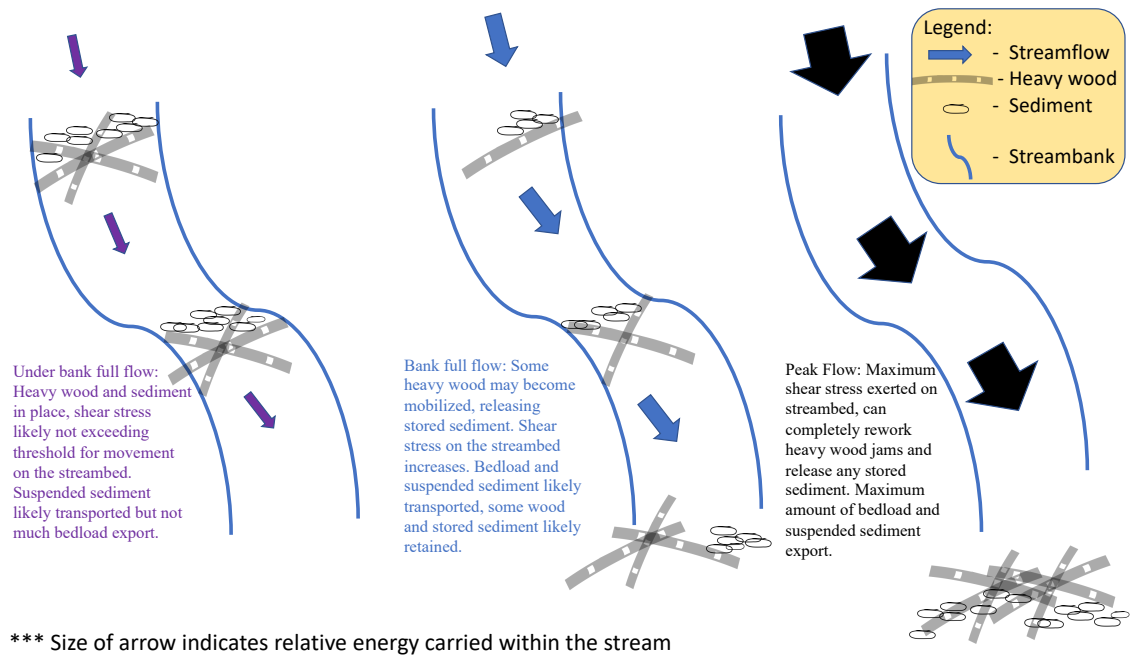
Figure 28. Schematic diagram of bedload export response to high flows in plan view (number and volume of days above bank full, maximum daily flow).
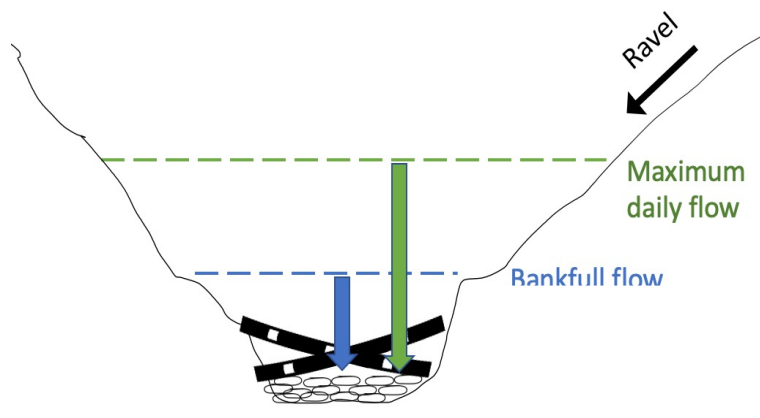
Figure 29. Schematic diagram of bedload export response to high flows in cross-section view

WS01. Prior to 100% clearcutting without roads, annual bedload export from WS01, controlling for the size of the maximum daily flow, was less than from WS02, but annual bedload export controlling for maximum daily flow magnitude from WS01 has remained well above that from WS02 even 30 to 50 year after clearcutting ($R^2 = 0.812$). The decay of in-stream wood increases fluvially transportable sediment within the valley floor. Mobilization of sediment formerly stored behind log jams may have contributed to the prolonged increase in annual bedload export after logging and the strong relationship of annual bedload export to maximum daily flow in WS01. WS01 has a long stretch of channel with stored sediment, relatively fine-textured material that is more readily moved by fluvial processes, and less trapping capacity by big wood. The wider valley floor of WS01 has a higher sediment storage capacity than other catchments in this study (Figure 30).

Large wood contributed to the channel before and during logging (1962 to 1966) has gradually decayed, and as wood decayed, much of this sediment has become available for fluvial transport and bedload export. Multiple linear regressions using bankfull flows and maximum daily flow showed that there was a moderately strong relationship between streamflow parameters and bedload export ($R^2 = 0.33$, multiple R = 0.57). Maximum daily flow was a significant predictor in the regression ($p < 0.01$), while days above bankfull and volume above bankfull were not. This may be because flows above bank full and the maximum daily flow inundate the same portions of the valley floor in this watershed.
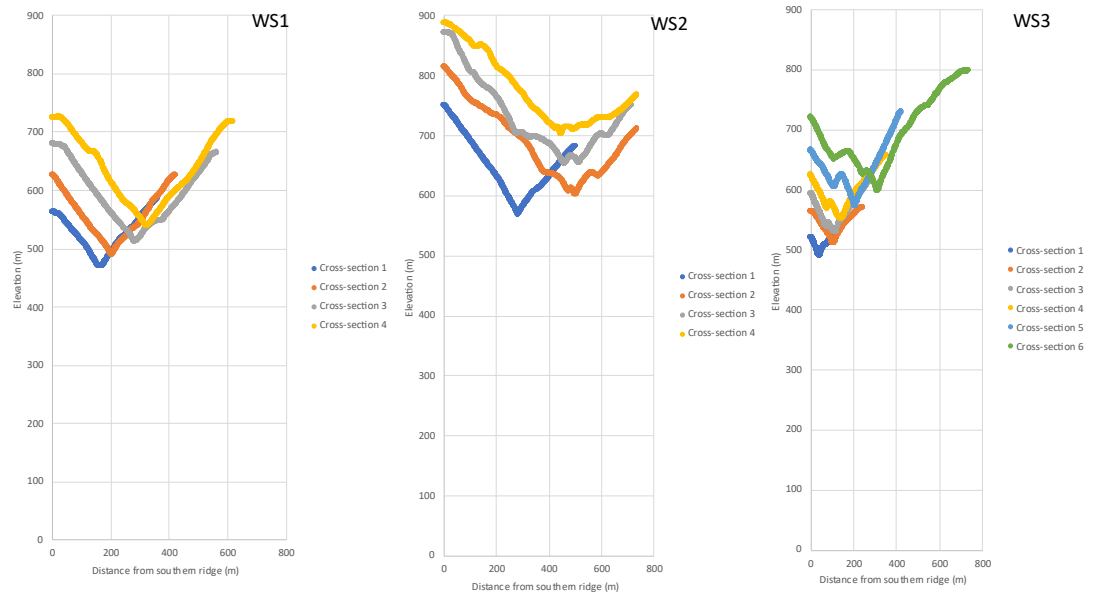
Figure 30. Valley cross-sections for WS01, WS02, and WS03.

WS02. The relationship between maximum daily flow and bedload export did

not vary through time in WS02, as expected, in this reference catchment with mature

and old-growth forest, which had no logging or roads, no debris slides or debris

flows, and no other disturbances until the wildfire of September 2020. The dominant

erosive processes that operated at the beginning of data collection likely continued at

the same rate and proportion, until the wildfire disturbance in 2020. I expect that this

relationship will change in the years to come due to the expected impact of wildfire

(see below). Bedload export variations were closely related to streamflow metrics in

WS02 ($R^2 = 0.69$, multiple R = 0.68). Maximum daily flow (p < 0.05), days above

bankfull (p < 0.001), and volume above bankfull (p < 0.001) were all significant

predictor variables, indicating that streamflow plays a dominant role in bedload

export. This finding is consistent with the interpretation that fluvial transport plays a

large role in annual sediment export in a catchment without human or natural

disturbances (Figure 24).

WS03. Annual bedload export was only weakly related to maximum daily

flow and bankfull flows, even when debris flows were excluded from the analysis

with debris flows removed from the record ($R^2 = 0.29$). This finding appears to be

due to complex effects of debris flows on sediment sources and transport in the

catchment. The relationship of annual bedload export to maximum daily flow

changed after debris flow events compared to before debris flow events. Annual

bedload export for a given maximum daily flow decreased in years after debris flows.

This finding indicated that debris flow events altered how streamflow interacts with

the catchment to export sediment. Although bedload export from WS03 excluding

debris flows was not well related to streamflow metrics, the volume of bedload export

from WS03 excluding debris flows was comparable to that from WS02, where

bedload export was strongly related to streamflow metrics. Bedload export from

WS03 may be limited by different processes than in WS02 or WS01. WS03 has a big

wedge of sediment in its lower reaches above the gage, probably deposited by debris

flows and is being held by large wood and a slump from the east just above the gage

(F. Swanson, personal communication). Large volumes of sediment and of this wood

was contributed over centuries, and some by early post-road debris flows from roads

(Fredriksen 1965). Debris flows removed huge amounts of sediment and large wood

from WS03 in 1964/1965 (Goodman et al., 2022), but the sediment retained within

the channel at WS03 was sufficient to support an alder stand in the 1964-1996 period

(F. Swanson, personal communication). The 1996 debris flows removed much of this

sediment, but some sediment and large wood was trapped in a debris-flow deposit upstream of the gage (F. Swanson, personal communication). Compared to WS01, WS03 has less sediment stored in the channel, more capacity to trap bedload in the channel, and less fine-grained material that can be mobilized by fluvial processes since debris flows of 1964/1965 (Figure 26 and Figure 27).

WS09. The relationship between maximum daily flow and bedload export did not vary through time in WS09, as expected, in this reference catchment with mature and old-growth forest, which had no logging or roads, no debris slides or debris flows, and no other disturbances until the wildfire of September 2020. Annual bedload export was related to streamflow metrics at WS09 ($R^2 = 0.48$, multiple R = 0.69), including maximum daily flow ($p < 0.05$) and days above bankfull flow ($p < 0.05$) in the multiple linear regression, indicating that fluvial transport of material was a principal process responsible for bedload export. The dominant erosive processes that operated at the beginning of data collection likely continued at the same rate and proportion in WS09, until the wildfire disturbance in 2020. I expect that the wildfire in 2020 will alter the relationship between the streamflow metrics and bedload export on an annual basis (see below).

WS10. Annual bedload export, excluding debris flows, was related to streamflow metrics at WS10 ($R^2 = 0.59$, multiple R = 0.77) including volume above bankfull ($p < 0.01$) and days above bankfull flow ($p < 0.001$), in the multiple linear regression, indicating that fluvial transport of material was a principal process responsible for bedload export. This is consistent with the observation that large roughness elements in the channel were removed during treatment (Swanson and

Fredricksen 1982), and sediment storage remained very low in the WS10 channel in 2022, more than 45 years after logging in 1975. Although debris flows dominated the total bedload export, streamflow plays a large role in bedload export in this catchment.

5.4 Effects of wildfire on bedload export

The 2020 wildfire burned 47 % of WS09, 21% of WS01, and 16% of WS02. In the two years after the fire, bedload export increased by 9 times in WS09 but did not increase in WS01 or WS02, although in November 2022 WS02 experienced a small, episodic export event that totaled ~5 to 10 m^3.

The export response in the catchments may reliant on several factors including: 1) the inherent geomorphic processes, and landforms in these catchments, 2) wind events prior to the wildfire, 3) the wildfire's effect on tree mortality, understory vegetation, precipitation reaching the surface, high flows, the decay of large roughness elements, and decreases in soil stability(Figure 31).

Wildfire was associated with moderate levels of tree mortality, with slightly higher rates in WS09, where up to 56% of the trees (414 of 735) were killed, whereas WS02 experienced 31 % mortality of surveyed trees, and WS01 experienced 25% mortality (Bell and Powers 2023). Charred cones, bark fragments, and needles dropped from killed trees to the ground surface, increasing the amount of large, charred organic sediment available to be entrained from the hillslope and delivered to the channel by precipitation, gravity, and wind. These processes may explain the high amounts of organic material and the large fraction of charred coarse organic matter in the bedload export in the first few months (October to December) after the wildfire.

Prior to the fire reaching the Andrews, winds reached 15 m/s at the CENMET meteorological station (Daly and McKee, 2019). Trees that have fallen from this event, or prior to this event in a different windstorm produce tip up mounds(root-throw) and increase the availability of coarse textured, loose sediment available on the hillslope. This sediment is consistent with a large proportion of the bedload sediment identified 1-2 years after the wildfire. The impact of a large tree falling and hitting the soil surface (tree slam) in conjunction with the creation of a tip up mound would increase sediment production. Toppling would also liberate bark and other organic sediment by breaking the tree. Without a wildfire disturbance, the understory vegetation would trap the loose sediment, prior to it reaching the channel. A wildfire removes the understory vegetation and can dramatically decrease the canopy, increasing the amount of precipitation that can reach the surface during rain events.

Burning removes vegetation and reduces surface roughness, and ravel increases following a fire event that (Bennett 1982, Mersereau and Dyrness 1972). Immediately after the fire, ravel likely increased dramatically and began to saturate the storage zones. This is likely a major source of the coarse-grained mineral material that was exported from WS09 during the first high flows after the wildfire.

Wildfire may cause in increase in streamflow because of a decrease in transpiration. Up to 56% of the trees were killed, which could lead to an increase in streamflow. More streamflow can lead to a larger drainage network and higher stage which would allow the flow to access more material than prior to the wildfire.

Annual bedload export from WS09 increased by almost an order of magnitude in the first two years after wildfire. Post-wildfire bedload export was high in organic

material and charred coarse (>4 mm) organic material in the first fall after the wildfire, and the fraction of organic matter and charred material decreased in the second year after wildfire. These findings imply that post-fire bedload export was contributed from the stream channel or hillslope sources that were connected to the stream channel and could be transported to the sediment basin. Much of the charred material in bedload export was bark fragments, which could have been sourced from trees on the hillslope near the stream and within the stream. Bark fragments may be more readily transported in dry ravel or by fluvial transport compared to twigs or cones because of their lower bulk density. Charred pieces of bark may have been detached from large wood in the channel. Alternatively, the bark may have been sourced from the hillslope. As the fire effected trees on the hillslope bark charred bark likely fell from the tree, additionally the fire could have impacted bark that was produce from trees falling prior to the fire. The charred bark, along with mineral sediment, on the hillslope may have been transported to the channel once the surface vegetation was consumed by the wildfire.

The alternative explanation is a more likely source of charred bark in this case, trees within the stream have likely already lost their bark through decay, it takes a long time for a tree that dies on the hillslope to enter the stream and begin to accumulate sediment. Similar to WS01, sediment stored by large wood in the channel of WS09 may continue to be exported for years to come, as the residual large wood decays. A debris flow could occur in the future and scour the sediment from the channel in WS09, as happened after logging in the paired catchment, WS10.

WS09: pre wildfire

Debris slide

Estimated storage volume of soil on hillslopes

Litterfall

Root-throw

Bioturbation

Soil creep

Debris flow

Estimated volume of sediment stored in valley floor.

Fluvial transport

Capacity of sediment basin

Hillslope storage may decrease or increase depending on the balance between sediment production and erosion

WS09: post wildfire

Estimated storage volume of soil on hillslopes

Sediment transfer from hillslope to valley floor increases from ground vegetation removal, possible consumption of large roughness elements on hillslope and organic litterfall from tree mortality. Storage zones may also increase post fire, if fire leads to trees falling and depositing in the channel

Litterfall

Soil creep

Root-throw

Bioturbation

Ravel + litterfall, fire suppression

Debris slide

Transportable organics and mineral material from the hillslope available to be exported during high flows, WS09 has been relatively stable – so far! The potential for a post-fire debris flow may persist for 5-10 years.

Estimated volume of sediment stored in valley floor.

Fluvial transport

Debris flow

Capacity of sediment basin

Figure 31: Schematic diagram of storages and flows of sediment in WS09, before and after wildfire in 2020.

Fire suppression occurred in WS02. A large fire line was created in WS02 on a relatively steep slope. By constructing a fire line, bare mineral soil was exposed to the surface for extended periods of time and stability of the soil was altered. In WS02, a small debris flow or wood-laden flood pulse occurred during a high flow event on November 5, 2022, two years after the wildfire. A pulse of sediment (including large wood and sediment ranging from fine to forearm size boulders, likely 5-10 m^3 of material) flowed into the sediment basin (G. Downing, personal communication). It is unclear whether this event was related to the wildfire because there was no evidence

of char on the material. It may have originated from a deposit of large wood and sediment that had occupied the WS02 channel just upstream of the waterfall, which is just upstream of the gage and sediment basin, for some decades, perhaps after a debris flow in WS02 in the 1940s (F. Swanson, personal communication). This deposit may have been mobilized from increased streamflow attributed to decreased transpiration. Alternatively, material might have been sources from soils disturbed by the fire suppression, but this remains to be investigated in the field.

WS01 and WS02 may have a delayed response to the fire. The valley floor in WS01 and WS02 is wider than WS09, and the area impacted by the fire in WS01 and WS02 was a considerable distance from the sediment basin. In contrast, the wildfire influenced areas near the sediment basin in WS09 (Figure 5), WS09 has a steeper channel gradient (Table 1), and the drainage area is considerably smaller in WS09 compared to WS01 and WS02 (Table 2). Differences in watershed characteristics and burn behavior between the WS01 and WS02 vs. WS09 may explain the immediate response in WS09 compared to a possible delayed response in WS01 and WS02.

5.5 Factors influencing quality (organic vs. mineral) and size distribution of bedload export after wildfire

Both biotic and abiotic processes contributed to the increase in bedload export from WS09 after wildfire (Figure 31 and Figure 32). Biotic processes include initial and ongoing tree mortality and litterfall, while abiotic processes include precipitation, ravel, and streamflow. Despite large differences in the volume of bedload export in WS09 after wildfire compared to WS10, the similarity in their grain size and organic

and mineral fractions indicates that similar geomorphic processes were operating in both catchments.

Bedload samples from WS09 in the first year after wildfire reveal the changes in bedload export composition during the water year. The <2 mm fraction was high in the early fall (October to December) and declined in the winter and spring (January to May), while the 2-4 mm and >4 mm size fractions increased during the winter of the first year following the wildfire. The 2-4 mm size fraction was mostly rounded aggregates or mineral material, indicating that this material was transported during the high flows of the winter. The decline in fine grained sediment from fall to winter may reflect a decrease in litterfall (especially needles small enough to be included in the <2 mm fraction) and an increase in the energy of high flows in winter. Higher precipitation may also entrain sediment from the hillslope, perhaps including coarse particles in tip-up mounds, possibly explaining larger 2 to 4 mm and >4 mm size fractions in bedload export during the winter.

Bedload export continued to have coarse organic matter, even two years after the fire, possibly explained by continued (delayed) mortality and litterfall. Large organic sediment such as cones could contribute to the bedload export. Another possible explanation for the continued increase in >4mm sediment would be the continual acceleration of ravel processes, due to a lack of regrowth.

Organic material was a smaller portion of the 2-4 mm fraction of bedload export from WS09 than from WS10. The wildfire may have broken down organo-mineral aggregates in WS09, creating more fine-grained organics, while organics were able to be retained in the 2-4 mm size fraction of WS10.

The 2-4 mm fraction of material initially exported from WS09 may have been sediment stored in the channel or mineral material produced from the wildfire breaking down aggregates in the soil, whereas the 2-4 mm fraction of material exported from WS10 may have been more dominated by litterfall and intact organo-mineral aggregates.

The highest proportion of organic material in bedload export from WS09 was in the > 4 mm fraction in the fall of the first year (October to December 2020). This coarse organic material may have originated from material that was fragmented by tree topping in the high winds that preceded the wildfire, or by turbulence during the wildfire. In the first winter after wildfire in WS09, the mineral portion of the > 4 mm fraction increased, perhaps because of higher energy fluvial processes that mobilized >4mm mineral grains in the winter. In the second year after wildfire in WS09, delayed mortality resulted in the death of at least eight large trees that were not killed initially by the fire. Organic material was a larger portion of the 2-4 mm fraction of bedload export from WS09 in the second year compared with the first year after wildfire, perhaps because delayed mortality contributes litterfall to hillslopes and the stream channel (Figure 32).
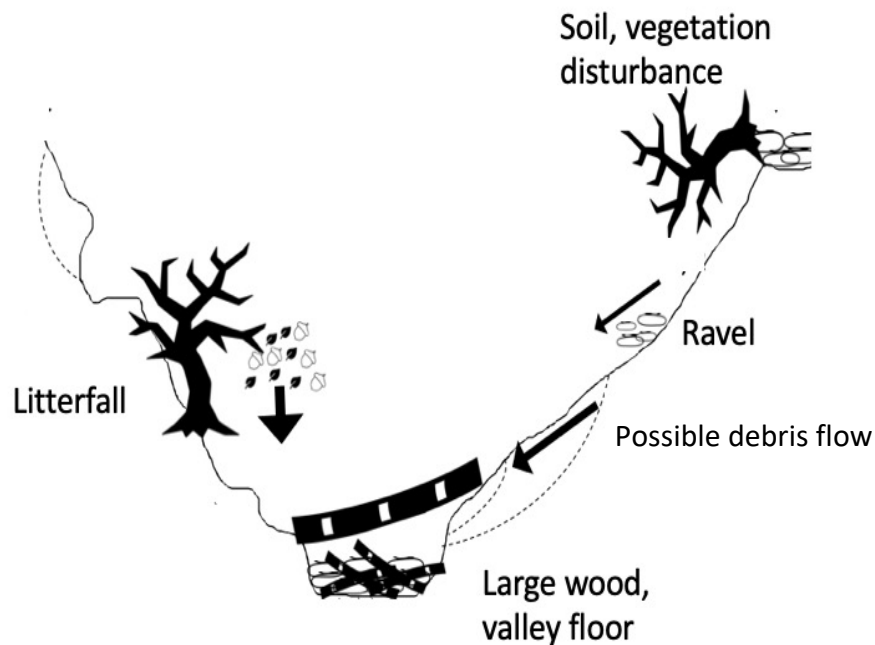
Figure 32: Schematic diagram of how the wildfire may have influenced abiotic and biotic bedload export processes

There are a few limitations involved with this research, first, the annual resolution of the bedload export data makes it difficult to identify exact processes that lead to increased export. We can look at variations in environmental parameters on an annual basis and see if variations in those parameters match variations in export, but we have no way to identify discrete erosional processes, other than debris flows. We lack data about sediment storage in stream channels prior to logging or wildfire disturbance. Samples were obtained from the interior of the deposits excavated from the sediment basins, but it is unclear how representative they are of the full deposit. The organic fractions of bedload may have been underestimated because of organic matter decomposition in the samples, or it may have been overestimated as a result of

litterfall directly into the sediment basin. Bedload export volumes may be overestimated because they include suspended sediment which may account for 25% of the bedload export. Lastly, although provisional data for 2018 to 2022 streamflow discharge was available, I was unable to convert that data into a usable format for this study.

Further research could: 1) test how inclusion of forest management related independent variables improve the fit of the multiple linear regression models; 2) test how inclusion of landscape metrics that account for changes in hillslope sediment supply affect regression model fit; 3) use lidar to quantify changes in sediment storage through time 4) investigate how the geologic structures influence debris flow susceptibility.

6.0 Conclusion

This study revealed that bedload export increased for multiple decades after logging and road construction in five small, steep, forested catchments in the western Cascade Range of Oregon. Annual bedload export from 100% clearcut catchments remained elevated by an order of magnitude for 45 to 55 years after clearcutting compared to reference catchments with mature and old growth forest (WS01 vs. WS02, WS10 vs. WS09). Annual bedload export in a 25% patch cut watershed with roads also was orders of magnitude higher for more than three decades compared to a reference watershed with mature and old growth forest (WS03 vs. WS02).

In addition, bedload export increased by an order of magnitude in the first two years following wildfire in a 9-ha watershed with mature and old forest (WS09), but

bedload did not increase in the first two years after wildfire in a 96-ha watershed with 50-year-old forest plantations (WS01) or a 60-ha watershed with mature and old forest (WS02). A bedload export response may be delayed in WS01 and WS02, because wildfire was lower severity and impacted locations farther from the watershed outlet (sediment basin) in WS01 and WS02 than in WS09.

Geomorphic processes of the study catchments regulated the response of bedload export to disturbance. Bedload export was dominated by episodic debris slide and debris flow processes in two catchments (WS03 and WS10) and by chronic hillslope and fluvial processes in three catchments (WS01, WS02, WS09). The long-term bedload export dataset showed this. In WS03 and WS10, debris flows in a few years accounted for a large proportion of the export over the entire data record (50-70 years). In contrast, catchments that did not experience debris flows had continual elevated export on an annual basis, and the relationship between high flow parameters and export was higher in those basins.

The greatest increases in bedload export occurred in the form of multiple debris flows that originated from roads constructed on benches of pre-existing mass movements in a 101-ha watershed (WS03) and from debris flows in a 10-ha watershed that originated from a bedrock hollow and a streamside slide (WS10). On the other hand, fluvial processes (represented by streamflow metrics including daily maximum flow and volume and number of days above bankfull flow) explained much of the variation over time in bedload export excluding debris flows especially in reference catchments (e.g., WS02, WS09).

Landforms and large wood in the study catchments also regulated the response of bedload export to disturbances including logging, roads, and wildfire. Differences in valley floor width and large wood in the stream channel influenced sediment storage and regulated bedload export response to natural and human disturbances. Prolonged elevated bedload export occurred from a 96-ha watershed with the widest valley floor, where large wood gradually decayed and released sediment that had accumulated before and during logging (WS01). Bedload export also was elevated after wildfire from a 9-ha watershed with a steep narrow valley floor, where sediment stored upstream of large wood pieces was apparently released by partial combustion of the wood in the channel (WS09). In contrast, bedload export excluding debris flows was no different from a watershed where debris flows had removed large wood and sediment from the channel (WS03) compared to the reference watershed (WS02).

Overall, this study demonstrated that forestry practices of the mid 20th century increased bedload export for up to 60 years after logging and road construction from five small catchments, and moderate to low severity wildfire increased sediment export initially in only one of three burned catchments (WS09). Differences in bedload export response to disturbance appear to be the result of differences in large scale geomorphic processes and landforms, as well as burn area and severity. The location of the disturbance in relation to the watershed outlet may also have regulated the timing and magnitude of bedload export response to disturbance.

Logging, roads, and wildfire increased bedload export by influencing sediment supply from hillslopes to channels, promoting sediment transport by fluvial processes, and increasing susceptibility to mass movements. Differences in geomorphic processes and landforms processes among catchments produced different responses of bedload export. These findings illustrate general principles that can be extended to predict how catchments may respond to future forestry practices and other disturbances including wildfire.

7. Literature Cited

Anderson, H.W. Storage and delivery of rainfall and snowmelt water as reated to forest environments. Int. Assoc. Sci. Hydrol., Publ. no.48.

Antoniazza, G., Nicollier, T., Boss, S., Mettra, F., Badoux, A., Schaefli, B., Rickenmann, D. and Lane, S.N. 2022. Hydrological drivers of bedload transport in an Alpine watershed. Water resources research, 58(3), p.e2021WR030663.

Bell, D.; Powers, M. 2023. Long-term growth, mortality and regeneration of trees in permanent vegetation plots in the pacific northwest, 1910 to present. Long-Term Ecological Research. Forest Science Data Bank, Corvallis, OR. [Database].Available:https://andlter.forestry.oregonstate.edu/data/abstractdetail.aspx?dbcode=TV010c

Benda, L., Dunne, T. 1997. Stochastic forcing of sediment supply to channel networks from landsliding and debris flow. Water Resour. Res., 33 (1997), pp. 2849-2863.

Bennett, K.A. 1982. Effects of slash burning on surface erosion rates in the Oregon Coast Range. M.S. Thesis, Oregon State University, Corvallis.

Bethlahmy, N. 1962. First Year Effects of Timber Removal on Soil Moisture. International Association of Scientific Hydrology. Bulletin, 7:2, pp. 34-38, DOI: 10.1080/02626666209493253.

Brown, G.W., Krygier, J.T. 1971. Clear-cut logging and sediment production in the Oregon Coast Range. Water Resour. Res. 7, pp. 1189–1198. https://doi.org/10.1029/WR007i005p01189.

Brunsden, D.,Thornes, J. B. 1979. Landscape Sensitivity and Change. Transactions of the Institute of British Geographers, 4(4),p. 463. doi:10.2307/622210

Bywater-Reyes, S., Segura, C., and Bladon, K. D. 2017. Geology and geomorphology control suspended sediment yield and modulate increases following timber harvest in temperate headwater streams. Journal of Hydrology, 548, pp. 754–769. doi:10.1016/j.jhydrol.2017.03.048

Bywater-Reyes, S., Bladon, K.D., Segura, C. 2018. Relative influence of landscape variables and discharge on suspended sediment yields in temperate mountain catchments. Water Resources Research. 54, pp. 5126–5142. https://doi.org/10.1029/ 2017WR021728.

Cheng, J. D. 1980. Hydrologic effects of a severe forest fire. In: Proceedings of Symposium on Watershed Management. American Society of Civil Engineers, New York, pp. 240-251.

Church, M. 2006.Bed material transport and the morphology of alluvial river channels. Annu. Rev. Earth Planet. Sci., 34 (2006), pp. 325-354, 10.1146/annurev.earth.33.092203.122721.

Czarnomski, N.M., Dreher, D.M., Snyder, K.U., Jones, J.A. and Swanson, F.J. 2008. Dynamics of wood in stream networks of the Western Cascades range, Oregon. Canadian Journal of Forest Research – Revue Canadienne De Recherche Forestiere, 38(8), pp. 2236–2248. Available from: https://doi.org/10.1139/x08-068

Czuba, J. Magirl, C., Czuba, C., Grossman, E., Curran, C., Gendaszek, A., Dinicola, R. 2011. Sediment Load from Major Rivers into Puget Sound and its Adjacent Waters. Fact Sheet 2011-3083. https://pubs.usgs.gov/fs/2011/3083/pdf/fs20113083.pdf

Daly, C.; Schulze, M.; McKee, W. 2019. Meteorological data from benchmark stations at the HJ Andrews Experimental Forest, 1957 to present. Long-Term Ecological Research. Forest Science Data Bank, Corvallis, OR. [Database]. Available: http://andlter.forestry.oregonstate.edu/data/abstract.aspx?dbcode=MS001. https://doi.org/10.6073/pasta/c021a2ebf1f91adf0ba3b5e53189c84f. Accessed 2023-05-26.

DiBiase, R. A., M. P. Lamb, V. Ganti, and A. M. Booth. 2017. Slope, grain size, and roughness controls on dry sediment transport and storage on steep hillslopes, J. Geophys. Res. Earth Surf.,122, pp. 941–960, doi:10.1002/2016JF003970.

Dietrich, W. E., Dunne, T., Humphrey, N., and Reid, L.M. 1982. Construction of sediment budgets for drainage basins. In: F. J. Swanson, R. J. Janda, T.Dunne, and D. N. Swanston (eds.), Sediment budgets and routing in forested drainage basins. Gen. Tech. Rep. USDA For. Ser. Pac. Northwest For. Range Expt. Stn. PNW-141. Portland, Oregon. pp. 5-23.

Dyrness, C.T. 1967. Soil surface conditions following skyline logging. U.S. Forest Service Research Note PNW-55, 8.

Dyrness, CT. 1967. Mass soil movements in the H.J. Andrews Experimental Forest. Res. Pap. PNW-42. Portland, OR: U.S. Department of Agriculture, Forest Service, Pacific Northwest Forest and Range Experiment Station. 13 p.

Eaton, L. S., Morgan, B. A., Kochel, R. C., and Howard, A. D. 2003. Role of debris flows in long-term landscape denudation in the central Appalachians of Virginia. Geology, *31(4), 339.* doi:10.1130/0091-7613(2003)031

Elliott, J. G. and Parker, R. S. 2001. Developing a post-fire flood chronology and recurrence probability from alluvial stratigraphy in the Buffalo Creek watershed, Colorado, USA. Hydrol. Process. 15, pp. 3039-3051.

Fredriksen, R. 1965. Christmas storm damage on the H.J. Andrews Experimental Forest, Research Note PNW-29. Portland, OR: U.S. Department of Agriculture, Forest Service, Pacific Northwest Forest and Range Experiment Station.

Fredriksen, R.L. 1970. Erosion and sedimentation following road construction and timber harvest on unstable soils in three small western Oregon watersheds. USDA For. Serv. Res. Pap. PNW-104, Pacific NW Res. Sta., Portland, Oregon.

Gomi, T., Sidle, R. C., and Richardson, J. S. 2002. Understanding Processes and Downstream Linkages of Headwater Systems. BioScience, 52(10), p.905. doi:10.1641/0006-3568(2002)052

Goodman, AC, Segura, C, Jones, JA, Swanson, FJ. Seventy years of watershed response to floods and changing forestry practices in western Oregon, USA. Earth Surf. Process. Landforms. 2022. Accepted Author Manuscript. https://doi.org/10.1002/esp.5537

Grant, G.E., Wolff, A.L. 1991. Long-term patterns of sediment transport after timber harvest, western Cascade Mountains, Oregon, USA. In: Walling, D.E., Peters, N. (Eds.), Sediment, and Stream Water Quality in a Changing Environment. Proceedings of the Vienna IAHS Symposium. IAHS Publication, pp. 31–40.

Greenland, D. 1993. Regional Context of the Climate of H.J. Andrews Experimental Forest, Oregon. KT Redmond and VL Tharp, Editors. 1994. Proceedings of the Tenth Annual Pacific Climate Workshop, April 4-7, 1993. California Department of Water Resources, Interagency Ecological Studie Program, Technical Report 36.

Harr, R. D. 1981. Some characteristics and consequences of snowmelt during rainfall in western Oregon. J.Hydrol. 53, pp.277-304

Harr, R. D., McCorison. 1979. Initial Effects of Clearcut Logging on Size and Timing of Peak Flows in a Small Waterhsed in Western Oregon. Water Resour. Res.15(1), pp. 90-94.

Harr, R.D., 1986. Effects of clearcutting on rain-on-snow runoff in Western Oregon: a new look at old studies. Water Resour. Res. 22, pp. 383–392. https://doi.org/10.1029/WR022i007p01095.

Harvey, A. M. 2001. Coupling between hillslopes and channels in upland fluvial systems: implications for landscape sensitivity, illustrated from the Howgill Fells, northwest England. Catena. *42(2-4), 225–250.* doi:10.1016/s0341-8162(00)0013

Hassan, M., Hogan, D., S.A. Bird, S., May, C., Gomi,T.,Campbel.D. 2005. Spatial and Temporal Dynamics of Wood in Headwater Streams of the Pacific Northwest. J. Am. Water Resour. Assoc. 41, pp. 899-919.

Hassan, M., Church, M., Lisle, T., Bardinoni, F., Benda, L., Grant, G. 2005. Sediment Transport and Channel Morphology of Small, Forested Streams. Journal of American Water Resources Assouciation, 41(4), pp. 853 – 876.

Heckmann, T., Schwanghart, W. 2013. Geomorphic coupling and sediment connectivity in an alpine catchment — Exploring sediment cascades using graph theory. Geomorphology, 182, pp. 89–103. doi:10.1016/j.geomorph.2012.10.

Helvey, J. D. 1973. Watershed behavior after forest fire in Washington. In: Proceedings of the Irrigation and Drainage Division Specialty Conference, American Society of Civil Engineers, April 22-24, 1973, Fort Collins, CO. pp. 403-422.

Hogan, D. L., S. A. Bird, and M. A. Hassan. 1998. Spatial and temporal evolution of small coastal gravel-bed streams: Influence of forest management on channel morphology and fish habitats, in Gravel-Bed Rivers in the Environment, edited by P. C. Klingeman et al., pp. 365– 392, Water Resour. Publ., Highlands Ranch, Colo.

Jackson, C.R., Martin, J.K., Leigh, D.S. and West, L.T. 2005. A southeastern piedmont watershed sediment budget: Evidence for a multi-millennial agricultural legacy. Journal of Soil and Water Conservation, 60(6), pp. 298-310.

Johnson, S., Rothacher, J. 2018. Stream discharge in gaged watersheds at the Andrews Experimental Forest, 1949 to present. Long-Term Ecological Research. Forest Science Data Bank, Corvallis, OR. [Database].Available: http://andlter.forestry.oregonstate.edu/data/abstract.aspx?dbcode=HF004(29 April 2019) https://doi.org/10.6073/pasta/ce70a42e1f637cd430d7b0fb64faefb4.

Johnson, S., Rothacher, J., 2017. Annual bedload accumulation from sediment basin surveys in small gauged watersheds in the Andrews Experimental Forest, 1957 to present. Long-Term Ecological Research. Forest Science Data Bank, Corvallis, OR.

[Database]. Available:
http://andlter.forestry.oregonstate.edu/data/abstract.aspx?dbcode=HS004 (29
April 2019)
http://dx.doi.org/10.6073/pasta/629412b84ff4bcf2bc74d9834ebc22b0.

Jones, J.A., 2000. Hydrologic processes and peak discharge response to forest
removal, regrowth, and roads in 10 small experimental basins, western
Cascades, Oregon. Water Resour. Res. 36, pp. 2621–2642.
https://doi.org/10.1029/2000WR900105.

Jones, J.A., Grant, G.E. 1996. Peak flow responses to clear-cutting and roads in small
and large basins, Western Cascades, Oregon. Water Resour. Res. 32, pp. 959–
974. https://doi.org/10.1029/95WR03493.

Kruse, C. G., Hubert, W. A., and Rahel, F. J. 1997. Geomorphic influences on the
distribution of Yellowstone cutthroat trout in the Absaroka Mountains,
Wyoming. Transactions of the American Fisheries Society, 126, pp. 418– 427.

Lancaster, S. T., and N. E. Casebeer. 2007. Sediment storage and evacuation in
headwater valleys at the transition between debris-flow and fluvial processes,
Geology, 35, 1027– 1030, doi:10.1130/G239365A.1

Lane, E.W. 1955. The Importance of Fluvial Morphology in Hydraulic Engineering.

Lanka, R. P., Hubert, W. A., and Wesche, T. A. 1987. Relations of geomorphology to
stream habitat and trout standing stock in small Rocky Mountain streams.
Transactions of the American Fisheries Society, 116, pp. 21– 28.

May, C., Gresswell, R. 2004. Spatial and temporal patterns of debris-flow deposition
in the Oregon Coast Range, USA. Geomorphology. 57, pp.135-149.
10.1016/S0169-555X(03)00086-2.

McClelland, D. E., Foltz, R. B., Wilson, W. D., Cundy, T., Heinemann, R., Saurbier,
J., and Schuster, R. L. 1997. Assessment of the 1995 and 1996 floods
andlandslides on the Clearwater National Forest. Part I: Landslide
Assessment. A report to the Regional Forester. USDA For. Serv. Northern
Region. Missoula, Montana

McNabb, D. H. and Swanson, F. J. 1990. Effects of fire on soil erosion. In: J. D.
Walsad, S. R. Radosevichand D. V. Sandberg (eds.) Natural and Prescribed
Fire in the Pacific Northwest Forests. Oregon State University Press.
Corvallis, pp. 159-176.

Megahan, W. F., Day, N. F., and Bliss, T. M. 1978.Landslide occurrence in the
western and central northern Rocky Mountain Physiographic Province in
Idaho. In: C. T. Youngberg (ed.), Forest Soils and Land Use. Proceedings of
the 5th North American Forest Soils Conference. Colorado State University,
Ft. Collins, pp. 116-139.

Megahan, W. F., King, J. G., and Seyedbagheri, K. A. 1995. Hydrologic and erosional responses of a granitic watershed to helicopter logging and broadcast burning. For. Sci. 41, pp. 777-795.

Mersereau, R., Dyrness, C., 1972. Accelerated mass wasting after logging and slash burning in western Oregon. J. Soil Water Conserv. 27, pp. 112–114.

Milhous, R. 1973. *Sediment transport in a gravel-bottomed stream.*: Oregon State University.

Minear, J.T., Kondolf, G.M. 2009. Estimating reservoir sedimentation rates at large spatial and temporal scales: A case study of California. Water Resour. Res. 45, pp. 1–8.

Murphy, M., Hawkins, C., Anderson, N. 1981. Effects of Canopy Modification and Accumulated Sediment on Stream Communities. American Fisheries society, 110(4), pp. 469 – 478.

Nakamura, F., Swanson, F. J., and Wondzell, S. M. 2000. Disturbance regimes of stream and riparian systems—a disturbance-cascade perspective. Hydrol. Process. 14, pp. 2849-2860.

Nelson, D.W., Sommers, L.E., 1996. Total carbon, organic carbon, and organic matter. pp. 961–1010. In: Sparks, D.L., Page, A.L., Helmke, P.A., Loeppert, R.H., Soltanpour, Tabatabai, M.A., Johnston, C.T., Sumner, M.E. (Eds.), Methods of Soil Analysis. Part 3. Chemical Methods. Soil Science Society of America and American Society of Agronomy, Madison, WI.

Parker, G., Klingeman, P. 1982. On why gravel bed streams are paved. Water Resources Research, 18(5), pp.1409 – 1424. https://doi.org/10.1029/WR018i005p01409

Pitlick, J. 1988. Variability of bed load measurement. *Water Resources Research*, *24*(1), pp.173-177.

Rapp, A., Li, J., and Nyberg, R. 1991. Mudflow disasters in mountainous areas. Ambio 20, pp. 210-218

Rice, S. and Church, M.1996. Sampling surficial fluvial gravels; the pre-cision of size distribution percentile sediments, J. Sediment. Res., 66, pp. 654–665.

Safeeq, M., Grant, G., Lewis, S., Hayes, S. 2020. Disentangling effects of forest harvest on long-term hydrologic and sediment dynamics, western Cascades, Oregon. Journal of Hydrology 580 (2020) 124259.

Shields, R., Pyron, M., Arsenault, E. R., Thorp, J. H., Minder, M., Artz, C., Costello, J., Otgonganbat, A., Mendsaikhan, B., Altangerel, S., and Maasri, A. 2021. Geomorphology variables predict fish assemblages for forested and endorheic rivers of two continents. Ecology and Evolution, 11, pp. 16745–16762. 10.1002/ece3.8300

Snyder, K. 2000. Debris Flows and Flood Disturbance in Small, Mountain Watersheds: M.S. Thesis, Oregon State University.

Sollins, P., Swanston, C., Kleber, M., Filley, T., Kramer, M., Crow, S., Caldwell, B.A., Lajtha, K. andBowden, R., 2006. Organic C and N stabilization in a forest soil: evidence from sequential density fractionation. Soil Biology and Biochemistry, 38(11), pp.3313-3324.

Swanson, F. J. 1981. Fire and Geomorphic Processes. In: Gen. Tech. Rep. USDA For. Serv. WO-26. Washington DC. pp. 401-420

Swanson, F. J., Dyrness, C. T. 1975. Impact of clear-cutting and road construction on soil erosion by landslides in the western Cascade Range, Oregon. Geology. 3(7), pp. 393-396.

Swanson, F. J.; Fredriksen, R. L.; McCorison, F. M. 1982. Material transfer in a western Oregon forested watershed. In: Edmonds, Robert L., ed. Analysis of coniferous forest ecosystems in the western United States. US/IBP Synthesis Series 14. Stroudsburg, PA: Hutchinson Ross Publishing Company: pp. 233-266.

Swanson, F.J., Fredriksen, R.L. 1982. Sediment Routing and Budget: Implications for Judging Impacts of Forestry Practices. In: Sediment Budgets and Routing in Forested Drainage Basins, USDA Forest Service, pp. 129-137

Swanson, F.J., James M.E., 1975. Geology and geomorphology of the H. J. Andrews Experimental Forest, Western Cascades, Oregon. USDA Forest Service Research Paper PNW-188, Portland, Oregon, 14 p.

Swanson, F.J., Swanston, D. 1977. Complex mass-movement terrains in the western Cascade Range, Oregon, Landslides, Donald R. Coates.

Swanson, Frederick J., Jones, Julia A. (2002) Geomorphology and hydrology of the H.J. Andrews Experimental Forest, Blue River, Oregon. Field guide to geologic processes in Cascadia: field trips to accompany the 98th annual meeting of the Cordilleran section of the Geological Society of America. (Pub. No: 3105, *Conference Proceedings*)

Swanston, D. N. 1971. Principal soil movement processes influenced by roadbuilding, logging and fire. In: Proceedings of a Symposium: Forest Land Uses and Stream Environment. Oregon State University, Corvallis. pp. 29-40.

Stephens, F, R. 1964. Soil Survey Report of the H.J. Andrews Experimental Forest Willamette National Forest. U.S. Forest Service Region 6, Division of Watershed Management.

Turowski, J., Richenmann, D., and Dadson, S. 2010.The partitioning of the total sediment load of a river into suspended load and bedload: a review of empirical data. Sedimentology, 57, pp. 1126-1146. https://doi.org/10.1111/j.1365-3091.2009.01140.x

Walter, R.C. and Merritts, D.J. 2008. Natural streams and the legacy of water-powered mills. Science, 319(5861), pp.299-304.

Wemple, B.C., Jones, J.A., Grant, G.E. 1996. Channel network extension by logging roads in two basins, western Cascades, Oregon. Water Resour. Bull. 32, pp. 1195–1207. https://doi.org/10.1111/j.1752-1688.1996.tb03490.x.

Wemple, B.C., Swanson, F.J., Jones, J.A. 2001. Forest roads and geomorphic process interactions, Cascade Range, Oregon. Earth Surf. Proc. Land. 26, pp. 191–204.

Whiting, P., Stamm, J.,Moog, D.,Orndorff, R.Sediment-transporting flows in headwater streams.1999. GSA Bulletin. 111 (3), pp. 450–466. doi: https://doi.org/10.1130/0016-7606(1999)111<0450:STFIHS>2.3.CO;2

Wohl E, Scott D, N. 2016. Wood and sediment storage and dynamics in river corridors. *Earth Surface Processes and Landforms*.

Wondzell, S. M. and Swanson, F. J. 1999. Floods, channel change, and the hyporheic zone. Water Resourc. Res. 35, pp. 555-567.

Wondzell, S.M., King. J.G. 2003.Post-fire erosional processes in the Pacific Northwest and Rocky Mountain regions. Forest Ecology and Management, 178 (2003), pp. 75-87.

Table of Contents (Appendix)

A. Long-term data analysis
Table A-1. Values used for multiple linear regression analyses. Data were available for this analysis only through the 2019 water year.

Year	Maximum mean daily flow (cfssm)					# of days that exceeded bankfull condition					Total volume of flow that exceeded bankfull condtion (cfssm)				
	WS01	WS02	WS03	WS09	WS10	WS01	WS02	WS03	WS09	WS10	WS01	WS02	WS03	WS09	WS10
1957	83	76	60	NA	NA	1	4	2	NA	NA	40	51	33	NA	NA
1958	99	103	85	NA	NA	4	6	6	NA	NA	82	118	94	NA	NA
1959	56	45	40	NA	NA	2	3	2	NA	NA	19	19	10	NA	NA
1960	30	28	26	NA	NA	0	0	0	NA	NA	0	0	0	NA	NA
1961	87	79	65	NA	NA	2	3	3	NA	NA	60	82	55	NA	NA
1962	76	59	58	NA	NA	2	5	3	NA	NA	52	49	41	NA	NA
1963	48	37	42	NA	NA	1	1	2	NA	NA	5	3	13	NA	NA
1964	54	30	36	NA	NA	1	0	1	NA	NA	11	0	3	NA	NA
1965	127	116	NA	NA	NA	11	11	NA	NA	NA	320	288	NA	NA	NA
1966	76	42	43	NA	NA	1	1	1	NA	NA	33	8	10	NA	NA
1967	51	47	44	NA	NA	2	1	2	NA	NA	10	13	12	NA	NA
1968	46	44	40	NA	NA	1	1	1	NA	NA	3	10	7	NA	NA
1969	76	49	51	NA	NA	3	5	4	NA	NA	62	39	26	NA	NA
1970	61	57	55	NA	NA	2	4	5	NA	NA	23	28	35	NA	NA
1971	89	74	67	NA	NA	5	3	3	NA	NA	81	85	68	NA	NA
1972	91	82	76	NA	NA	11	14	14	NA	NA	260	197	184	NA	NA
1973	38	27	26	NA	NA	0	0	0	NA	NA	0	0	0	NA	NA
1974	66	33	37	39	50	2	0	1	2	1	24	0	4	6	50
1975	73	51	47	51	62	3	1	1	4	2	30	17	14	32	62
1976	88	82	66	74	77	2	2	2	7	2	72	69	50	77	77
1977	18	12	11	14	27	0	0	0	0	0	0	0	0	0	27
1978	77	68	65	55	98	4	6	6	5	5	89	110	96	53	98
1979	64	45	44	44	74	2	1	1	2	2	23	11	11	12	74
1980	71	59	49	44	71	3	3	3	2	2	46	48	35	21	71
1981	72	64	59	50	79	4	3	4	5	4	49	42	35	27	79
1982	71	66	59	57	74	6	6	8	9	8	79	80	66	79	74
1983	46	43	40	44	57	3	4	3	3	5	6	17	10	17	57
1984	87	71	66	65	82	3	2	2	3	3	66	44	38	50	82
1985	32	25	23	37	41	0	0	0	1	0	0	0	0	2	41
1986	97	92	76	NA	NA	2	3	2	NA	NA	97	118	84	NA	NA
1987	40	33	31	32	50	0	0	0	0	1	0	0	0	0	50
1988	66	47	42	42	66	1	1	2	1	1	23	13	9	7	66
1989	68	51	48	57	68	2	2	1	2	3	28	20	19	34	68
1990	55	38	34	46	64	2	1	1	2	3	14	4	1	11	64

Year														
1991	41	26	27	32	47	0	0	0	0	0	0	0	0	0	47
1992	48	29	31	39	52	1	0	0	1	1	5	0	0	4	52
1993	38	34	30	34	39	0	0	0	0	0	0	0	0	0	39
1994	46	28	32	32	56	1	0	0	0	1	3	0	0	0	56
1995	67	46	44	56	64	2	3	2	3	4	26	24	14	29	64
1996	160	164	NA	99	144	5	4	NA	6	5	209	242	NA	121	144
1997	100	87	86	74	92	7	9	9	8	8	161	194	163	127	92
1998	41	28	28	30	49	0	0	0	0	1	0	0	0	0	49
1999	90	103	107	72	118	4	6	7	6	4	70	124	162	66	118
2000	66	70	64	62	66	2	4	3	6	2	36	71	67	40	66
2001	12	14	14	17	21	0	0	0	0	0	0	0	0	0	21
2002	50	49	44	43	61	1	2	3	2	2	7	20	28	13	61
2003	52	42	44	47	60	1	2	3	2	2	9	11	21	16	60
2004	60	56	55	54	67	1	3	2	1	1	17	31	28	19	67
2005	34	30	28	32	42	0	0	0	0	0	0	0	0	0	42
2006	82	80	85	72	90	3	6	7	6	5	63	123	136	89	90
2007	42	45	48	40	58	0	1	2	1	2	0	11	17	5	58
2008	32	33	29	34	41	0	0	0	0	0	0	0	0	0	41
2009	73	67	64	67	74	4	6	5	4	5	53	106	105	72	74
2010	NA	NA	NA	64	64	NA	NA	NA	0	1	NA	NA	NA	0	64
2011	74	70	69	67	80	1	3	3	2	2	31	45	61	33	80
2012	84	78	76	42	93	2	4	8	6	4	42	85	79	51	93
2013	47	44	44	54	54	1	3	3	2	1	4	16	23	10	54
2014	69	60	59	62	77	1	4	4	2	2	26	44	182	20	77
2015	80	74	66	53	84	1	2	2	2	1	37	49	38	31	84
2016	51	56	48	53	54	2	3	4	1	2	8	34	31	18	54
2017	62	65	57	28	65	2	2	3	2	1	21	43	33	29	65
2018	30	32	27	53	32	0	0	0	0	0	0	0	0	0	32
2019	63	63	61	53	67	2	2	3	2	2	24	40	44	26	67

Table A-2: Relationship of annual bedload export to maximum daily flow based on linear regressions using (1) untransformed data, (2) natural log-transformed data, and (3) natural log-transformed data with zeros filled with values of 0.01.

Site Name	(1)	(2)	(3)
WS01	0.32	0.27	0.257
WS02	0.58	0.103	0.46
WS03	0.016	0.1792	0.24
WS09	0.35	0.47	0.35
WS10	0.13	0.41	N/A

Watershed 1 valley cross sections
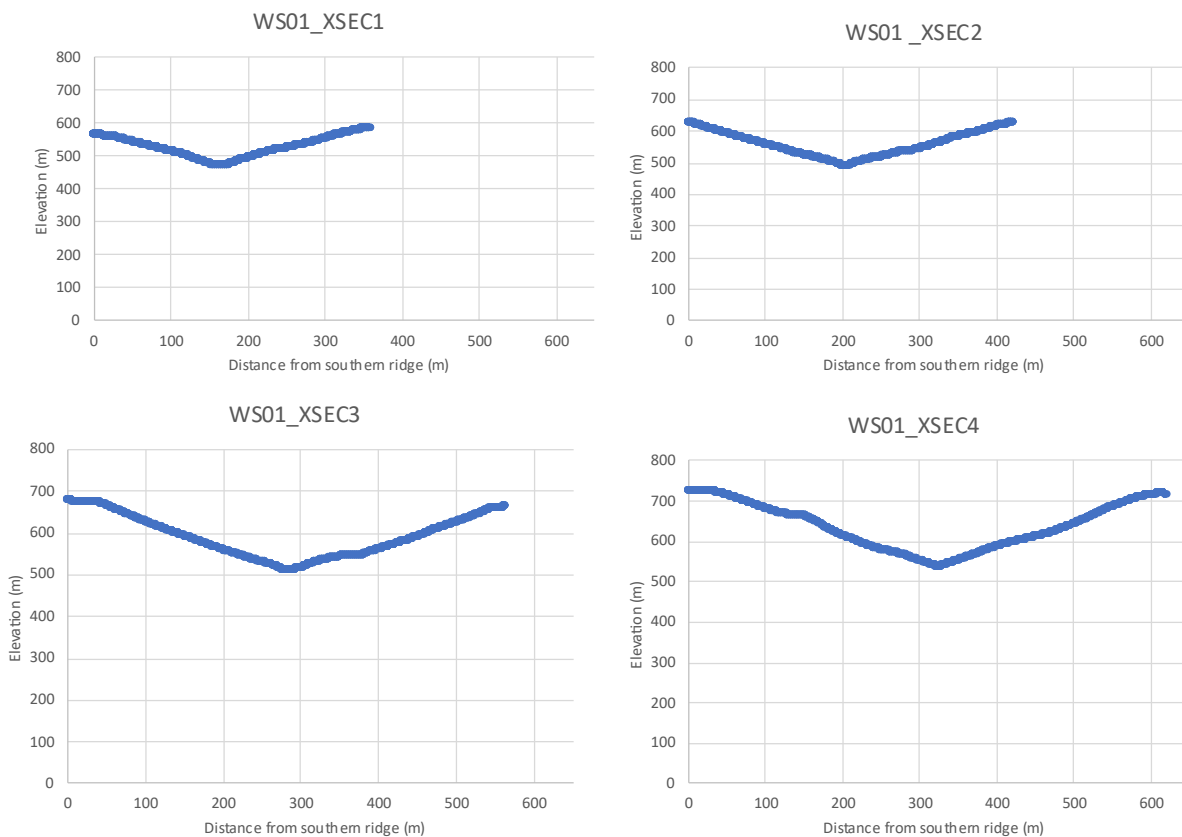
Figure A-1. Valley cross-sections, WS01.

Watershed 2 valley cross sections
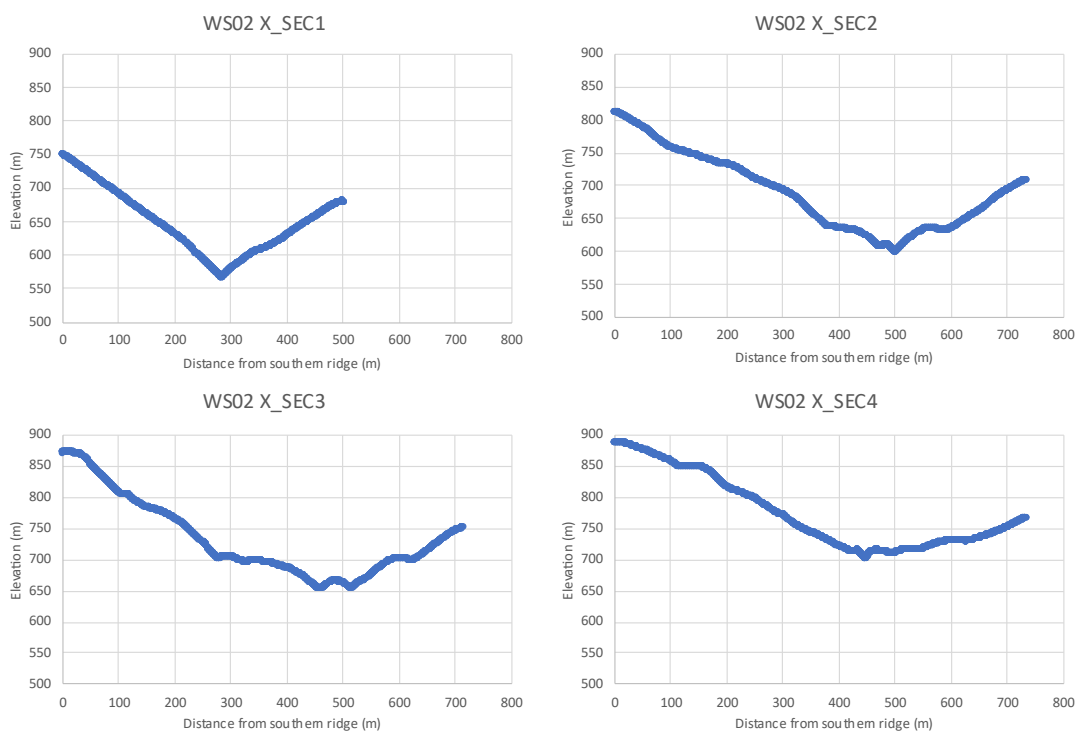
Figure A-2. Valley cross-sections, WS02.

Watershed 3 valley cross sections
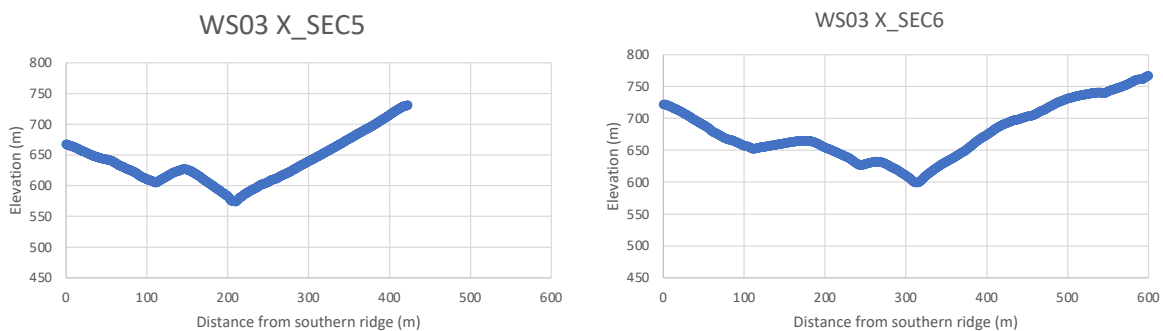
Figure A-3. Valley cross-sections, WS03.

Watershed 1 longitudinal profiles from 3 tributary channels
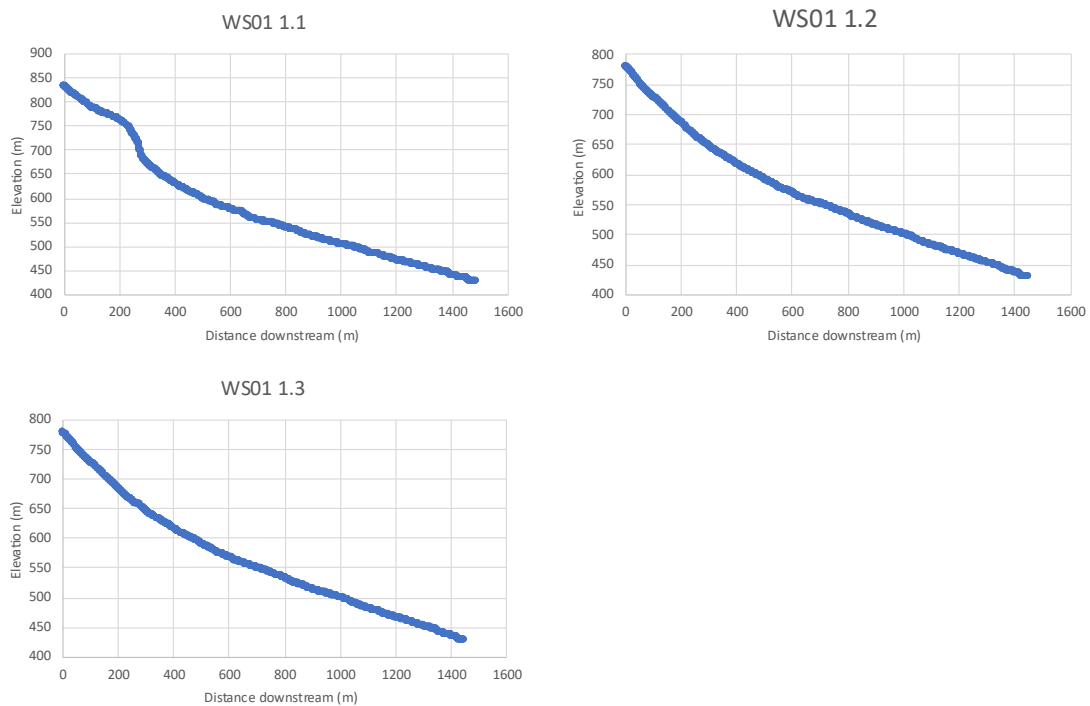
Figure A-4. Longitudinal profiles, WS01.
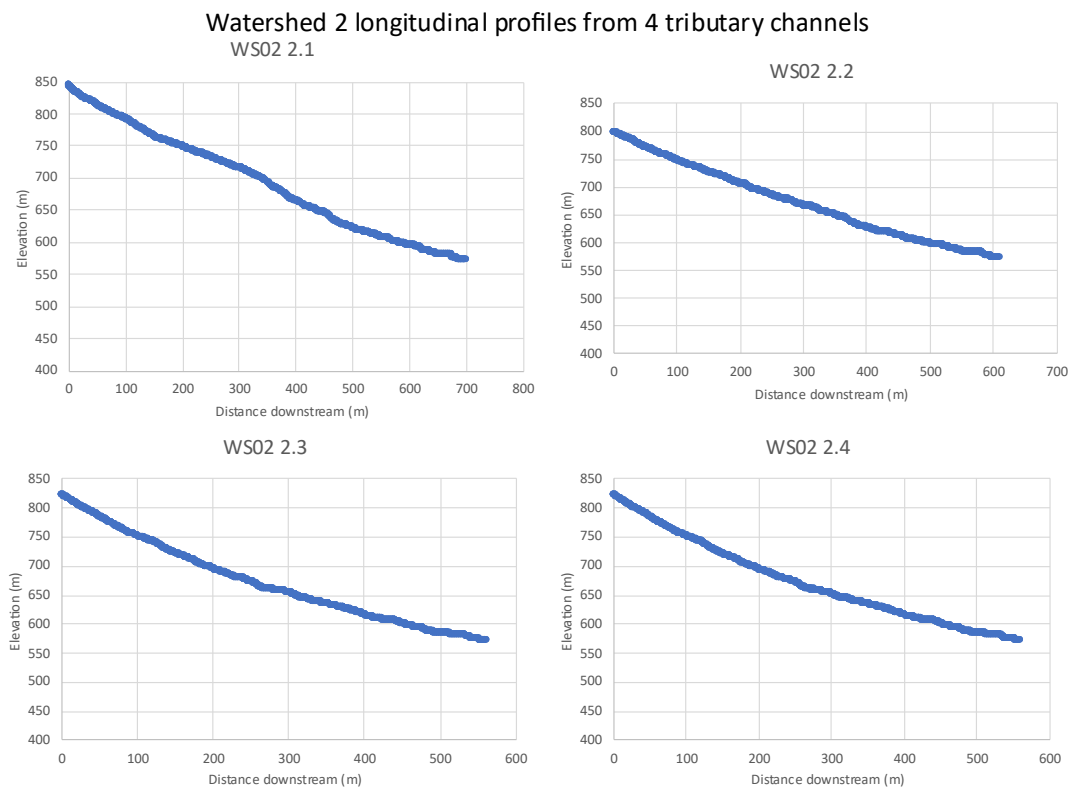
Figure A-5. Longitudinal profiles, WS02.
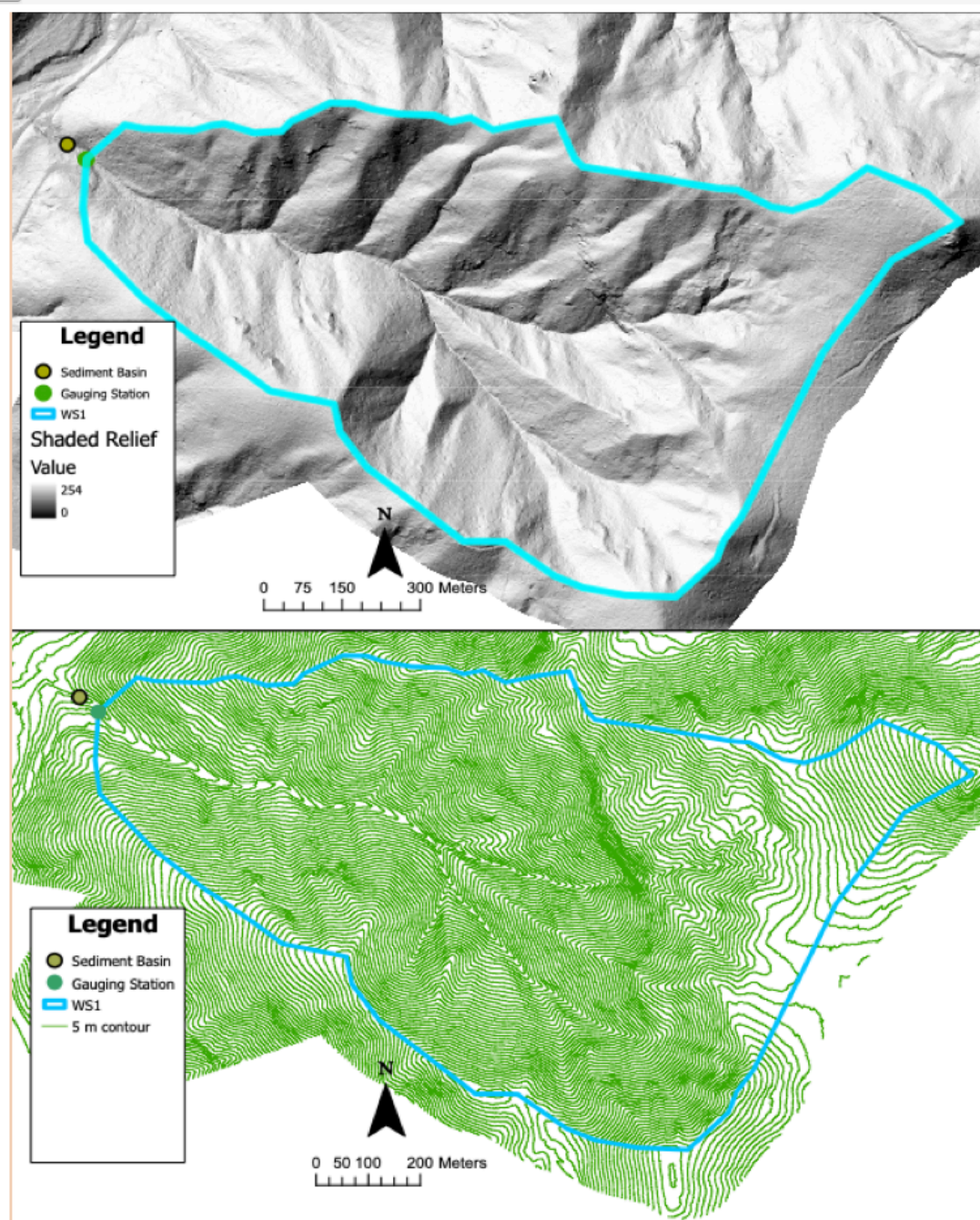
Figure A-6. Topographic map of WS01.
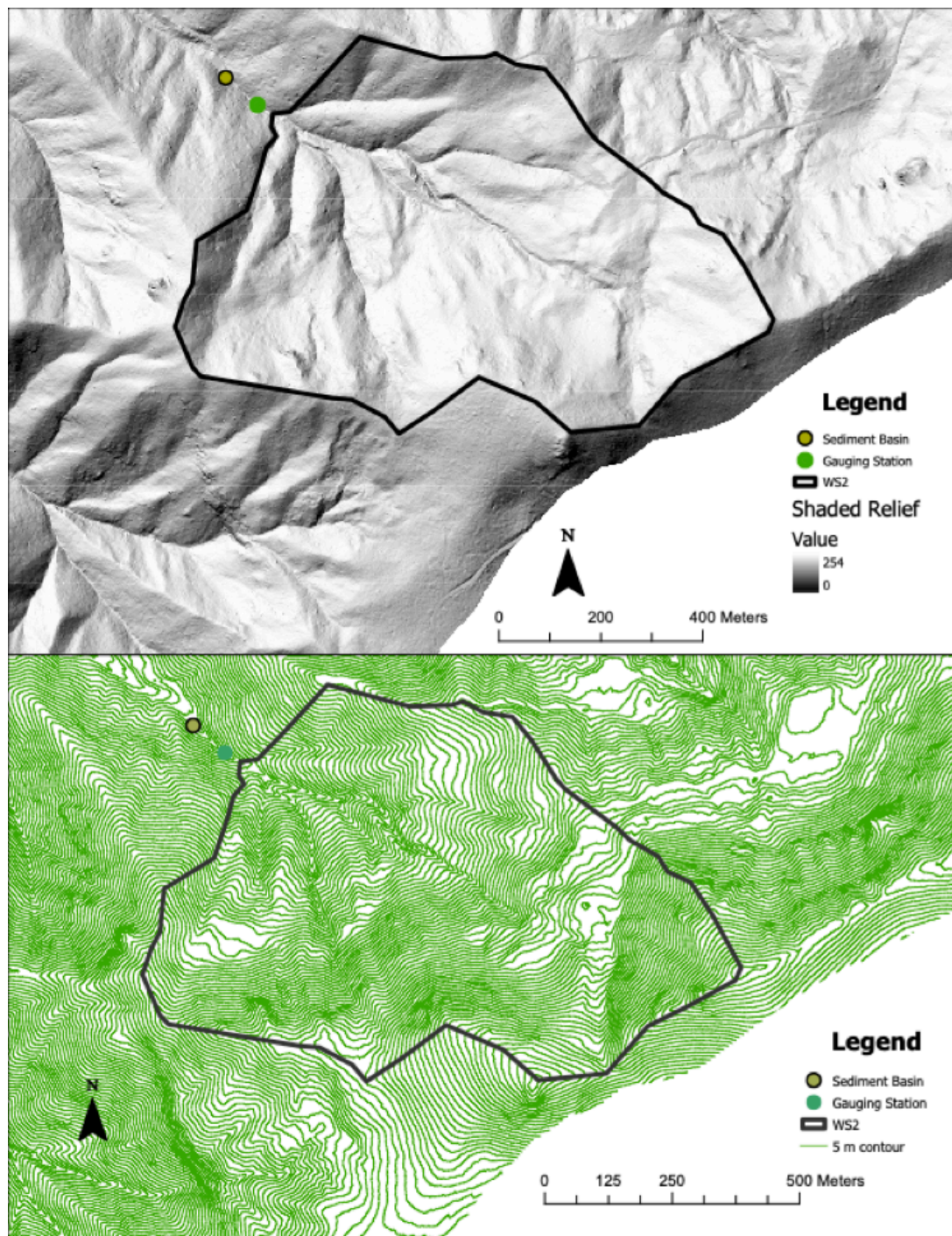
Figure A-7. Topographic map of WS02.
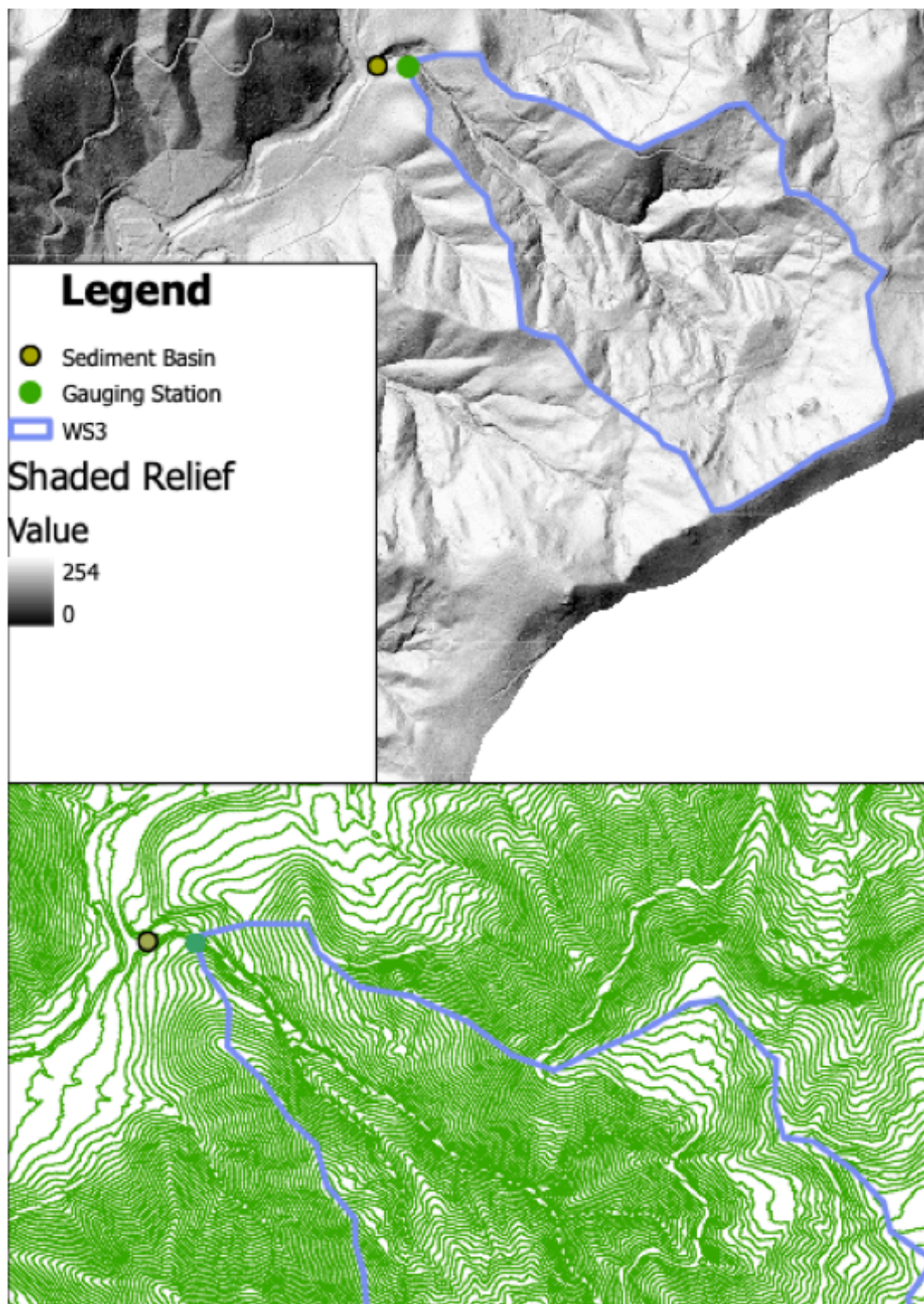
Figure A-8. Topographic map of WS03.
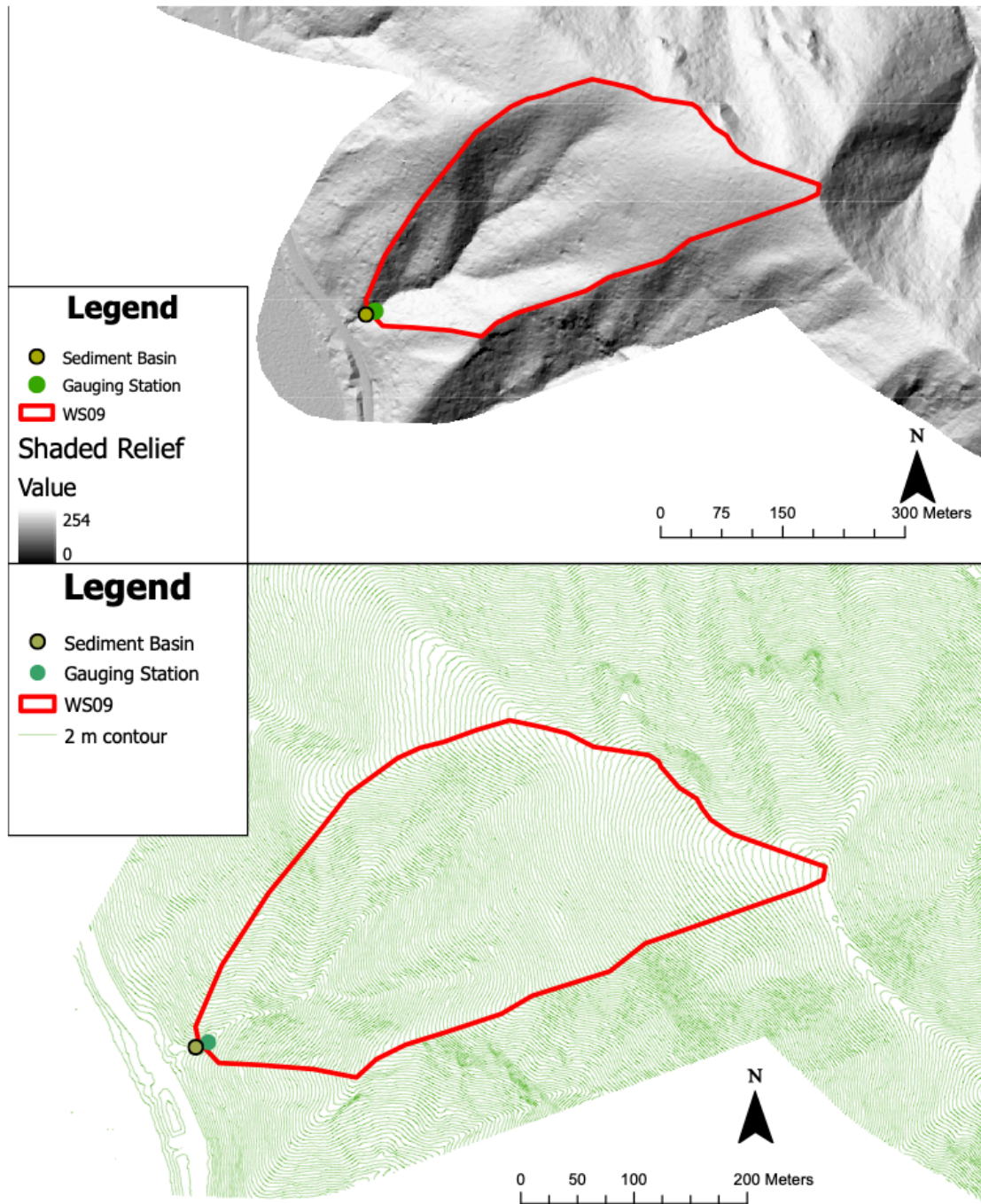
Figure A-9. Topographic map of WS09.
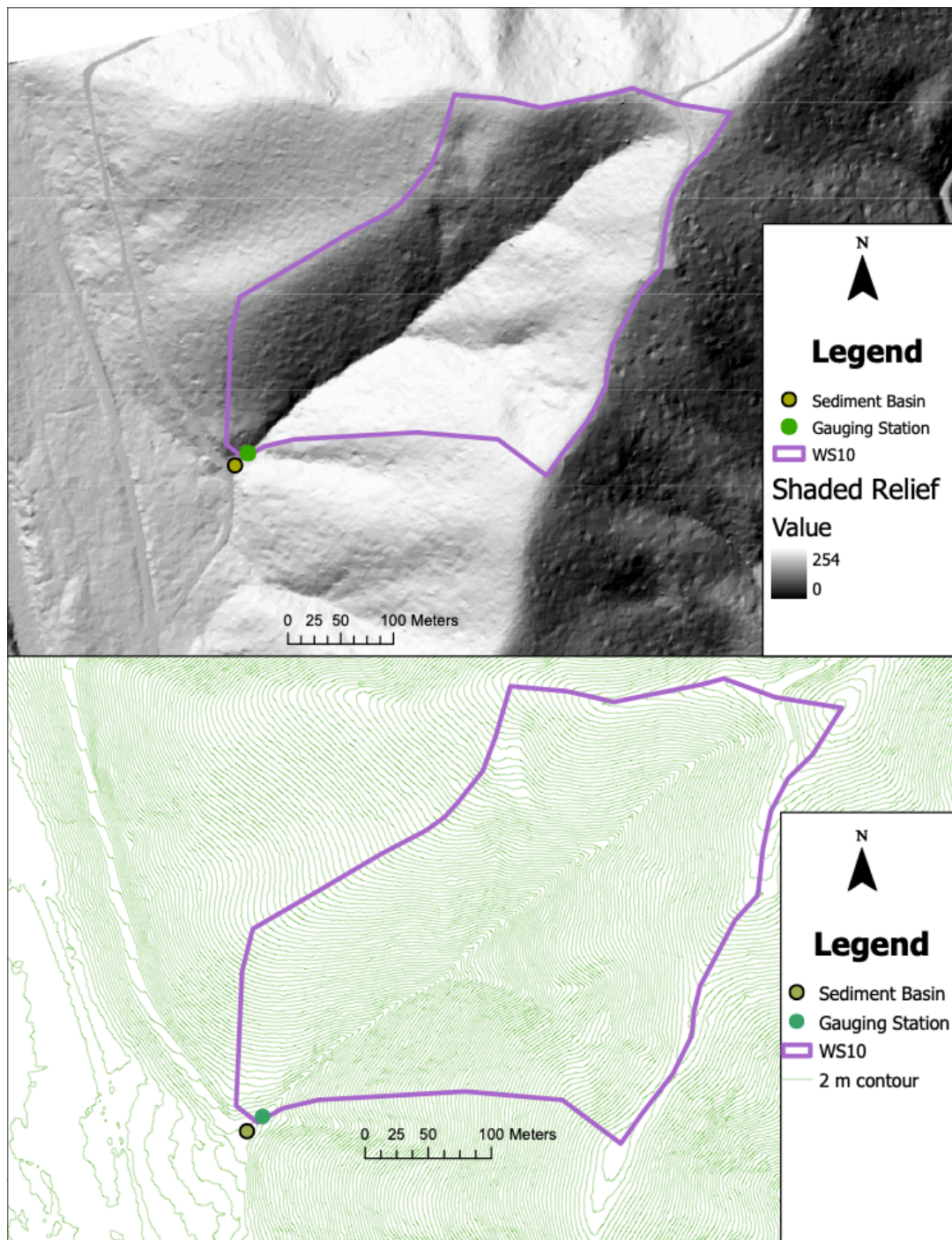
Figure A-10. Topographic map of WS10.

- Broadcast burn + stream cleaning increased export
- Wide valley floor and residual large wood trapped and stored LOTS of sediment
- Continual decay of wood + high amount of stored sediment contribute to increased export 50 -60 years post treatment

WS01: 100% clearcut, slash burn, no roads

27

1964: pre-cut

1964: post-cut, pre-yarding, pre-broadcast burn

1966: post-broadcast burn, pre-cleaning

1966 – post-stream cleaning, sediment stored in wide valley floor and by wood
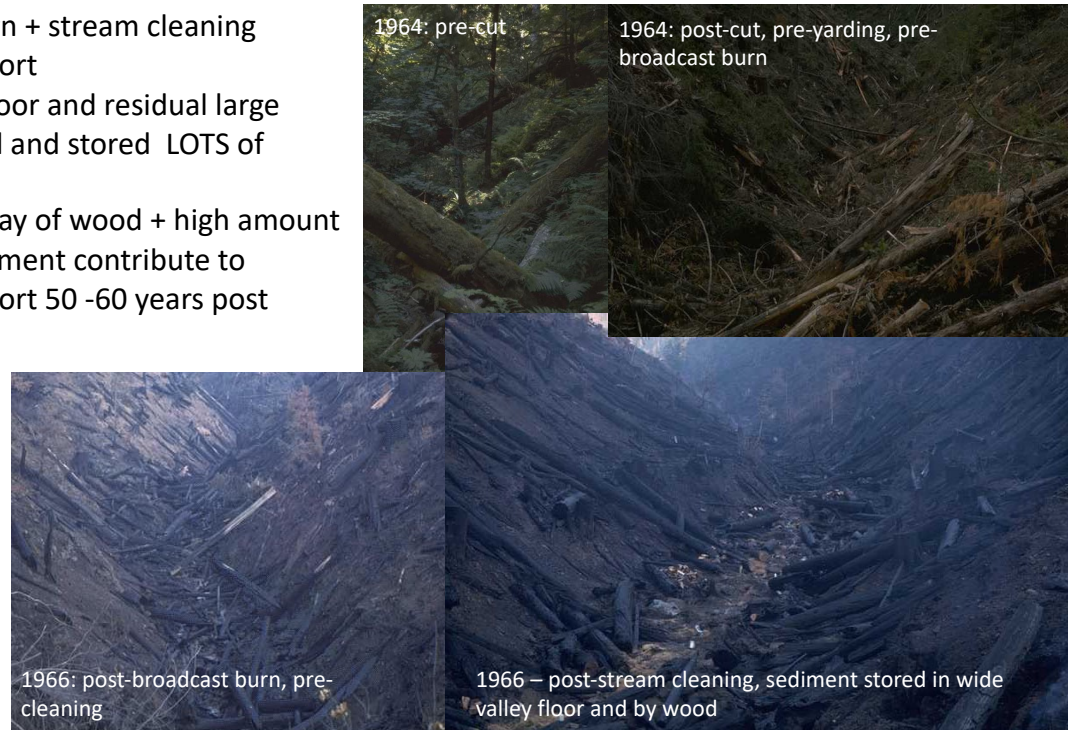
Figure A-11. WS01 historical photos with labels

- Debris flows 1964, 1996
- Channel scoured
- Bedload export was reduced following debris flows

WS03: 25% patch cut, roads,

pre-flood 1964

1972 post-debris flow scoured channel

Rebuilt gauging station post-debris flow

1996 debris flow deposit

Post-debris flow 1996

Figure A-12. WS03 historical photos with labels

- Debris flows 1986, 1996
- Channel scoured
- Bedload export was elevated after debris flows, possibly due to steep unstable slopes with little to no channel storage

WS10: 100% clearcut, no roads
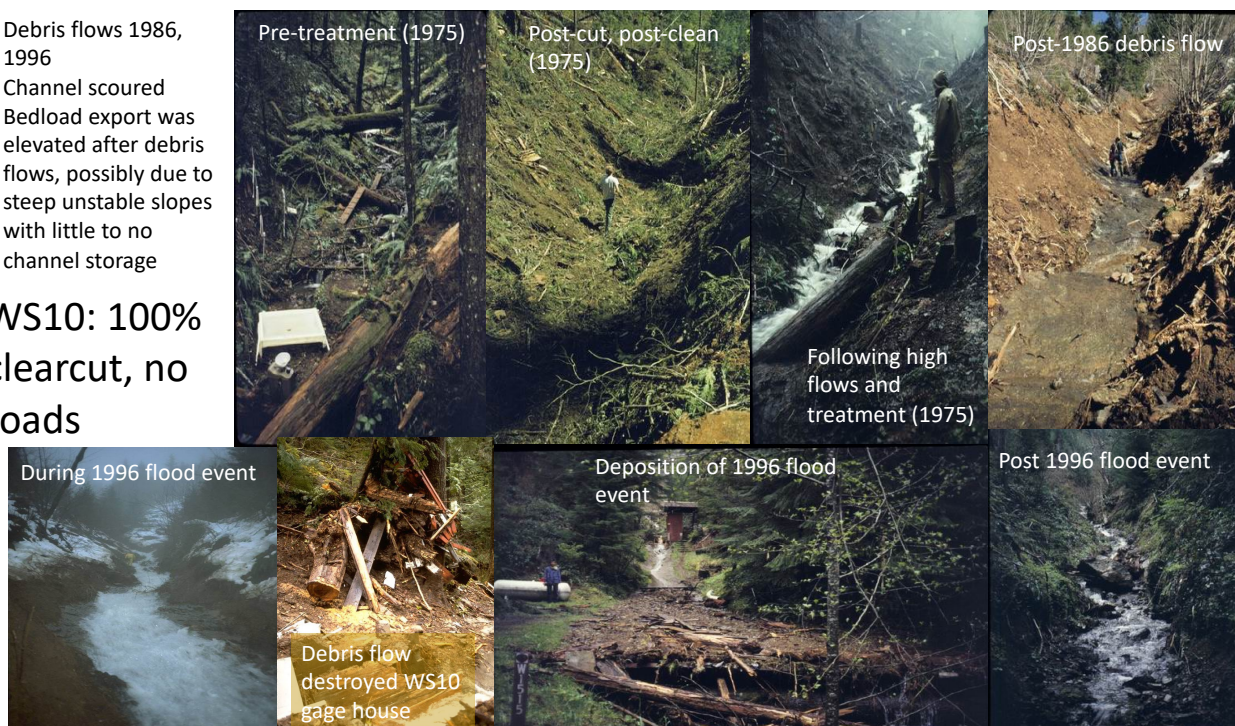
Figure A-13. WS10 Historical photos with labels

B. Bedload sample characterization
Table B-1. Grain size fractions (g) of all samples (n=31), subdivided by organic and mineral fractions. No = Sample number, Loc = location, WY = water year, Min = mineral, Org = organic.

			<2 mm		2-4 mm		>4 mm		Total		Min+Org
No	Loc	WY	Min	Org	Min	Org	Min	Org	Min	Org	Org
WS09 early fall of first year after fire, October -December 2020											
1	WS09	2020	95.6	35.3	3.5	0.7	13.4	73.0	112.5	109.0	221.4
2	WS09	2020	104.9	45.2	2.7	0.7	18.0	43.4	125.6	89.3	214.9
3	WS09	2020	149.4	69.2	2.9	0.0	15.5	53.2	167.8	122.4	290.2
4	WS09	2020	89.2	49.0	2.4	0.0	12.2	48.6	103.8	97.6	201.3
5	WS09	2020	244.6	102.5	0.4	1.0	19.8	127.5	264.8	231.0	495.8
6	WS09	2020	40.6	18.3	40.7	9.1	18.3	93.2	99.6	120.6	220.2
Ave			120.7	53.3	8.8	1.9	16.2	73.2	145.7	128.3	274.0
%			44.1	19.4	3.2	0.7	5.9	26.7	53.2	46.8	100.0
WS09 winter and spring of first year after fire, January - May 2021											
7	WS09	2021	45.0	6.4	33.4	0.0	288.5	0.0	366.9	6.4	373.3
8	WS09	2021	29.8	3.5	39.8	0.0	329.6	0.0	399.2	3.5	402.7
9	WS09	2021	30.8	2.8	39.1	0.0	327.3	0.0	397.2	2.8	400.0
10	WS09	2021	65.6	9.7	63.7	7.5	0.0	3.6	129.3	20.8	150.2
11	WS09	2021	48.7	6.9	294.9	39.1	0.0	10.2	343.6	56.2	399.9
12	WS09	2021	66.8	9.0	65.7	14.0	237.7	5.7	370.2	28.7	398.9
13	WS09	2021	57.3	6.0	58.4	8.6	251.6	9.2	367.3	23.8	391.2
14	WS09	2021	14.1	2.0	29.0	0.0	206.6	0.0	249.7	2.0	251.7
15	WS09	2021	45.9	7.8	49.0	0.0	184.8	0.0	279.7	7.8	287.4
16	WS09	2021	51.8	7.1	49.9	0.0	156.8	0.0	258.5	7.1	265.6
Ave			45.6	6.1	72.3	6.9	198.3	2.9	316.2	15.9	332.1
%			13.7	1.8	21.8	2.1	59.7	0.9	95.2	4.8	100.0
WS09 fall, winter and spring of second year after fire, May 2021 - June 2022											
17	WS09	2022	30.6	14.2	10.3	1.4	169.9	53.3	210.8	68.9	279.8
18	WS09	2022	92.4	31.7	33.8	19.3	180.1	16.4	306.3	67.4	373.6
19	WS09	2022	63.2	28.2	10.7	4.2	115.8	50.6	189.7	83.0	272.8
20	WS09	2022	40.5	15.3	11.7	9.0	258.1	38.7	310.3	63.0	373.4
21	WS09	2022	86.6	33.2	8.3	3.7	177.5	61.5	272.4	98.4	370.8
22	WS09	2022	134.4	46.4	23.0	9.1	68.3	10.3	225.7	65.8	291.5
Ave			74.6	28.2	16.3	7.8	161.6	38.5	252.5	74.4	327.0
%			22.8	8.6	5.0	2.4	49.4	11.8	77.2	22.8	100.0
WS10, year preceding wildfire, August 2019 - August 2020											
23	WS10	2020	57.0	15.0	47.8	12.7	249.9	14.7	354.7	42.4	397.1

24	WS10	2020	92.8	26.9	69.5	17.0		32.9	162.3	76.8	239.1
Ave			74.9	21.0	58.7	14.9	249.9	23.8	258.5	59.6	318.1
%			23.5	6.6	18.4	4.7	78.6	7.5	81.3	18.7	100.0

WS10, first year after wildfire in WS09, August 2020 - August 2021

25	WS10	2021	145.2	60.7	71.0	36.9	197.1	45.4	413.3	143.0	556.3
Ave			145.2	60.7	71.0	36.9	197.1	45.4	413.3	143.0	556.3
%			26.1	10.9	12.8	6.6	35.4	8.2	74.3	25.7	100.0

WS10, second year after wildfire, August 2021 - August 2022

26	WS10	2022	75.3	34.2	39.5	15.1	32.1	18.8	146.9	68.1	215.0
27	WS10	2022	89.9	29.5	22.0	9.6	40.1	20.1	152.0	59.2	211.2
28	WS10	2022	69.7	26.2	30.5	9.4	46.2	16.9	146.4	52.5	198.9
29	WS10	2022	91.3	32.8	21.8	9.8	51.2	6.0	164.3	48.6	212.8
30	WS10	2022	75.6	25.4	20.5	10.0	56.8	12.1	152.9	47.5	200.6
31	WS10	2022	100.5	39.2	19.0	7.8	38.4	4.5	157.9	51.5	209.3
Ave			83.7	31.2	25.6	10.3	44.1	13.1	153.4	54.6	208.0
%			40.3	15.0	12.3	4.9	21.2	6.3	73.8	26.2	100.0

WS09, first two years after fire, October 2020 - June 2022

Ave, WS09			74.0	25.0	39.7	5.8	138.6	31.7	252.3	62.5	314.8
%			23.5	7.9	12.6	1.8	44.0	10.1	80.1	19.9	100.0

WS10, year before and two years after fire, August 2019 - June 2022

Ave, WS10			88.6	32.2	38.0	14.3	89.0	19.0	205.6	65.5	271.1
%			32.7	11.9	14.0	5.3	32.8	7.0	75.8	24.2	100.0